EFFECTS OF CONSTRUCTION PROCEDURES ON BOND IN BRIDGE DECKS

by

Rex C. Donahey

David Darwin

A Report on Research Sponsored by

THE KANSAS DEPARTMENT OF TRANSPORTATION

Project No. P 0255

UNIVERSITY OF KANSAS

LAWRENCE, KANSAS

January 1983

50272-101

REPORT DOCUMENTATION PAGE	1. REPORT NO.	2.	3. Recipient's Accession No.

4. Title and Subtitle

Effects of Construction Procedures on Bond in Bridge Decks

5. Report Date

6. January 1983

7. Author(s)

Rex C. Donahey and David Darwin

8. Performing Organization Rept. No.

SM Report No. 7

9. Performing Organization Name and Address

University of Kansas Center for Research, Inc.
2291 Irving Hill Drive, West Campus
Lawrence, Kansas 66045

10. Project/Task/Work Unit No.

11. Contract(C) or Grant(G) No.

(C) P 0255

(G)

12. Sponsoring Organization Name and Address

Kansas Department of Transportation
State Office Building
Topeka, Kansas 66612

13. Type of Report & Period Covered

14.

15. Supplementary Notes

16. Abstract (Limit: 200 words)

The effects of consolidation method and two-course construction on concrete-steel bond in concrete bridge decks are studied as functions of slump, bleed, and depth of slab. Consolidation was varied by vibrator spacing and insertion time. Four top covers were studied: 3/4, 1, and 3 inch monolithic and 3 inch two-course. Bond test specimens were of two types: shallow, with 8 inches of concrete below the reinforcement, and deep, with 24 inches of concrete below the reinforcement. All specimens were modified cantilever beam type specimens. Concrete densities were obtained using core samples.

Based on the experimental work, high density internal vibration provides improved bond over low density internal vibration. 3 inch monolithic cover provides higher bond strength than 3 inch two-course cover. Increased concrete slump has a negative effect on bond strength for top-cast reinforcement. Deep specimens made with stiff, well consolidated concrete can provide the same bond strengths as shallow specimens.

17. Document Analysis a. Descriptors

air entrainment, bond, bleeding (concrete), bridge decks, concrete construction, consolidation, cover, overlays, reinforced concrete, reinforcing steel, slump, vibration

b. Identifiers/Open-Ended Terms

c. COSATI Field/Group

18. Availability Statement	19. Security Class (This Report)	21. No. of Pages
Release unlimited	Unlimited	
	20. Security Class (This Page)	22. Price
	Unlimited	

(See ANSI–Z39.18) *See Instructions on Reverse* OPTIONAL FORM 272 (4–77) (Formerly NTIS–35) Department of Commerce

Acknowledgements

This report is based on a thesis presented by Rex C. Donahey in partial fulfillment of the requirements for the MSCE degree from the University of Kansas. Support for this project was provided by the State of Kansas Department of Transportation under a research contract with the University of Kansas Center for Research, Inc. Vibrating and finishing equipment was supplied by Allen Engineering Corporation. Reinforcing steel was provided by ARMCO INC. and Sheffield Steel. High-range water-reducer was supplied by Gifford-Hill and Company, Inc. The water blaster was supplied by District I of the Kansas Department of Transportation. Additional support was provided by the University of Kansas Department of Civil Engineering.

Table of Contents

Table of Contents (continued)

List of Tables

List of Figures

List of Figures (continued)

List of Figures (continued)

List of Figures (continued)

List of Figures (continued)

Chapter 1

Introduction

1.1 General

Attempts to solve the problem of corrosion of reinforcing steel in concrete bridge decks have led to the introduction of innovative procedures for new deck construction. Two of these procedures, two-course bonded deck construction and high density internal vibration. are relatively untested for their effects on concrete-steel bond strength.

Two-course bonded deck construction places a high quality concrete wearing surface on a previously placed and cured first course. It has been found, however, that due to the low cover initially used over the top steel, the procedure can can cause settlement cracks in the first course, which may, in turn, affect the concrete-steel bond.

Bridge deck concrete in Kansas is currently consolidated using high density internal vibration, which limits maximum vibrator spacing to one foot. This method is intended to be an improvement over consolidation using hand-held vibrators. Although it is generally accepted that good consolidation leads to good concrete, it is not clear what effect the high density vibration has on the concrete-steel bond.

Concrete-steel bond is affected by many factors, including the reinforcing bar diameter and spacing; the strength, slump, settlement. and bleeding characteristics of the concrete; the consolidation method used; the depth of the member; and the minimum cover. Current AASHTO Bridge Specifications (1) and ACI Building Code provisions (4) consider only four of these factors (bar diameter and spacing, concrete strength, and depth of the member).

The bond between concrete and steel is critical for structural safety. An understanding of the interaction between the two materials and an understanding of the parameters affecting that interaction is therefore necessary. The effects of the degree of consolidation and the type and thickness of the cover above the reinforcement are not well documented and are not considered in the current design codes. It is the purpose of this study to provide additional information on these parameters.

1.2 Background

Deterioration of concrete bridge decks has been a major concern in the United States since the early 1960's (18, 21). Investigations have indicated that the major problem in most states is surface spalling caused by internal expansive forces in the concrete, generated by corrosion of the top reinforcing steel. Cracks over bars, shallow concrete covers over bars. and permeable concrete allow deicing chemicals to reach the top reinforcement and cause corrosion (18, 21). In response to these problems, new construction procedures have been implemented.

Current Kansas Department of Transportation bridge deck construction specifications require that deck concrete be consolidated using internal vibrators (23). These vibrators must be mounted on a device designed to maintain a maximum vibrator spacing of one foot. Although multiple vibrators are not explicitly required, typical devices in use have four to eight vibrators mounted on a moveable frame (Fig. 1.1). Multiple, frame-mounted vibrators can provide adjacent vibrator interaction, consistent insertion spacing, and consistent insertion timing; however, such assemblies are more expensive than hand-held vibrators. Research conducted by the Kansas Department of Transportation indicates that high density vibration results in lower permeability than consolidation using hand-held vibrators (11). The relative permeability of samples obtained from a deck consolidated using high density vibration is just one-fifth that of decks consolidated using a hand-held vibrator.

Two-course bonded deck construction has recently been implemented in many states to improve the quality of the top surface concrete in bridge decks. A major benefit of such construction is that it slows the rate of deterioration of decks, primarily by slowing the rate of penetration of deicing chemicals to the top reinforcing steel (18).

The two-course construction procedure used in Kansas consists of placing the first course concrete with a 3/4 inch design top cover, followed by a 2-1/4 inch bonded concrete overlay. The first course contains all of the deck reinforcement and is made using concrete with a maximum slump of 2-1/2 inches and a water-cement ratio of 0.44. The second course consists of concrete with a maximum 3/4 inch slump and a 0.35 water-cement ratio. The first course is internally vibrated, while the second is consolidated using a vibratory screed (Fig. 1.2).

The Kansas two-course deck procedure combines two of the currently recommended practices designed to protect top reinforcement: Bonding of a low water-cement ratio concrete overlay to the deck (21), and use of a 3 inch top cover (37).

The procedure has, however, resulted in the formation of settlement cracks over the top reinforcement within the first course in some decks, as shown in Fig. 1.3. These cracks are aggravated by the low cover and the removal of coarse aggregate above the top reinforcement during the finishing operation. Because this cracking resembles incipient bond failure, the concrete-steel bond is of concern.

The concrete-steel bond is critical, both during the construction phase. when only a 3/4 inch cover exists, and during the service phase. It is especially of interest over the piers of haunched slabs where the depth of concrete below the top reinforcement can be 24 inches or more. and the deck is subjected to a negative moment. The negative moment places the top reinforcement in tension, while the increased concrete depth at these sections may reduce the bond strength due to increased bleeding and settlement of the concrete.

1.3 Previous Work

Although it has been established for a number of years that initial or delayed consolidation using vibration can provide improved concrete-steel bond when compared with hand rodding, it has also been shown that repeated vibration of plastic concrete can have a negative effect on bond.

In 1938, Davis, Brown, and Kelly found that external vibration by jigging improved the maximum bond strength approximately 14 percent over hand rodding (17). A 45 percent improvement over hand rodding was achieved by axially vibrating the test bars. Specimens used in this study were 6 by 6 inch cylinders with vertically cast deformed bars. 4 inch slump concrete was used.

Davis et al. also studied the effect of delayed vibration on bond. They used methods and specimens similar to those used to study the effects of vibration, but vibration was applied at 3, 6, and 9 hours after the concrete had been placed by hand.

This work on the effects of delayed vibration on bond has been referenced in other papers as evidence of the positive effect of revibration (32, 33). However, because the specimens used in this study were not initially vibrated, the improvement in bond can only be attributed to delayed vibration, not revibration.

In 1942, Robin, Olsen, and Kinnane used 3 to 4 inch slump concrete and horizontally cast bars to compare external vibration with hand rodding (30). The specimens used were 3 inches wide and 10 inches deep. Smooth test bars were located from 1-1/2 to 7-1/2 inches above the bottom of the molds. External vibration resulted in lower bond strengths than hand rodding for bars located 1-1/2 or 3 inches from the bottom of the forms. External vibration resulted in higher bond strengths than hand consolidation, however, for bars located 6 or 7-1/2 inches from the form bottoms.

Menzel found that, with a 2 inch slump concrete, internal vibration provided a dramatic improvement in bond strength over hand rodding for top-cast bars (27). Using the specimens shown in Fig. 1.4, Menzel conducted pullout tests on both top-cast and bottom-cast deformed bars. The maximum steel stresses obtained in the tests are shown in Fig. 1.5. The value shown for the bottom-cast bar (with 2-1/8 inches of concrete below it) is the average for all specimens consolidated in the same manner. The other stresses are individual results. Although not all specimen depths were tested for both consolidation methods, the results indicate a trend of increasing strength with improved consolidation, as the height of the bar above the base is increased. The bottom-cast bars appear to have almost the same bond, regardless of the consolidation method. Only the average bond strengths for the bottom-cast bars were published, and no data were provided on the scatter in the results.

Negative effects of revibration on bond were obtained by Larnach (24) and by Menzel (27). The tests conducted by Larnach used a 4 inch square by 6 inch long specimen, with a horizontally cast smooth bar centered in the mold. Concrete was initially consolidated in the molds using external and surface vibration. Concrete was revibrated using external vibration. 4 by 4 inch cubes were consolidated and revibrated in a similar manner. Revibration at 3 hours produced a maximum reduction in bond of 33 percent and caused a 16 percent reduction in the concrete compressive strength. Revibration at 30 minutes and 1 hour reduced bond strengths by 6 and 9 percent, respectively, while the reconsolidation caused a decrease in compressive strength of 14 percent in both cases. It is of interest to note that the reduction in compressive strength noted by Larnach contradicts trends shown more recently by Vollick (36). Internal vibration was used in Vollick's tests. Although Vollick provided detailed descriptions of the plastic concrete properties from his tests, Larnach did not. The contradictory trends are therefore difficult to explain.

Menzel (27) used deformed bars in the 18 inch deep molds used in his consolidation tests (Fig. 1.4). His tests indicated that neither over-vibration nor revibration after one hour had adverse effects on the bottom-cast bars in each mold. However, over-vibration increased bond strength slightly for top-cast bars, while revibration reduced bond strength by over 28 percent. 2 inch slump concrete was used. Over-vibrated specimens were described as being vibrated "about 25 percent longer than necessary". It should be noted that this is the only study of the effects of revibration on bond strength that used both internal vibration and deformed bars.

Prior to the current work, the effects of two-course construction on concrete-steel bond have not been explicitly investigated. However. the controlling factors in settlement cracking have been studied, and the bond in top-cast reinforcement (reinforcement with less than 3 inches top cover) has been investigated.

Dakhil, Cady, and Carrier (16) found that the incidence of longitudinal settlement cracks formed above top reinforcement tends to increase with increases in slump and bar size and with decreases in top cover (Fig. 1.6). Specimens made in the above study were consolidated by internal vibration. Menzel (27) noted settlement cracks above top-cast, one inch diameter bars with a 2 inch cover in specimens placed with 6 inch slump, hand rodded concrete. Cracks were not noted. however, in specimens placed with 3 inch slump, internally vibrated concrete.

There have been individual investigations studying the bond in top-cast reinforcement as a function of one or more of the following parameters:

1) The depth of the concrete member.

2) The concrete sedimentation properties (settlement and bleed).

3) The minimum cover.

4) The concrete slump.

Although the ACI Building Code (4) and the AASHTO Bridge Specifications (1) currently require a 40 percent increase in bonded length for horizontally cast bars with 12 inches or more concrete below them, there has been only one investigation, by Menzel (27), which has studied the effects of the depth of concrete below the steel alone. Many investigations have compared the bond strength of top-cast reinforcement with that of bottom-cast bars. Top-cast bars normally display lower bond strengths than bars cast lower in the same or similar specimens (12, 13. 14, 19, 20, 28, 31, 35). This type of comparison is useful, but it includes the effects of depth of concrete above the bottom bars and low top covers (including the effects of settlement cracking), as well as depth of concrete below the top-cast bars.

Menzel's work showed that top-cast deformed bar bond strength decreases as the specimen depth increases (24). This change was quite pronounced as the height of the top bar was increased from 2-1/8 inches to 33-1/8 inches using 5 to 6 inch slump, hand-rodded concrete. For example, the maximum steel stress at splitting was 72000 psi for 2-1/8 inches of concrete below the bar, but only 40000 psi for 33-1/8 inches. Decreasing the slump of hand rodded concrete to 2 to 3 inches reduced the rate of decrease in bond strength as the depth of concrete below the bar increased. The smallest "top bar effect", however. was achieved using 2 to 3 inch slump, internally vibrated concrete. With stiff, well consolidated concrete, the maximum load developed by a bar cast with 33-1/8 inches of concrete below it was over 90 percent of the bond strength of a bar with 2-1/8 inches of concrete below it, while a bar cast with 15-1/8 inches of concrete below it had the same strength.

In the same study, Menzel made direct settlement measurements, which indicated that bond decreased with increased settlement. Welch and Patten (38) confirmed this work by showing that increased settlement tended to decrease bond in both top and bottom-cast bars. The top-cast bars in these tests had 8-5/8 inches of concrete below them and a 2-5/8 inch top cover. Slumps were between 2-1/2 and 4 inches. Both settlement and bleed were measured for each specimen. Most specimens with deformed bars were internally vibrated, but the authors noted no difference in behavior between specimens consolidated by vibration and those consolidated by hand rodding. Settlements measured on the pullout specimens with deformed bars were between 0.15 and 0.62 percent of the total specimen height. Bleed test results for the specimens were not published, and no trends were shown between bleed and bond.

The Commissie Voor Uitvoering Van Research Ingesteld door de Betonvereniging in the Netherlands (CUR) conducted tests in 1963 (15) using the cantilever beam pullout type specimen shown in Fig. 1.7. Among other trends noted, it was determined that an increase in the cover tends to increase the ratio of top-cast bar strength to bottom-cast bar strength. The top-cast bar/bottom-cast bar ratio is shown in Fig. 1.8

as a function of cover for "Hi-Bond" bars from the CUR tests. The embedment lengths for the data points shown were 140, 265, and 350mm for the 10, 18, and 26mm bars, respectively.

Beam tests conducted by Ferguson and Thompson (19) illustrate the effects of both slump and cover on the ratio of top-cast bar bond strength to bottom-cast bar bond strength. Ferguson and Thompson noted that the bond strength for top-cast #11 bars decreased between 3 and 13 percent as the slump was increased from one to three inches. Although it was not noted by Ferguson and Thompson, their test data also show the same trends with respect to cover as those found by the CUR. The depth of concrete below the test bars in these tests varied as the top cover was varied; however, it was approximately 12 inches for all tests. A plot of the relative bond efficiency of top-cast bars compared to bottom-cast bars as a function of top cover (Fig. 1.9) confirms the trend noted by the CUR.

Zekany, Neumann, Jirsa, and Breen (39) conducted tests using beams with both top-cast and bottom-cast splices. All beams used were 16 inches high and had 2 inch top and bottom covers. The ratio of top-cast splice strength to bottom-cast splice strength was found to decrease as slump was increased from 3-1/2 to 10-1/2 inches. Also, for both top and bottom bars, bond tended to decrease with increasing slump. This effect was more pronounced, however, for the top-cast bars.

Luke, Hammad, Jirsa and Breen (25) used 72 inch deep wall specimens in their investigation of the influence of casting position on development and splice length (Fig. 1.10). Their data (Fig. 1.11) show that the top-cast bars were significantly affected by the concrete slump.

Top-cast #9 and #7 bars developed normalized stresses of 31 and 40 ksi when placed with 3 inch slump concrete, but developed only 18.5 and 19.1 ksi, respectively, when placed with 8-1/2 inch slump concrete. These were 40 and 52 percent decreases in bond caused primarily by an increase in slump. The researchers also noted that settlement cracks formed above the top-cast bars in the high slump test specimen, but not in the low slump specimen.

Although the effect of slump was noted in other test bars within the same specimens, it was most pronounced for the top-cast bars. In fact, the normalized stresses for test bars cast below the specimen mid-height were approximately the same in the high slump specimen as in the low slump specimen.

1.4 Empirical Bond Relationships

Experimental bond test results have historically been used in the derivation of design relationships. The current ACI Building Code (4) and AASHTO Bridge Specifications (1) limit ultimate bond stresses in reinforcement by setting development length requirements. However, the relationships used for the development length requirements are based on the ultimate bond stresses specified in the 1963 ACI Building Code (3). These stresses, in turn, are based on tests at the University of Texas (20) and the Bureau of Standards (26) which indicate that the ultimate average bond force per unit length, U, (in pounds per inch) is

$$U = 35\sqrt{f'_c} \qquad (1.1)$$

in which f'_c is the concrete compressive strength. The total bond force will then be

$$T = 35L\sqrt{f'_c} \tag{1.2}$$

in which L = the embedment length.

The 1977 ACI Building Code (4) and AASHTO Bridge Specifications (1) basic development length requirements are based on the force necessary to develop 125 percent of the yield strength. Incorporation of this factor and rounding results in an ultimate bond force (in pounds) of

$$T_a = 25L\sqrt{f'_c} \tag{1.3}$$

which is the total force developed by a bar of embedment length L, in inches.

A limiting bond stress of 800 psi was also introduced in the 1963 ACI Building Code (3) requirements. Conversion of this into an equivalent bond force, application of the factor of 1.25, and rounding results in a limiting bond force (in pounds) of

$$T_a = 625\pi Ld \tag{1.4}$$

This requirement has also been retained by ACI (4) and AASHTO (1) for #11 bars and smaller.

Untrauer (34) pointed out that bars with small covers (less than 1-1/4 inch) tend to have bond strengths less than the 1963 ACI Building Code (3) bond strengths. This was found using data obtained primarily from top-cast bar tests.

One of the more recent bond relationships was developed by Jimenez, White, and Gergely at Cornell (22). The Jimenez bond equation is based on the assumption that the predominant failure mode is longitudinal splitting along the bar. Using a regression analysis applied to 174 development and splice length tests, and assuming that concrete tensile strength is given by $7.5(f'_c)^{\frac{1}{2}}$, the axial force (in kips) at which splitting failure occurs is:

$$T_j = \frac{dLc\sqrt{f'_c}}{(35.4d+0.573L)} \qquad (1.5)$$

in which c = the minimum concrete cover, and d = the bar diameter, both in inches.

This relationship tends to provide very conservative values for bars with covers less than 1/2 the bar diameter. For covers greater than the bar diameter, it tends to produce better results. The maximum cover to bar diameter ratio used in the analysis was 2.21.

Another recently derived bond relationship was developed by Morita and Fujii (29). This relationship has been shown to provide excellent correlations between calculated and measured bond stresses from several sources.

Three separate failure modes are considered in the Morita relationship: A horizontal split between closely spaced reinforcement, a corner split, and a "V-notch" type split. The V-notch failure is assumed to occur when reinforcing bars are placed at wide spacings with relatively small covers. The axial load (in kips) at which failure will occur in the V-notch mode is:

$$T_m = dL[0.0126c/d+0.0114]\sqrt{f'_c} \tag{1.6}$$

1.5 <u>Object and Scope</u>

The effects of consolidation method and two-course construction on concrete-steel bond strength in bridge decks are studied as functions of slump, bleed, and depth of slab. Bond strength and concrete density obtained with high density consolidation (insertions at one foot centers) are compared with the values obtained with low density consolidation (vibrator insertions at 2 foot centers). The bond strength with two-course top cover is compared with the bond strength obtained with monolithic top cover. Bond strengths obtained with small first-course covers (before overlay placement) are also studied.

The study used eighteen 4 by 8 foot deck specimens, with 8 inches of concrete below the top reinforcement. and six-3 by 4 foot deck specimens, with 24 inches of concrete below the top reinforcement. Four top covers were studied: 3/4, 1, and 3 inch monolithic top covers and 3 inch two-course top covers. #5 and #8 bars were used. A total of 117 bars were tested.

All bond tests utilized modified cantilever beam specimens. During each test. load, loaded end slip, and unloaded end slip were monitored and recorded. Concrete densities were obtained using core samples.

Test results are plotted and analyzed. Bond values obtained from the tests are compared with values obtained from other tests in this series and with empirical relationships developed by other researchers. Recommendations are made for bridge deck design and construction.

Chapter 2

Experimental Investigation

2.1 General

To study the effects of consolidation method and top cover on bond in concrete bridge decks, the specimen designs,placement procedures, and test procedures were selected to reflect actual deck thicknesses, placement procedures, and loading. Consolidation with multiple vibrators was a requirement. Also, it was important to select a bond test procedure that would place realistic loads on the reinforcement and the concrete.

Consolidation using multiple vibrators requires specimens with large plan areas. Large areas provide room for the vibrators and reduce the settlement restriction imposed by the sides of small forms. They also provide room for multiple test bars within a single specimen and similar concrete for bars with different top covers.

In order to make valid comparisons of bond strengths, both the reinforcement and the surrounding concrete should be placed in tension, as they would be in an actual structure. Modified cantilever beam specimens were selected since they provide realistic loading of the reinforcement, while allowing multiple test bars in each specimen.

2.2 Test Specimens

Two types of test specimen were used. Shallow slabs (those with 8 inches of concrete below the steel) were 4 feet by 8 feet in plan (Fig. 2.1). As many as three top covers were used on a specimen. One third of each slab had a 3 inch top cover. The remaining two thirds of the specimen were placed with a 3/4 inch top cover, one-half of which was, on 11 slabs, eventually covered with a 2-1/4 inch overlay. In order to maintain a constant 8 inch depth below the reinforcement, the bottom of the form was stepped down 2-1/4 inches in the third of the form containing the 3 inch monolithic cover. Twelve dummy deformed bars (not tested) were installed in the form to allow aggregate bridging, which tends to restrict settlement.

Deep slabs (24 inches of concrete below the steel) were 3 feet by 4 feet in plan (Fig. 2.2). The reduced plan area was required because of weight restrictions imposed by the available lifting capacity. Each specimen had one cover type--3/4, 1, or 3 inch monolithic or 3 inch two-course--and contained 2 test bars and 4 dummy bars.

Test specimens were constructed using timber forms. 3/4 inch A-B plywood was used as form sheathing for the shallow forms, while 3/4 inch B-B Plyform was used for the deep forms. The sheathing was protected using 3 coats of polyurethane clear gloss finish.

Form sides were butted against the form bases and held in position using double 2 x 4 wales. Wales were connected with ties at each corner and, on the shallow forms, transverse ties at the third points. Ties consisted of 1/4 inch diameter all-thread rod.

The shallow slabs were reinforced with a bottom layer of #5 bars on one foot centers, supported by 1-1/2 inch chairs. The deep slabs were reinforced with 4x4-3/4 - D16 x D16 welded wire fabric, supported on 4 inch chairs. Lifting inserts were installed at each corner of the slabs to allow the specimens to be transported. The inserts projected out of the ends of the specimens, so as not to interfere with the slab finishing operations.

Test bars and dummy bars were supported at holes drilled through the side forms. Bonded lengths of the test bars were limited by bond-breaking collars fabricated from polyvinyl chloride (PVC) pipe, with an inside diameter just large enough to accommodate the test bar (Fig. 2.3). Steel pipe was butted against the unloaded end of the test bar and coupled to the bar using a second piece of PVC pipe. The steel pipe had the same outside diameter as the test bar. Its purpose was to permit access to the the test bar to obtain unloaded end slip measurements. Couplings and bond-breakers were sealed against mortar seepage using Dow Corning Silicone Seal. Silicone Seal was applied between the PVC and the test bar and allowed to cure before concrete placement.

Test bars extended 22 inches from the faces of the test specimens. These bars were held in place during concrete placement by supports constructed from 2x4 dimension lumber and plywood. The supports were installed 12 inches from the form sides and connected to the forms using plywood, on the shallow forms, or 2x4 braces, on the deep forms.

2.3 Test Bar Embedment Length

Initial embedment lengths used in the study were selected based on the empirical bond relationship developed by Jimenez et al. (22), Eq. 1.4, using a steel stress of 60 ksi, a cover of 3 inches, and a concrete strength of 3000 psi. It was found in the early tests that it would be difficult to limit the concrete strength to 3000 psi and that the initial embedments would have to be adjusted to prevent yielding of the test bars with 3 inch covers. Bars with 3/4 inch covers were, however, found to pull out at loads far below yield. The embedment lengths were therefore increased for bars with a 3/4 inch cover on some placements.

Table 2.1 shows the embedment lengths used for each test bar. The cover type and consolidation method are also listed for each bar. Bars are numbered in order of pullout. Slabs and slab groups are numbered in order of placement.

2.4 Materials

2.4.1 Concrete

The concrete used in all first course placements was supplied by a local ready-mix concrete plant. Type I Portland cement and 3/4 inch nominal maximum size coarse aggregate (locally described as 1/2 inch rock) were used. The coarse aggregate was crushed limestone, and the fine aggregate was Kansas River sand. Aggregate properties are listed in Table 2.2.

Overlay concrete was prepared in the laboratory using Type I cement, Kansas River sand, and 3/4 inch maximum size coarse aggregate. The coarse aggregate for the overlays was obtained by removing all material retained on a 3/4 inch sieve from crushed limestone obtained from the same ready mix plant which provided the concrete for the first course placements. Mix designs for the first and second course concretes in each Slab Group are shown in Table 2.2.

Concrete properties were tested in accordance with ASTM procedures. Compressive strength specimens were prepared in accordance with ASTM C 31 (6), and concrete slump was measured per ASTM C 143 (7). Air content was measured using a volumetric air meter (Rollameter) per ASTM C 173 (8). All first-course concrete was tested for bleeding using the standard bleed test per ASTM C 232 (9). Concrete properties for each Slab Group are shown in Table 2.3.

2.4.2 Steel

ASTM A 615 Grade 60 reinforcing bars were used for all tests. Stress-strain curves for the two bar sizes are shown in Fig. 2.4. The deformation patterns for both sizes are shown in Fig. 2.5, and deformation dimensions and bearing areas are shown in Table 2.4.

Deformation data were obtained per ASTM A 615 (5). Deformation bearing areas were calculated using rib heights measured at three points along each rib and bar diameters measured at two locations. Rib heights were measured at the locations specified in ASTM A 615 (5). Bar diameters (between ribs) were measured at the rib origins and at 90 degrees to the gap between the rib origins.

2.5 Placement

Specimen placement was an important portion of the study. Construction procedures were selected to be as consistent as possible within and between individual slab groups.

The first course concrete was placed in the forms using a one cubic yard bucket and an overhead crane. Shallow forms were filled in one lift, and deep forms were filled in two lifts (each lift was vibrated equally). Forms were filled with a one inch surcharge to allow for settlement during consolidation.

Because construction procedures were being compared within each slab group, it was important that the concrete within each group be consistent. Placement procedures for the first two slab groups were found to be inadequate and were therefore modified.

Slab Groups 1 and 2 were placed by completely filling each form in turn. Slab bleed tests indicated that the first concrete out of the truck bled more than the rest of the batch. To provide greater uniformity in later placements. a portion of each bucket of concrete was placed in each form.

In the first two placements, consolidation was started as soon as the first form was filled. For the remaining placements, the filled forms were allowed to rest for ten minutes before vibration was started. Consolidation was obtained using 1-7/8 inch diameter Allen Engineering Corporation Model AV1 pneumatic vibrators. Vibrators were rated at 11,500 vibrations per minute at 90 psi air pressure. Vibrator amplitude was 0.04 inch. High density vibration was obtained using either one or two vibrators inserted at one foot centers. Low density vibration was achieved using a single vibrator inserted at two foot centers. With the exception of Group 6, low density consolidation slabs were vibrated one foot from each form side. The low density slab from Group 6 was vibrated at the slab centerline only. Vibrator patterns used for all shallow slabs are shown in Fig. 2.6. The vibrator pattern used for all deep slabs is shown in Fig. 2.7. Vibrators were inserted rapidly, held in place for 10 seconds in most slabs, and withdrawn slowly. The low density vibration slab from Group 7 was vibrated until the surface began to glisten (approximately 7 seconds). Indexing marks on both the vibrator frame and the formwork were used to insure correct vibrator positioning. Consolidation of a slab is shown in Fig. 2.8.

Slabs were hand screeded using a metal-edged screed. Two passes were made, with screed travel perpendicular to the top reinforcement in each pass.

Immediately upon completion of screeding, the specimens were floated using a magnesium bull float. Bleed and settlement tests were then started.

Special bleed tests for the slabs used preweighed, 5-1/2 inch square paper towels (from the same lot). The towels were placed on the surface of the concrete and covered with a glass plate to prevent evaporation (Fig. 2.9). When fully saturated, the towels were replaced. The time on the surface was recorded for each pad. This provided data on the amount of bleed water reaching the slab surface as a function of the time after finishing. The tests were not soley a measure of bleed, because it was clear that the pads drew water from the slab surface. Since this occurred on all specimens, however, it was considered to be a constant. Bleed testing was conducted at both ends of the shallow specimens and one end of the deep specimens.

Settlement tests used linear variable differential transformers (LVDT's). Two inch square balsa wood pads were placed on the concrete surface, and an LVDT core rod was allowed to bear on the center of each pad, as shown in Fig. 2.9. LVDT outputs were recorded by a Hewlett-Packard data acquisition system at 30 second intervals.

Bleed and settlement tests continued for a minimum of 2 hours after finishing. Following the tests, the slabs were covered with 4 mil polyethylene until a strength of 3000 psi was attained. The polyethylene sheet was then removed, and the forms were stripped.

At this point some of the slabs were overlaid. The first step in overlay application was waterblasting the surface of the slabs. Surfaces were blasted until all traces of laitence and carbonation were removed. The surfaces were allowed to dry for two hours, and a 50 percent sand-50 percent cement (by weight) grout was applied using a stiff brush. The water-cement ratios for the grout varied but were approximately the same as used for the overlay concrete for each group. For Group 8, a water reducing agent was added to the grout to compensate for a lowered water-cement ratio. In all cases, the grout was the consistency of thick cream.

Overlays for the first 7 slab groups had water-cement ratios of 0.44 and cement contents of 600 pounds/cubic yard. The Group 8 overlay had a water cement ratio of 0.35 and a cement content of 835 pounds/cubic yard. Group 7 and 8 overlays were mixed with Gifford-Hill PSI-Super high-range water-reducer to improve workability. Overlay concrete was mixed in the laboratory in 0.07 cubic yard batches. Overlay concrete was placed on the wet grout and consolidated using a 12HD

Razorback pneumatic vibratory screed manufactured by Allen Engineering Corporation (Fig. 2.10). The screed rode on 2-1/4 inch high forms. The overlays were then hand floated using a magnesium float to remove local imperfections. Polyethylene sheets were applied to the surface immediately after floating. Overlays were allowed to cure until a strength of 4000 psi was attained or until the overlay strength was as high as the first-course strength (one exception to this practice was Group 6, where the overlay strength was only 2600 psi at the time of the pullout tests). Curing material was removed at least 5 hours before pullout tests were started.

2.6 Test Apparatus

The pullout apparatus shown in Fig. 2.11 was used for the bond tests. The machine was designed so that the test bar could be loaded in tension without placing the surrounding concrete in compression. Although the machine was designed for multiple bar pullout (a maximum of three #11 bars), it was used only for single bar pullout in this study.

In the single bar mode, the load was provided by two-60 ton hollow-core rams powered by an Amsler hydraulic testing machine. Load was transferred through two 1 inch diameter cold-rolled steel load rods. Each load rod was instrumented with two longitudinal and two transverse 350 ohm strain gages. Load was transferred through rockers to two 2 inch by 5 inch cold-rolled steel plates, which transferred load through a single rocker and wedge grip assembly to the test bar.

The test machine was tied to the structural floor using two wide flange beams and two tension rods which extended through the structural floor. The test slab was tied down in a similar manner, as shown in Fig. 2.11.

Test bars were instrumented at both the loaded and unloaded ends. At the loaded end, two LVDT's were attached to the test bar, 1-1/4 inches from the exterior face of the concrete. Because each bar was placed with a bond breaker at the vertical face, the distance from the LVDT attachment to the actual loaded end of the bar was 5 inches. Measurements taken by the LVDT's therfore included deformation of the bar between the two points. A single LVDT was mounted on the projecting end of the steel pipe embedded behind the test bar. All LVDT core rods were spring loaded so that movement of the bar would cause movement of the core.

2.7 Pullout Tests

Each slab group was tested during a 24 hour period at ages ranging from 6 to 43 days. 6 inch x 12 inch compression test cylinders were tested at the time of the bond tests to determine the slab and overlay strengths.

The two load cells and three LVDT's were monitored using a Hewlett-Packard data aquisition system. Bars were loaded at approximately 3.0 kips per minute. Load and loaded end slip were plotted as the tests progressed. During the first half of each test, the load was monitored at 10 second intervals. As the bar reached ultimate, the sample interval was reduced to 5 seconds.

2.8 Core Tests

Four inch diameter core samples were taken from Groups 6 and 7. Samples were taken from the locations shown in Fig. 2.12. Core density and void percentage were determined using ASTM C 642 (10) procedures with the following exceptions: Dry weights were obtained using air dried specimens rather than oven dried specimens. Saturated weights after immersion were used in place of saturated weights after boiling.

2.9 Test Results

2.9.1 Plastic Concrete

Bleed results for each slab are presented in Figs. 2.13-2.20. All bleed plots are referenced to the completion of the finishing operation for each slab. Total bleed values at two hours are listed in Table 2.5.

The bleed results were significantly affected by the method of distribution of concrete among the forms. Because the concrete used was transit mixed in a tilted mixer, some segregation occurred and the initial discharge from the truck contained a higher percentage of mix water than the later portions of the batch. The first form filled in Slab Groups 1 and 2 displayed more bleeding than forms filled later. Group 3 also had one slab that had much higher bleed than the others in the placement. Although some concrete from each bucket was placed in each form during this placement, most of the first bucket out of the truck was inadvertently placed in Slab 3a (Fig. 2.15).

With the exception of Groups 1, 2, and 3, bleed varied only slightly between individual slabs in a given group. For most of the slab groups, bleeding was initially rapid but slowed substantially after 90 minutes.

The small range of the LVDT's used in the measurement of slab settlement (0.2 inches) made it difficult to place the LVDT's within range on the plastic concrete. A number of LVDT outputs indicated that the core was out of range and that the output was therefore not valid. The valid settlements recorded at 2 hours for all slabs are listed in Table 2.5. An example of a valid settlement versus time curve is shown in Fig. 2.21.

Settlements were small for all slab groups and depths. At 2 hours, the maximum total settlement recorded was only 0.012 inches (Slab 8b). The lowest settlement , 0.003 inches, was recorded for the slab group with 10 percent air content (Group 6). It was observed during this placement that the slab surface swelled after screeding.

2.9.2 Hardened Concrete

Settlement cracking above the test bars was noted in 4 slab groups. Cracks were noted above bars with 3/4 inch cover in Slab Groups 2, 4, 5, and 6. Group 2 contained #8 bars and was placed with 8-1/2 inch slump concrete. The other three groups contained #5 bars.

Load versus loaded end slip and load versus unloaded end slip curves are presented in Figs. 2.22-2.44. Each load-slip curve is labeled with the test bar number. Bar numbers are listed in Table 2.1, with the cover and consolidation method used for each. Concrete strengths for each slab group are shown in Table 2.3. Ultimate pullout forces are summarized in Chapter 3.

For both bar sizes tested, the behavior and failure mode in the pullout tests were dependent upon the cover. All failures could be described as splitting type failures, except those for #5 bars with 3 inches total cover, which rarely displayed any cracking.

#8 bars with 3/4 inch cover initially displayed longitudinal cracks above the steel. These cracks started at the vertical slab face (above the PVC bond breaker) and advanced toward the unloaded end of the test bar. As this longitudinal crack advanced, the crack growth rate increased, and transverse cracking appeared. As the ultimate load was attained, the crack width increased and the top cover spalled away from the bar. The spalling was accompanied by a rapid drop-off in load. Ultimate loads were attained at relatively low unloaded end slips as compared to those for bars with 3 inch covers (Fig. 2.22). After failure, vertical cracks were sometimes noted below the #8 test bars at the slab face.

#8 bars with 3 inch cover displayed the same initial cracking behavior as the bars with 3/4 inch cover; cracks advanced from the loaded to the unloaded end of the bar. When the crack had advanced to the unloaded end of the bar, transverse cracking was observed. In many cases, longitudinal cracks progressed beyond the slab centerline. After ultimate, the load did not fall off rapidly for the #8 bars with 3 inch cover. Instead, the load remained close to the ultimate, even at high unloaded end slips. For example, Fig. 2.24 shows that bars with 3 inch cover sustained high loads even at unloaded end slips above 0.035

inches. At the completion of the tests, a crack was observed below the bar in almost every case. This crack extended to the bottom of the shallow slabs and approximately 2/3 of the distance to the bottom of the deep slabs. Typical crack patterns for #8 bars are illustrated in Fig. 2.45.

#5 bars with 3/4 inch cover displayed longitudinal cracking and some transverse cracking. The load remained near ultimate, even at high unloaded end slips, and there was no rapid drop in load (Fig. 2.31). No spalling occurred.

#5 bars with 3 inch cover displayed little, if any, cracking. Bond failure was apparently caused by shearing of the concrete between the lugs. Again, the load did not fall off rapidly at the ultimate load (Fig. 2.34).

All bars displayed significant loaded end slip before unloaded end slip was noted. This was partially the result of elastic deformation of the test bar over the 5 inch distance from the LVDT attachment to the bonded portion of the bar. Before failure, however, the unloaded end slip increased at approximately the same rate as the loaded end slip. Bars with 3/4 inch cover failed at lower loads than bars with 3 inch cover, and bars with two-course cover normally failed at loads between the failure loads for the bars with 3/4 and 3 inch monolithic covers.

The pullout data for #8 bars with 3 inch cover (both two-course and monolithic) indicate that the second bar pulled usually reached the maximum load at a lower slip than the first bar. The second bar also displayed a lower ultimate load. This was probably caused by the longitudinal crack which crossed the slab centerline on some tests.

Core samples from high density consolidation slabs had higher densities and lower void percentages than those from slabs consolidated using low density consolidation. Table 2.6 presents the apparent specific gravities and void percentages obtained from Group 6 and 7 shallow slabs. These results indicate that density was increased by 4 and 2 percent, and void percentages were reduced by 3 and 5 percent, respectively, when high density consolidation was used.

Chapter 3

Evaluation and Discussion of Results

3.1 General

The test results described in Chapter 2 are used to examine the effects of consolidation method and cover type on concrete-steel bond strength and to compare bond values with those predicted by the 1977 ACI Code (4) and the 1977 AASHTO Specifications (1), by Jimenez et al. (22), and by Morita and Fujii (29). Results are also used to determine the effects of slump, bleed, and embedment length on concrete-steel bond. Core sample measurements are used determine the effects of consolidation method on concrete density.

3.2 Bond Forces

3.2.1 Ultimate Load

The ultimate loads are listed in Table 3.1 and represent the maximum recorded load for each test. Some bars yielded before reaching the ultimate load. In addition, longitudinal splitting cracks crossed the slab centerline for most #8 bars with 3 inch covers. Therefore, only the first #8 bar with 3 inch cover pulled from a slab was used in comparisons.

3.2.2 Unloaded End Slip Criteria

Since accurate ultimate loads could not be obtained for all bars, two other criteria for bond force comparisons were considered: a selected loaded end slip, and a selected unloaded end slip. The unloaded end slip was selected because the load obtained at a given loaded end slip is dependent upon local effects near the loaded end of the bar, while the load obtained at a given unloaded end slip is more dependent on the bond over the entire bonded length. There is also some question as to where the actual "loaded end" is located.

Bond forces were obtained at unloaded end slips of 0.010 inches and 0.005 inches for the #5 and #8 bars, respectively. These slip values occurred before the ultimate load was attained for all tests. In almost all tests, the forces corresponding to these slip values exceeded 60 percent of the ultimate bond force.

The recorded unloaded end slip was not always a smooth function of load. For some bars, such as bar 4 in Fig. 2.28, the end slip was initially negative. This was probably caused by the movement of the slab relative to the LVDT mounting. Other test bars, such as bar 55 in Fig. 2.36, displayed a sudden positive slip before a significant load developed. This could have been caused by improper seating of the LVDT core rod against the test bar.

The erratic behavior of the end slip for many test bars created the need for a correction of the data. To make the correction, a maximum load was selected at which zero slip would normally be expected (this was based on load-slip curves which showed a smooth transition throughout the loading). Loads of 1 and 10 kips were used for #5 and #8 bars, respectively, and any recorded slip at 1 or 10 kips was considered to be a shift in the data. The correction procedure is illustrated in Fig. 3.1.

Bond forces at 0.005 and 0.010 inch end slips are listed in Table 3.1. A few bars yielded before reaching these slip values.

3.3 Normalization of Data

Bond forces were converted to bond forces per unit length so that comparisons could be made between individual tests. The bond forces per unit length were normalized to a strength of 4000 psi and to embedment lengths of 10 inches and 3-1/2 inches for the #8 and #5 bars, respectively.

Strength normalization was accomplished using the assumption that bond strength is proportional to the tensile capacity of the concrete, which, in turn, is proportional to the square root of the compressive strength. Bond values were, therefore, multiplied by $\sqrt{4000/f'_c}$. This type of correction has been made by other researchers (20, 25, 35).

Length was normalized assuming that total bond strength is not directly proportional to the bonded length. Eq. 1.5, developed by Jimenez et al. (22), gives bond force as a nonlinear function of the bonded length and was used to determine normalized embedment lengths, which are presented in Table 3.2. Bond forces were divided by these normalized lengths. The normalized results are presented in Table 3.1.

3.4 Evaluation of Test Results

3.4.1 Effect of Consolidation Method

The results indicate that high density vibration improves bond strength in most cases and that the effectiveness of high density vibration is at least partially a funtion of concrete slump. In addition, the core density measurements indicate that high density vibration provides higher unit weights and lower void contents than does low density vibration.

The improvements in bond strength obtained with high density vibration are illustrated in Figs. 3.2 and 3.3 and Table 3.3 using "bond vibration efficiency ratios", i.e., the ratios of bond forces obtained with high density vibration to bond forces obtained with low density vibration. Comparisons are made for Slab Groups 2, 3, and 7, which all contained #8 bars. For each group, average bond forces for both consolidation methods were calculated, and these averages were used in the calculation of the efficiency ratios.

The efficiency ratios for bond forces determined at a 0.005 inch unloaded end slip are shown in Fig. 3.2, which includes all data from the three slab groups. Overall, high density vibration provided a higher bond force in 6 out of the 9 cases. An increase in the effectiveness of high density vibration with increasing slump is evident for bars with 3/4 and 3 inch covers. For bars with 3/4 inch cover, the efficiency ratios ranged from 0.96 to 1.11, with two-course cover, the ratios ranged from .95 to 1.08, and with 3 inch monolithic cover, the ratios ranged from 1.27 to 1.32.

Fig. 3.2 clearly shows that high density vibration provided greater benefit for bars with monolithic 3 inch cover than for bars with either 3/4 inch or two-course 3 inch covers. While high density consolidation does provide increased concrete density, the formation of settlement cracks in the thin top cover may dominate for bars with a 3/4 inch initial cover. These settlement cracks may allow early slip of the bars. Test bars with 3 inch initial top cover, therefore, would benefit more from improved consolidation than test bars with only 3/4 inch initial top cover.

Fig. 3.3 illustrates the effect of slump on the bond vibration efficiency ratios based on bond strength. Fig. 3.3 includes only the valid data for the first 3 inch cover bars pulled from each slab. The figure indicates increasing relative performance of high density vibration with increasing slump. The relative improvement provided by high density vibration is, however, much less at ultimate load than it is at slip of 0.005 inch, being approximately the same for all three covers. It is interesting to note that high density vibration provides the greatest improvement in bond in the high slump concrete, which should need the least amount of consolidation.

All three slabs in Group 1 were consolidated using high density vibration. Two slabs were vibrated using double vibrators inserted at one foot centers, and one slab was vibrated using a single vibrator inserted at one foot centers. For the 3/4 inch cover bars, the slab vibrated with a single vibrator had an average strength of 1.04 times that for the doubly vibrated slab (Note: due to problems discussed in Section 3.2.1, valid strengths were not obtained for bars in Group 1 with 3 inch cover). This may be an indication of a slight overvibration of the doubly vibrated slabs.

While considerable scatter exists, the results indicate that high density vibration also improved the bond strength for the #5 bars. Results for Groups 5 and 6 indicate that bond is improved by high density vibration, while the results for Group 4 indicate that the opposite is true. Figs. 3.4 and 3.5 illustrate the relative efficiencies of the two types of consolidation in improving bond strength at 0.010 inch end slip and at ultimate load, respectively. As shown in Fig. 3.4, Slab Groups 5 and 6, which had 2-3/4 and 4-1/2 inch slumps, respectively, had efficiency ratios ranging from 1.06 to 1.35 for all cover types. Slab Group 4, with a slump of 3 inches, however, had efficiency ratios ranging from 0.83 to 0.86. The higher bleed characteristics of the relatively stiff concrete used in Slab Group 4 may have had an effect (Table 3.4).

Within individual slab groups, the vibration density did not appear to affect the bleed or the settlement of the concrete. The bleed test results indicate that low density and high density consolidation produced the same bleed results for 3 out of the 4 groups used for comparison (Table 3.4). Settlement test results were too limited for comparison. If the settlement is expressed as a percentage of specimen depth, the maximum recorded settlement was 0.15 percent. This is the minimum settlement recorded by Welch and Patten (38). The settlements recorded in this study were therefore quite small. In effect, internal vibration provided low settlement in both the high and low density configurations.

3.4.2 Effect of Cover Thickness and Type

3.4.2.1 General

Almost without exception, bars with 3/4 inch cover had lower bond strengths than bars with 3 inch, two-course cover. Also, bars with 3 inch, two-course cover typically had lower unit bond strengths than bars with 3 inch, monolithic cover.

Figs. 3.6 and 3.7 show the variation in normalized bond forces per unit length at 0.005 inch end slip and ultimate, respectively, for #8 bars in shallow, high density vibration slabs as a function of slump and cover. Figs. 3.6 and 3.7 are limited to Groups 2, 3, and 8, which had similar concrete strengths and embedment lengths. Figs. 3.8 and 3.9 show similar results at ultimate for tests from all high density and low density vibration slabs, respectively. In every case, the bond forces for bars with 3 inch, two-course cover fall between those for bars with 3/4 inch cover and bars with 3 inch monolithic cover at both the end slip value and at the ultimate load.

Figs. 3.10 and 3.11 illustrate the test results at 0.010 inch end slip and ultimate, respectively, for #5 bars in high density vibration slabs. Although considerable overlap exists for the three cover types at 0.010 inch end slip, the bond strengths associated with the three cover types clearly separate at ultimate (Fig. 3.11).

3.4.2.2 Two-course versus Monolithic Cover

Fig. 3.12 illustrates the considerable variation in the bond strength of bars with two-course covers as compared with those of bars with monolithic covers. The ordinate in Fig. 3.12 is the ratio of the bond strengths for the two cover types, while the abscissa is the ratio of the overlay concrete strength to the first-course concrete strength. The majority of bars with two-course cover have lower bond strengths than those with monolithic cover. Even in the case where the strength of the overlay concrete is 1-1/2 times that of the first-course concrete, the bond strengths of the bars with two-course cover are only 92 percent of those of bars with monolithic cover.

Fig. 3.12 suggests that the bond strength achieved in two-course construction is a function of the strength of the overlay concrete. As the ratio of the overlay strength to the first-course strength increases, the bond strength for two-course construction approaches that for monolithic construction. This is true for both bar sizes tested, even though the failure modes differ for #5 and #8 bars.

The lower bond strengths of bars in two-course decks, compared with bars in monolithic decks (Figs. 3.6-3.12) probably result from a weakened first-course cover produced by settlement cracks above the reinforcement. Even though settlement cracks were not noted above most of the #8 test bars, they were noted above all of the #5 bars with 3/4 inch cover. The crack incidences reported by Dakhil et al. (16) indicate that the #8 bars should have had more cracking than the #5 bars. It is possible then, that although the cracks were too small to identify on the #8 bar test slabs, they were present and influenced the bars with two-course covers.

The finishing operation also had an effect on the concrete above bars with low cover. It has been observed that the coarse aggregate is worked away from the bar during the screeding operation. This would have affected the bond strength of bars with either the 3/4 inch cover or the 3 inch, two-course cover.

The results also strongly indicate that the concrete-steel bond strength achieved with two-course construction must be dependent upon the bond between the first and second courses. Delamination of the second course will reduce the bond strength to the bond strength obtained with a low first-course cover.

3.4.2.3 3/4 Inch versus 3 Inch Cover

The strengths of the bars with 3/4 inch cover were approximately 60 percent of those with 3 inch monolithic cover for both #5 and #8 bars (Fig. 3.13). The test results indicate that the variation of bond with changes in cover is not linear, as assumed by Jimenez (Eq. 1.5). The Jimenez equation was, however, developed from a data base in which the maximum cover to bar diameter ratio was 2.27. In this study, the maximum ratios were 3.0 for the #8 bars and 4.8 for the #5 bars. Jimenez also assumed a splitting failure. While this was the case for the #8 bars with 3 inch cover, the failure mode for the #5 bars with 3 inch cover was a direct pullout and does not fit Jimenez's requirement that failure is accompanied by longitudinal splitting. The effect of cover thickness does not appear to change markedly with concrete slump.

3.4.3 Effect of Slump

Although it was not originally an objective of this study, the results confirm earlier work (25, 27, 39) indicating that increased slump will reduce bond strength.

The effect of slump on bond strength can best be shown using the normalized bond forces from Groups 2, 3, and 8, which all had #8 bars with 10 inch embedment lengths and approximately 4000 psi concrete. Fig 3.6 shows the pullout values at an end slip of 0.005 inches for three slabs consolidated using high density vibration. All three cover types show a trend of decreasing bond with increasing slump (lines shown through the data points are least-squares fits). Ultimate strengths for the same slabs are plotted in Fig. 3.7. 3/4 inch cover bars no longer show a decrease in bond with slump. In fact, there is a slight increase. Bond strengths for bars with two-course bonded construction are below those for bars with 3 inch monolithic cover, and both continue to show a decrease in bond with an increase in slump. The decrease is approximately 2-1/2 percent per inch increase in slump.

It must be noted that Group 2 concrete, which had a slump of 8-1/2 inches, was vibrated immediately after being placed in the forms, while Groups 3 and 8, which provide the closest comparison in terms of bonded length and concrete strength, were vibrated after a 10 minute delay. Data obtained by Davis et al. (17) show that delayed vibration can provide improved bond over immediate vibration. The delays in the Davis study were 3 and 6 hours. Although 10 minutes is quite small compared with 3 hours, the delay for Group 3 and Group 8 placements might have been adequate to provide some of the improvement in bond over that obtained with Group 2. However, Fig. 3.8, which includes all valid ultimate bond values for all high density vibration slabs, confirms the trends evident in Fig. 3.7.

Data are too limited to reach any clear conclusions on the effect of slump for the low density vibration results illustrated in Fig. 3.9.

The data for #5 bars show no clear trends. Only a limited range of slump was available for the three test groups with #5 bars. There were also wide variations in both bonded lengths and concrete strengths, which may have been too great for the normalization procedure used. Any effects of slump have been overshadowed by these other factors (Figs. 3.10 and 3.11).

A definite correlation between bleed and slump exists for this series of tests (Fig. 3.14). The trends of decreased bond with increased slump could, therefore, be trends of decreased bond with increased bleed. Air contents ranged from 4-1/2 to 10 percent and are noted beside each data point in Fig. 3.14. For the range of air contents used, there is no apparent effect of air content on bleed.

3.4.4 Effect of Depth of Specimen

Both AASHTO (1) and ACI (4) require a 40 percent increase in embedment length for horizontally cast bars with more than 12 inches of concrete cast below them. These bars are classified as top bars. Using this definition, all test bars cast with 24 inches of concrete below them would be expected to have significantly lower bond strengths than bars cast with 8 inches of concrete below them. This was not found to be the case.

The ratios of deep specimen bond strength to shallow specimen bond strength were calculated for the valid tests in Groups 7 and 8. The results are shown in Table 3.5. The bond strengths are very close, with the exception of those in Group 7, which actually indicate a higher bond strength with the deep specimen.

Menzel's tests (27) indicated that even for low slump, highly consolidated concrete, the depth of concrete below the top reinforcement should have at least some affect on bond. Menzel's specimens were, however, prepared so that they were the same size at the time of testing. It is possible, then, that there is a geometry effect on the bond results in the current study.

The vertical crack that was observed below the #8 test bars often extended to the bottom of the shallow slabs. While the vertical cracks did not extend to the bottom of the deep slabs, they did grow to more than 8 inches in length. Therefore, test bars in deep slabs actually cracked more concrete than bars in shallow slabs. The additional energy required to crack the deep slabs may have been reflected in the high bond strengths for deep specimens. This fact does not reduce the validity of the results, since, in practice, deeper bridge decks will have more concrete available to crack.

The current work indicates an approximate decrease in bond strength of 2-1/2 percent per inch increase in slump for top-cast bars with 8 inches of concrete cast below them (Fig. 3.7). Other research indicates a decrease in bond strength of 8-1/3 percent per inch increase in slump for top-cast bars with 70 inches of concrete below them (25). This difference indicates that the effect of slump may be more pronounced as the specimen depth is increased. Also, this comparison strongly suggests that the effect of the concrete depth below a bar will be more pronounced as the slump is increased. This observation seems reasonable, since higher slump concretes will exhibit increased settlement and increased bleed, both of which are expected to reduce bond strength.

3.4.5 Effect of Bonded Length

A limited comparison can be made of bond force per unit length versus bonded length. Fig. 3.15 shows normalized bond strengths for #8 bars with 3/4 inch cover at ultimate load. Fig. 3.16 shows normalized bond forces for #5 bars with 3/4 inch cover at 0.010 inch unloaded end slip. Both high and low density consolidation tests are included. As has been shown in earlier work (19, 20), the bond force per unit length tends to decrease with increasing embedment length.

3.5 Comparisons With Empirical Bond Equations

Ideally, the ACI (4) and AASHTO (1) bond requirements should be conservative when compared with experimental data. This was not found to be the case for all tests. Empirically derived bond equations, such as Eq. 1.5 and 1.6, must reflect the data used in their derivations. They would, therefore, be expected to have good correlation with similar data.

For ACI and AASHTO comparisons, the bond force is calculated using either Eq. 1.3 or 1.4. For #8 bars, the minimum bond force is found using Eq. 1.3, while for #5 bars, the minimum bond force is found using Eq. 1.4. Both the ACI Code (4) and the AASHTO Specifications (1) allow a 20 percent reduction in development length (equivalent to a 25 percent increase in bond strength) for bars with a lateral spacing of at least 6 inches. This factor was applied in the comparisons that follow.

Fig. 3.17 illustrates the ratios of test loads to ACI and AASHTO loads for #5 and #8 bars with 3/4 inch and 3 inch monolithic covers. The ACI and AASHTO requirements were found to be conservative for bars with 3 inch covers with both bar sizes. While #8 bars with 3 inch cover were found to have very conservative Code values (the lowest test load to code load ratio was 2.23), neither the #8 bars with 3/4 inch cover nor the #5 bars had overly conservative values. One #5 bar with 3/4 inch cover from Group 4 fell below the load calulated using Eq. 1.4. Two other #5 bars had loads within 6 percent of the calculated load. One #8 bar with 3/4 inch cover from Group 7 was within 4 percent of the load calculated using Eq. 1.3. Test bars from Group 4 were #5 bars with 5 inch embedments and a concrete strength of 3570 psi. Test bars from Group 7 were #8 bars with 15 inch embedments and a concrete strength of 4970 psi. The lack of conservatism for low cover, top-cast bars agrees with earlier observations made with respect to the 1963 ACI Building Code (34).

The ratios of test loads for bars with two-course cover to ACI and AASHTO loads are shown as functions of first-course concrete strength in Fig. 3.18. The ACI and AASHTO loads are conservative for both bar sizes. The minimum test load to calculated load ratio was 1.43 for a #5 bar from Group 6.

The Jimenez bond relationship, Eq. 1.5, was found to be conservative for 3/4 inch covers, but not conservative for 3 inch covers (Fig. 3.19). The lack of conservatism in the Jimenez relationship for 3 inch covers is probably caused by the shift from a splitting type failure to a direct pullout for the #5 bars. The basic Jimenez relationship was developed using an assumed splitting failure, and empirical test results used to evaluate the constants in the basic relationship were all from splitting type failures. The failure mode of #5 bars with 3 inch total cover (direct pullout) therefore excludes them from valid comparison with the relationship. It is interesting to note, however, that test loads for #8 bars with 3 inch cover show good aggreement the Jimenez relationship. #8 bars with 3 inch cover did fail in a splitting type mode.

The bond relationship developed by Morita and Fujii, Eq. 1.6, also was found to be conservative for bars with 3/4 inch covers, but produced better results for bars with 3 inch covers and somewhat better results overall than the Jimenez relationship (Fig. 3.20). This relationship was, however, derived using a wider data base than the Jimenez relationship.

3.6 Recommendations

The construction procedures currently in use for concrete bridge decks were implemented primarily to improve the deck quality and to prolong the deck life. However, the procedures also have both positive and negative effects on the concrete-steel bond.

The use of high density internal vibration results in improved bond over low density consolidation in most cases. The procedure reduces the percentage of voids in the concrete and can provide reduced permeability when compared with low density consolidation (11). Continued use of the procedure is recommended.

The continued use of low slump concrete (maximum 2-1/2 inches) for the first course is also recommended. The detrimental effect of increased slump on bond is significant. The use of thorough consolidation with relatively low slump concrete is an effective method of providing improved bond, especially in top-cast reinforcement.

In most cases, two-course construction results in lower bond strengths than monolithic construction. Although the bond strengths achieved with 2-course construction are conservative as compared with ACI and AASHTO requirements, the data are based on tests using high-strength, well-bonded overlays. Low strength, or poorly bonded overlays will lead to much lower bond strengths. The current work indicates that bond strengths for reinforcement with only 3/4 inch cover can be less than the current ACI (4) or AASHTO (1) requirements. This is not only a problem during the construction phase of a deck, but it can also be a problem during the service phase, if delamination of the overlay occurs. Continued use of two-course bonded deck construction is only warranted if it can be shown that high-strength, well bonded overlays are used and that the procedure results in more corrosion protection than 3 inch monolithic cover.

Longitudinal settlement cracking, longitudinal depressions, and aggregate tears in the concrete have been noted above the top reinforcement in first-course placements. All of these can be detrimental not only to the concrete-steel bond strength, but to the durability of the deck as well. Longitudinal settlement cracking has been shown to be a function of top cover (16). Longitudinal depressions and aggregate tearing are brought about in the finishing operation and are probably both caused by the combination of a low cover with a relatively large maximum aggregate size. The current specified first-course top cover is the same as the specified nominal maximum aggregate size. The lack of adequate spacing between the top reinforcement and the finishing equipment causes the coarse aggregate to be worked away from the reinforcement, resulting in depressions. It also causes the aggregate particles to be trapped between the reinforcement and the finishing equipment, resulting in tearing of the concrete surface. The first-course cover should be increased to a 1 inch minimum, or 4/3 of the maximum size aggregate, as is recommended in ACI 211.1 (2). This would then allow the use of 3/4 inch maximum size aggregate. Field studies have shown that installed concrete covers have a standard deviation of about 3/8 inch (37). Therefore, using a standard deviation of 3/8 inch and assuming a normal distribution, a design first-course cover of 1-1/2 inches would provide that at least 90 percent of the top reinforcement would have the 1 inch minimum cover. The specified overlay thickness could then be decreased to 2 inches, if required for economy.

Chapter 4

Summary and Conclusions

4.1 Summary

The purpose of this investigation was to study the effects of high density vibration and two-course deck construction on concrete-steel bond in concrete bridge decks. One hundred seventeen pullout tests were conducted using #5 and #8 deformed bars. The major variables in the study were the consolidation method, the top cover, and the specimen depth. Individual pullout specimens had either 8 inches of concrete below the reinforcement and 6 test bars, or 24 inches of concrete below the reinforcement and 2 test bars. The test results are compared to evaluate the effects of the major test variables on concrete-steel bond. The test results are also compared with bond values predicted by the ACI (4) and AASHTO (1) bond requirements, Jimenez et al. (22), and Morita and Fujii (29).

4.2 Conclusions

The following conclusions are based on the tests and analysis described in this report:

1) Based on the experimental work, high density internal vibration provides improved bond over low density internal vibration.

2) 3 inch monolithic covers provide higher bond strengths than 3 inch two-course covers.

3) 3/4 inch covers provide approximately 60 percent of the bond strength of 3 inch monolithic covers.

4) The current ACI Building Code (4) and AASHTO Specification (1) provisions are not always conservative for top-cast bars with 3/4 inch covers.

5) 3 inch two-course covers will provide adequate bond strength only if high strength, well bonded overlays are used. For this type of construction, increased overlay strength will increase the bond strength, but equivalence to bond strength in monolithic decks is difficult to attain.

6) Deep specimens made with stiff, well consolidated concrete can provide the same bond strengths as shallow specimens. However, the data are very limited.

7) Increased concrete slump has a negative effect on the bond strength of top-cast reinforcement.

4.3 Recommendations for Future Study

Although the current code provisions use only the depth of the concrete below the reinforcement as a criterion in defining a "top bar", the data from this and other studies tend to support the use of two other criteria, slump and top cover.

The effects on bond of slump, top cover, and depth of concrete below the reinforcement are interactive and cannot be quantified without research considering all three simultaneously. Since the relative effects are of primary concern, it would be possible to determine the relationships using smaller specimens than were used in the current study.

Any relationships developed from a study considering all three parameters could be applied to data obtained from more realistic tests and specimens (for example, beam tests). All data used for a final empirical bond relationship must, of course, be based on some common datum. A reasonable datum would be results of tests using only bottom-cast reinforcement in specimens no more than 30 inches deep. The independently derived relationship between cover, slump, and member depth could then be applied to obtain design relationships.

Much confusion exists in the literature in the area of the effect of revibration on bond in concrete. Available test data are very limited and quite dated. There is, therefore, a need for new research that will quantify the effects of revibration on bond, using current deformed bars and realistic construction procedures.

The linear relationship between bleed and slump, combined with the apparent independence of this relationship from air content, raises an important question about one of the acknowledged major advantages of entrained air: i.e., that it reduces bleeding. This suggests that some additional work on the effects of entrained air and slump on bleeding would be useful.

References

1. AASHTO Subcommittee on Bridges and Structures, Standard Specifications for Highway Bridges, 1977, American Association of State Highway and Transportion Officials, Washington, D.C., 1977.

2. ACI Committee 211, Recommended Practice for Selecting Proportions for Normal and Heavyweight Concrete (ACI 211-77), American Concrete Institute, Detroit, Michigan, September, 1977, 20 pp.

3. ACI Committee 318, Building Code Requirements for Reinforced Concrete (ACI 318-63), American Concrete Institute, Detroit Michigan, June 1963, 144 pp.

4. ACI Committee 318, Building Code Requirements for Reinforced Concrete (ACI 318-77), American Concrete Institute, Detroit, Michigan, 1977.

5. ASTM A 615, "Standard Specification for Deformed and Plain Billet-Steel Bars for Concrete Reinforcement," Annual Book of ASTM Standards, Part 4, American Society for Testing and Materials, Philadelphia, Pennsylvania, 1980, pp. 588-593.

6. ASTM C 31, "Standard Method of Making and Curing Concrete Test Specimens in the Field," Annual Book of ASTM Standards, Part 14, American Society for Testing and Materials, Philadelphia, Pennsylvania, 1980, pp. 7-12.

7. ASTM C 143 "Standard Test Method for Slump of Portland Cement Concrete," Annual Book of ASTM Standards, Part 14, American Society for Testing and Materials, Philadelphia, Pennsylvania, 1980, pp. 101-109.

8. ASTM C 173 "Standard Test Method for Air Content of Freshly Mixed Concrete by the Volumetric Method," Annual Book of ASTM Standards, Part 14, American Society for Testing and Materials, Philadelphia, Pennsylvania, 1980, pp. 127-129.

9. ASTM C 232, "Standard Test Method for Bleeding of Concrete," Annual Book of ASTM Standards, Part 14, American Society for Testing and Materials, Philadelphia, Pennsylvania, 1980, pp. 167-172.

10. ASTM C 642 "Standard Test Method for Specific Gravity, Absorption, and Voids in Hardened Concrete," Annual Book of ASTM Standards,

Part 14, American Society for Testing and Materials, Philadelphia, Pennsylvania, 1980, pp. 388-390.

11. Bukovatz, John E., Unpublished data from a Kansas Department of Transportion Study.

12. Clark, Arthur P., "Bond of Concrete Reinforcing Bars, "ACI Journal, Proceedings, Vol. 46, No. 3, Nov. 1949, pp. 161-184.

13. Clark, Arthur P., "Comparitive Bond Efficiency of Deformed Concrete Reinforceing Bars," ACI Journal, Proceedings, Vol. 18, No. 4, Dec. 1946, pp. 381-400.

14. Collier, S.T., "Bond Characteristics of Commercial and Prepared Reinforcing Bars," ACI Journal, Proceedings, Vol. 18, No. 10, June 1947, pp. 1125-1133.

15. Commissie voor Uitvoering van Research Ingesteld door de Betonvereniging, "Onderzoek naar de samenwerking van geprofileered staal met beton," Report No. 23, 1963, The Netherlands (Translation No. 112, 1964, Cement and Concrete Association, London, "An Investigation of the Bond of Deformed Steel Bars with Concrete"), 28 pp.

16. Dakhil, F.H.; Cady, P.D.; and Carrier, R.E., "Cracking of Fresh Concrete as Related to Reinforcement," ACI Journal, Proceedings, Vol. 72, No. 8, Aug. 1975, pp. 421-428.

17. Davis, Raymond E.; Brown, Elwood H.; and Kelly, J.W., "Some Factors Influencing the Bond Between Concrete and Reinforcing Steel," Proceedings of the Forty-first Annual Meeting of the American Society for Testing Materials, Vol. 38, Part II, Philadelphia, 1938, pp. 394-406.

18. Durability of Concrete Bridge Decks, NCHRP Synthesis No. 57, Transportation Research Board, Washington, D.C., May 1979, 60 pp.

19. Ferguson, Phil M. and Thompson, J. Neils, "Development Length for Large High Strength Reinforcing Bars," ACI Journal, Proceedings, Vol. 62, No. 1, Jan. 1965, pp. 71-91.

20. Ferguson, Phil M. and Thompson, J. Neils, "Development Length of High Strength Reinforcing Bars in Bond," ACI Journal, Proceedings, Vol. 59, No. 7, July 1962, pp. 887-922.

21. Freyermuth, Clifford L; Klieger, Paul; Stark, David C.; and Wenke, Harry N., "Durability of Concrete Bridge Decks--A Review of Cooperative Studies," Highway Research Record No. 328, Highway Research Board, Washington, D.C., 1970, pp. 50-60.

22. Jimenez, Rafael; Gergely, Peter; and White, Richard N., Shear Transfer Across Cracks in Reinforced Concrete, Department of Structural Engineering, Cornell University, Ithaca, N.Y., Aug. 1978, 357 pp.

23. Kansas Department of Transportation, Standard Specifications for State Road and Bridge Construction, KDOT, Topeka, Kansas, 1980, 914 pp.

24. Larnach, William J., "Changes in Bond Strength Caused by Revibration of Concrete and the Vibration of Reinforcement," Maganzine of Concrete Research, London, No. 10, July 1952, pp. 17-21.

25. Luke, J.J.; Hamad, B.S.; Jirsa, J.O.; Breen, J.E., The Influence of Casting Position on Development and Splice Length of Reinforcing Bars, Research Report No. 242-1, Center for Transportion Research, Bureau of Engineering Research, The University of Texas at Austin, June 1981, 153 pp.

26. Mathey, Robert G. and Watstein, David, "Investigation of Bond in Beam and Pull-out Specimens with High-strength Deformed Bars," ACI Journal, Proceedings, Vol. 57, No. 2, March 1961, pp. 1071-1098.

27. Menzel, Carl A., Effect of Settlement of Concrete on Results of Pullout Tests, Research Department Bulletin 41, Research and Development Laboratories of the Portland Cement Association. Nov. 1952, 49 pp.

28. Menzel, Carl A. and Woods, William M., An Investigation of Bond, Anchorage and Related Factors in Reinforced Concrete Beams, Research Department Bulletin 42, Portland Cement Association, Nov. 1952, 114pp.

29. Morita, S. and Fujii, S., "Bond Capacity of Deformed Bars Due to Splitting of Surrounding Concrete," Bond in Concrete, edited by P. Bartos, Applied Science Publishers, London, 1982, pp. 331-341.

30. Robin, R.C.; Olsen, P.E.; and Kinnane, R.F., "Bond Strength of Reinforcing Bars Embedded Horizontally in Concrete," Journal of the Institute of Engineers, Vol. 14, Sept. 1942, pp. 201-217.

31. Thompson, M.A.; Jirsa, J.O.; Breen, J.E.; and Meinheit, D.F., "Behavior of Multiple Lap Splices in Wide Sections," ACI Journal, Proceedings, Vol. 76, No. 2, Feb. 1979, pp. 227-248.

32. Tuthill, Lewis H. and Davis, Harmer E., "Overvibration and Revibration of Concrete," ACI Journal, Proceedings, Vol. 35, No. 4, September 1938, pp. 41-47.

33. Tuthill, Lewis H. "Revibration Reexamined," Concrete Construction, Vol. 22, No. 10, October 1977, pp. 537-539.

34. Untrauer, R.E., Discussion of "Development Length for Large High Strength Reinforcing Bars," ACI Journal, Proceedings, Vol. 62, No. 1, Jan. 1965, pp. 71-88.

35. Untrauer, Raymond E. and Warren, George E., "Stress Development of Tension Steel in Beams," ACI Journal, Proceedings, August 1977, pp. 368-372.

36. Vollick, C.A., "Effects of Revibrating Concrete," ACI Journal, Proceedings, Vol. 54, No. 39, Mar. 1958, pp. 721-732.

37. Weed, Richard M., "Recommended Depth of Cover for Bridge Deck Steel," Transportation Research Record No. 500, Transportation Research Board, Washingtion, D.C., 1974, pp. 32-55.

38. Welch, Geoffry B. and Patten, Bruce J.F., "Bond Strength of Reinforcment Affected by Concrete Sedimentation," ACI Journal, Proceedings, Vol. 62, No. 2, Feb. 1965, pp. 251-263.

39. Zekany, A.J.; Neumann, S.; Jirsa, J.O.; Breen, J.E., The Influence of Shear on Lapped Splices in Reinforced Concrete, Research Report 242-2, Center for Transportation Research, Bureau of Engineering Research, The University of Texas at Austin, July 1981, 88 pp.

Table 2.1 Test Bar Variables

Slab	Bar Number	Embedment Length in.	Total Cover in.	Cover Type*	Consolidation Type+
1c	4	12	3/4	1	H2
	5		3/4	1	
	6		3	1	
	7		3	1	
	8		3/4	1	
1b	9	12	3/4	1	H1
	10		3/4	1	
	11		3	1	
	12		3/4	1	
	13		3/4	1	
	14		3	1	
1a	15	12	3/4	1	H2
	16		3/4	1	
	17		3/4	1	
	18		3/4	1	
	19		3	1	
	20		3	1	
2c	39	10	3/4	1	L1
	40		3	2	
	41		3	2	
	42		3/4	1	
	43		3	1	
	44		3	1	
2b	45	10	3/4	1	H2
	46		3	2	
	47		3	2	
	48		3/4	1	
	49		3	1	
	50		3	1	
2a	51	10	3/4	1	H2
	52		3/4	1	
	53		3/4	1	
	54		3/4	1	
	55		3	1	
	56		3	1	
3a	21	10	3/4	1	H2
	22		3	2	
	23		3	2	
	24		3/4	1	
	25		3	1	
	26		3	1	
3c	27	10	3/4	1	L1
	28		3	2	
	29		3	2	
	30		3/4	1	
	31		3	1	
	32		3	1	

Table 2.1 (continued)

Slab	Bar Number	Embedment Length in.	Total Cover in.	Cover Type*	Consolidation Type+
3b	33	10	3/4	1	H2
	34		3/4	1	
	35		3/4	1	
	36		3/4	1	
	37		3	1	
	38		3	1	
4b	57	5	3/4	1	H2
	58		3/4	1	
	59		3/4	1	
	60		3/4	1	
	61		3	1	
	62		3	1	
4a	63	5	3/4	1	L1
	64		3/4	1	
	65		3/4	1	
	66		3/4	1	
	67		3	1	
	68		3	1	
5b	69	3.5	3/4	1	H2
	70		3	2	
	71		3	2	
	72		3/4	1	
	73		3	1	
	74		3	1	
5a	75	3.5	3/4	1	L1
	76		3	2	
	77		3	2	
	78		3/4	1	
	79		3	1	
	80		3	1	
6b	81	12	3/4	1	L2
	82		3	2	
	83		3	1	
	84		3/4	1	
	85		3	2	
	86		3	1	
6a	87	12	3/4	1	H2
	88		3	2	
	89		3	1	
	90		3/4	1	
	91		3	2	
	92		3	1	

Table 2.1 (continued)

Slab	Bar Number	Embedment Length in.	Total Cover in.	Cover Type*	Consolidation Type+
7a	93	15	3/4	1	H2
	94	10	3	2	
	95	10	3	1	
	96	15	3/4	1	
	97	10	3	2	
	98	10	3	1	
7b	99	15	3/4	1	L3
	100	10	3	2	
	101	10	3	1	
	102	15	3/4	1	
	103	10	3	2	
	104	10	3	1	
7c	105	10	3	1	H2(D)
	106		3	1	
7d	107	15	3/4	1	H2(D)
	108		3/4	1	
8a	109	10	3/4	1	H2
	110		3	2	
	111		3	1	
	112		3/4	1	
	113		3	2	
	114		3	1	
8b	115	10	3	1	H2(D)
	116		3	1	
8c	117	10	3	3	H2(D)
	118		3	3	
8d	119	10	3	2	H2(D)
	120		3	2	

* Cover Type Designations:
1 = Monolithic.
2 = Two-course w/ 3/4 inch first course.
3 = Two-course w/ 1 inch first course.
\+ Consolidation Type Designations:
H1 = High density vibration using one vibrator.
H2 = High density vibration using two vibrators.
L1 = Low density vibration at two foot centers.
L2 = Low density vibration at the slab centerline at two foot centers.
L3 = Low density vibration at two foot centers for seven seconds.
(D) = Deep slab.

Table 2.2 Concrete Mix Designs
(Cubic Yard Batch Weights)

	First Course Concrete				Second Course Concrete			
			Aggregate				Aggregate	
Slab Group	Cement #	Water #	Fine+ #	Coarse* #	Cement #	Water #	Fine+ #	Coarse* #
1	591	262	1470	1455	--	--	--	--
2	636	282	1381	1455	563	248	1491	1491
3	591	262	1470	1455	563	248	1491	1491
4	555	244	1545	1455	--	--	--	--
5	591	262	1470	1455	563	248	1491	1491
6	584	257	1484	1455	563	248	1491	1491
7	591	243	1515	1455	620	248	1447	1491
8	591	262	1470	1455	825	289	1316	1316

* Crushed limestone--Hamm's Quarry, Perry, KS
Bulk Specific Gravity = 2.52, Absorption = 3.5%,
Maximum size = 3/4 inch.

\+ Kansas River sand--Lawrence Sand Co., Lawrence, KS
Bulk Specific Gravity = 2.62, Absorption = 0.5%,
Fineness Modulus = 3.0.

Air entraining agent--vinsol resin

Table 2.3 Concrete Properties

Slab Group	First Course Concrete				Second Course Concrete	
	Slump in.	Air %	Bleed* ml	f'_c psi	Slump in.	f'_c psi
1	2-1/2	4-1/2	0	4510	--	--
2	8-1/2	9	10.8	3820	1/2	5920
3	5-1/2	7	13.5	3970	1/2	4380
4	3	7	3.5	3570	--	--
5	2-3/4	5	0	4910	1/4	5670
6	4-1/2	10	2	4060	0	2600
7	1-3/4	5	0	4950	0	5100
8	2-1/4	7	0	3970	1/2	5350

* ASTM C 232, at 100 minutes.

Table 2.4 Test Bar Data

Bar Size	#8	#5
Deformation Spacing, in.	0.545	0.345
Deformation Height, in.	0.057	0.040
Deformation Angle, deg.	50	50
Deformation Gap, in.	0.313	0.125
Nominal Weight, #/ft.	2.650	1.010
Deformation Bearing Area, sq.in./in. length	0.239	0.162
Yield Strength, ksi	63.47	60.23
Tensile Strength, ksi	104.6	101.0
Deformation Pattern--Sheffield		

Table 2.5 Slab Bleed and Settlement at 2 Hours

Slab	Consolidation Type+	Total Avg. Bleed gm	Settlement In.
1a	H2	14.4	0.010
1b	H1	8.8	0.008
1c	H2	9.5	0.006
2a	H2	57.3	0.010
2b	H2	43.5	No Data
2c	L1	39.4	No Data
3a	H2	41.3	0.004
3b	H2	26.2	0.007
3c	L1	28.2	0.009
4a	L1	31.0	0.010
4b	H2	29.0	No Data
5a	L1	21.4	0.011
5b	H2	17.9	0.009
6a	H2	26.3	0.007
6b	L2	26.0	0.003
7a	H2	17.7	0.010
7b	L3	17.6	0.011
7c	H2(D)	18.3	0.005
7d	H2(D)	16.4	0.008
8a	H2	11.1	0.011
8b	H2(D)	10.6	0.012
8c	H2(D)	9.3	0.003
8d	H2(D)	11.6	0.005

+ See Table 2.1 for notation.

Table 2.6 Core Test Results for Slab Groups 6 and 7

Slab	6a	6b	7a	7b
Consolidation Method+	H2	L2	H2	L3
Core Numbers	2,6,7	8,9,10	13,14	15,16,17,18
Apparent Specific Gravities	2.16,2.08, 2.14	2.05,2.05, 2.04	2.24,2.26	2.21,2.19, 2.25,2.17
(Average)	(2.13)	(2.05)	(2.25)	(2.21)
Percents Voids	6.89,6.59, 7.45	7.30,7.22, 7.12	7.29,7.13	7.90,7.68, 7.28,7.68
(Average)	(6.98)	(7.21)	(7.21)	(7.62)
Ratio of Specific Gravities++	1.04		1.02	
Ratio of Percents Voids++	0.97		0.95	

\+ See Table 2.1 for notation.
++ Ratio of average quantities from High Density and Low Density Vibration slabs from the same Group.

Table 3.1 Bond Forces

Slab	Bar Number	Bar Size	Concrete Strength (Slump, in.) 1st Course psi	Concrete Strength (Slump, in.) 2nd Course psi	Consolidation Type+	Embedment Length in.	Total Cover in.	Cover Type*	End Slip Load° kips	Ultimate Load kips	Normalized Bond Forces Per Unit Length End Slip Load kips/in.	Normalized Bond Forces Per Unit Length Ultimate Load kips/in.
1c	4	#8	4510	N.A.	H2	12	3/4	1	29.3	35.3	2.36	2.48
	5		(2-1/2)				3/4	1	32.3	35.2	2.60	2.84
	6						3	1	45.8	56.4Y	3.69	4.55Y
	7						3	1	46.3	48.3	3.73	3.89
	8						3/4	1	29.4	31.4	2.37	2.53
1b	9	#8	4510	N.A.	H1	12	3/4	1	31.0	33.1	2.50	2.67
	10		(2-1/2)				3/4	1	37.0	37.8	2.98	3.05
	11						3	1	49.5Y	57.5YT	3.99Y	4.64YT
	12						3/4	1	33.5	34.3	2.70	2.76
	13						3/4	1	37.8	38.2	3.04	3.08
	14						3	1	46.6	47.9	3.76	3.86
1a	15	#8	4510	N.A.	H2	12	3/4	1	37.0	38.7	2.98	3.12
	16		(2-1/2)				3/4	1	31.3	33.3	2.52	2.69
	17						3/4	1	29.8	30.3	2.40	2.44
	18						3/4	1	37.0	38.0	2.89	3.06
	19						3	1	52.8Y	56.7YT	4.26Y	4.57YT
	20						3	1	43.8	51.3YT	3.53	4.13YT
2c	39	#8	3820	5920	L1	10	3/4	1	19.1	22.8	1.95	2.33
	40		(8-1/2)				3	2	25.3	39.1	2.58	3.99
	41						3	2	28.0	37.6	2.86	3.84
	42						3/4	1	21.3	27.1	2.17	2.77
	43						3	1	29.0	43.1	2.96	4.40
	44						3	1	22.0	35.2	2.24	3.59
2b	45	#8	3820	5920	H2	10	3/4	1	19.8	26.8	2.02	2.73
	46		(8-1/2)				3	2	24.8	40.1	2.53	4.09
	47						3	2	30.2	40.3	3.08	4.11
	48						3/4	1	24.8	28.5	2.53	2.91
	49						3	1	30.8	44.3	3.14	4.52
	50						3	1	35.0	38.8	3.57	3.96
2a	51	#8	3820	5920	H2	10	3/4	1	24.0	26.8	2.44	2.74
	52		(8-1/2)				3/4	1	22.0	25.9	2.24	2.64
	53						3/4	1	22.8	24.6	2.33	2.51
	54						3/4	1	21.6	24.3	2.20	2.47
	55						3	1	34.0	46.1	3.47	4.70
	56						3	1	33.8	40.0	3.45	4.08
3a	21	#8	3970	4380	H2	10	3/4	1	24.2	25.8	2.42	2.58
	22		(5-1/2)				3	2	30.8	42.9	3.08	4.29
	23						3	2	26.3	41.4	2.63	4.14
	24						3/4	1	23.5	29.7	2.35	2.97
	25						3	1	42.0	47.3	4.20	4.73
	26						3	1	38.5	43.6	3.85	4.36
3c	27	#8	3970	4380	L1	10	3/4	1	23.8	26.2	2.38	2.62
	28		(5-1/2)				3	2	29.3	43.8	2.93	4.38
	29						3	2	30.5	39.4	3.05	3.94
	30						3/4	1	28.5	30.0	2.85	3.00
	31						3	1	34.0	48.6	3.40	4.86
	32						3	1	29.8	41.5	2.98	4.15

Table 3.1 (continued)

Slab	Bar Number	Bar Size	Concrete Strength (Slump, in.) 1st Course psi	2nd Course psi	Consolidation Type+	Embedment Length in.	Total Cover in.	Cover Type*	End Slip Load° kips	Ultimate Load kips	Normalized Bond Forces Per Unit Length: End Slip Load kips/in.	Ultimate Load kips/in.
3b	33	#8	3970	4380	H2	10	3/4	1	28.8	31.2	2.88	3.12
	34		(5-1/2)				3/4	1	28.0	31.3	2.80	3.13
	35						3/4	1	28.5	31.0	2.85	3.10
	36						3/4	1	28.5	29.4	2.85	2.94
	37						3	1	34.3	47.8	3.43	4.78
	38						3	1	39.0	45.5	3.90	4.55
4b	57	#5	3570	N.A.	H2	5	3/4	1	6.10	8.17	1.34	1.79
	58		(3)				3/4	1	5.50	7.00	1.21	1.54
	59						3/4	1	6.30	8.43	1.39	1.86
	60						3/4	1	7.33	8.55	1.61	1.88
	61						3	1	7.88	13.6	1.74	3.00
	62						3	1	5.75	11.8	1.27	2.59
4a	63	#5	3570	N.A.	L1	5	3/4	1	5.80	8.39	1.28	1.85
	64		(3)				3/4	1	6.55	8.03	1.44	1.77
	65						3/4	1	10.2	10.9	2.25	2.40
	66						3/4	1	8.00	9.40	1.76	2.07
	67						3	1	17.2	18.2Y	3.78	4.01Y
	68						3	1	8.00	14.4	1.76	3.17
5b	69	#5	4910	5670	H2	3.5	3/4	1	9.75	10.8	2.50	2.77
	70		(2-3/4)				3	2	10.3	17.6	2.64	4.54
	71						3	2	13.0	17.9	3.35	4.61
	72						3/4	1	10.9	11.1	2.80	2.86
	73						3	1	12.5	21.2Y	3.22	5.46Y
	74						3	1	8.40	14.9	2.16	3.83
5a	75	#5	4910	5670	L1	3.5	3/4	1	7.13	8.68	1.84	2.73
	76		(2-3/4)				3	2	8.55	13.9	2.20	3.58
	77						3	2	11.4	15.0	2.92	3.87
	78						3/4	1	8.20	9.24	2.11	2.38
	79						3	1	7.00	14.4	1.80	3.70
	80						3	1	10.0	15.5	2.57	3.98
6b	81	#5	4060	2600	L2	12	3/4	1	17.3	18.2	1.71	1.81
	82		(4-1/2)			3.5	3	2	5.60	8.93	1.58	2.53
	83					3.5	3	1	6.35	11.0	1.80	3.12
	84					12	3/4	1	19.0Y	20.4Y	1.88Y	2.02Y
	85					3.5	3	2	5.55	7.74	1.57	2.19
	86					3.5	3	1	6.75	9.50	1.91	2.68
6a	87	#5	4060	2600	H2	12	3/4	1	17.3	19.0Y	1.72	1.88Y
	88		(4-1/2)			3.5	3	2	7.00	10.9	1.98	3.09
	89					3.5	3	1	7.75	12.5	2.19	3.54
	90					12	3/4	1	21.5Y	22.5Y	2.13Y	2.23Y
	91					3.5	3	2	6.30	9.66	1.78	2.23
	92					3.5	3	1	9.40	13.2	2.65	3.74

Table 3.1 (continued)

Slab	Bar Number	Bar Size	Concrete Strength (Slump, in.) 1st Course psi	2nd Course psi	Consolidation Type+	Embedment Length in.	Total Cover in.	Cover Type*	End Slip Load° kips	Ultimate Load kips	Normalized Bond Forces Per Unit Length End Slip Load kips/in.	Ultimate Load kips/in.
7a	93	#8	4950	5100	H2	15	3/4	1	40.5	41.3	2.62	2.66
	94		(1-3/4)			(10	3	2	40.0	47.5	3.60	4.28
	95					10	3	1	44.7	48.9Y	4.04	4.42Y
	96					15	3/4	1	30.3	34.0	1.95	2.19
	97					10	3	2	40.4	48.9Y	3.64	4.41Y
	98					10	3	1	41.3	47.7	3.72	4.30
7b	99	#8	4950	5100	L3	15	3/4	1	34.1	36.2	2.19	2.33
	100		(1-3/4)			10	3	2	35.2	50.1Y	3.17	4.51Y
	101					10	3	1	32.5	48.0	2.93	4.32
	102					15	3/4	1	40.0	40.1	2.57	2.58
	103					10	3	2	39.8	46.2I	3.59	4.16I
	104					10	3	1	38.3	43.6	3.45	3.93
7c	105	#8	4950	5100	H2	10	3	1	44.2	53.7Y	3.98	4.84Y(D)
	106		(1-3/4)				3	1	37.5	54.6Y	3.38	4.91Y(D)
7d	107	#8	4950	5100	H2	15	3/4	1	45.8	48.1	2.95	3.10(D)
	108						3/4	1	44.4	45.4	2.86	2.92(D)
8a	109	#8	3970	5350	H2	10	3/4	1	23.8	27.2	2.38	2.72
	110		(2-1/4)				3	2	33.3	48.3	3.33	4.83
	111						3	1	38.3	49.2E	3.83	4.92E
	112						3/4	1	27.0	28.4	2.70	2.84
	113						3	2	37.5	43.0	3.75	4.30
	114						3	1	38.3	46.3	3.83	4.63
8b	115	#8	3970	5350	H2	10	3	1	38.0	46.2	3.80	4.62(D)
	116		(2-1/4)				3	1	30.8	45.5	3.08	4.55(D)
8c	117	#8	3970	5350	H2	10	3	3	36.5	47.1	3.65	4.71(D)
	118		(2-1/4)				3	3	28.6	48.4	2.86	4.84(D)
	119	#8	3970	5350	H2	10	3	2	42.5	46.8	4.25	4.68(D)
	120		(2-1/4)				3	2	21.3	48.4	2.13	4.84(D)

° End slip = 0.005 inches for #8 bars and 0.010 for #5 bars.
* Cover Type Designations:
1 = Monolithic.
2 = Two-course w/ 3/4 inch first course.
3 = Two-course w/ 1 inch first course.
\+ Consolidation Type Designations:
H1 = High density vibration using one vibrator.
H2 = High density vibration using two vibrators.
L1 = Low density vibration at two foot centers.
L2 = Low density vibration at the slab centerline at two foot centers.
L3 = Low density vibration at two foot centers for seven seconds.
Y after load indicates pullout force exceeded yield strength.
YT is same as Y, but loading terminated before pullout.
I after load indicates loading rate ≈ 10 times normal rate.
(D) after load indicates deep slab.
E after load indicates estimated value based
on single load cell output.

Table 3.2 Length Normalization

Bar Size	Actual Embedment in.	Normalized Embedment in.
#8	10.0	10.0
	12.0	11.7
	15.0	14.0
#5	3.5	3.5
	5.0	4.83
	12.0	9.98

Table 3.3 Bond Vibration Efficiency Ratios (Ratio of Bond Strengths for High Density Vibration to Bond Strengths for Low Density Vibration)

Bar	Group	Slump	End Slip Value+ Cover Type*			Ultimate Force Value° Cover Type*		
Size	#	in.	1	2	3	1	2	3
#5	4	3	0.83		0.86	0.88		0.88
	5	2-3/4	1.35	1.16	1.23	1.22	1.23	1.11
	6	4-1/2	1.06	1.19	1.32	Y	1.23	1.25
#8	2	8-1/2	1.11	1.03	1.32	1.05	1.02	1.08
	3	5-1/2	1.00	.95	1.27	1.05	.98	.98
	7	1-3/4	.96	1.08	1.28	.99	Y	Y

+ End slip = 0.005 inches for #8 bars and 0.010 for #5 bars.
° Y indicates yield in one or more test bars.
* Cover Type Designations
1 = 3/4 inch monolithic cover.
2 = 3 inch two-course cover.
3 = 3 inch monolithic cover.

Table 3.4 Bleed for Slabs
With Well-Distributed Concrete

Group Number	Vibration Method Low Density	High Density
	gm	gm
4	28.84	29.01
5	21.37	17.87
6	26.02	26.30
7	17.25	17.74

Table 3.5 Comparison of Bond Strengths for
Deep Slabs and Shallow Slabs

Group Number	Bar Size	Embedment Length	Cover	Ultimate Bond Force Deep	Shallow	Deep/Shallow Ratio
		in.	in.	kips	kips	
7	#8	15	3/4	48.1(F)	41.3(F)	1.16
8	#8	10	3/4+2-1/4	46.8(F)	48.3(F)	0.97
8	#8	10	3	45.5(S)	46.3(S)	0.98

(F)--First Bar Pulled for a given cover.
(S)--Second Bar Pulled for a given cover.
(First bar data lost for shallow slab in Group 8)

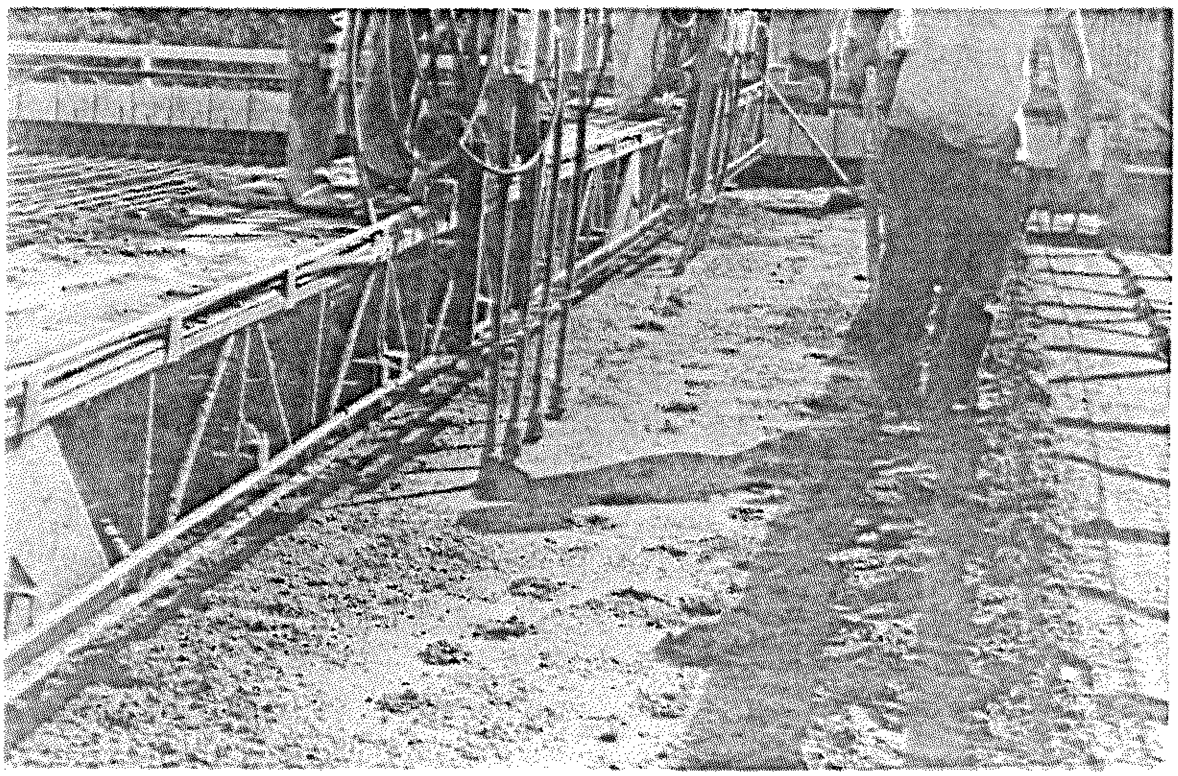

Fig. 1.1 Deck Consolidation Using Frame-Mounted, Internal Vibrators.

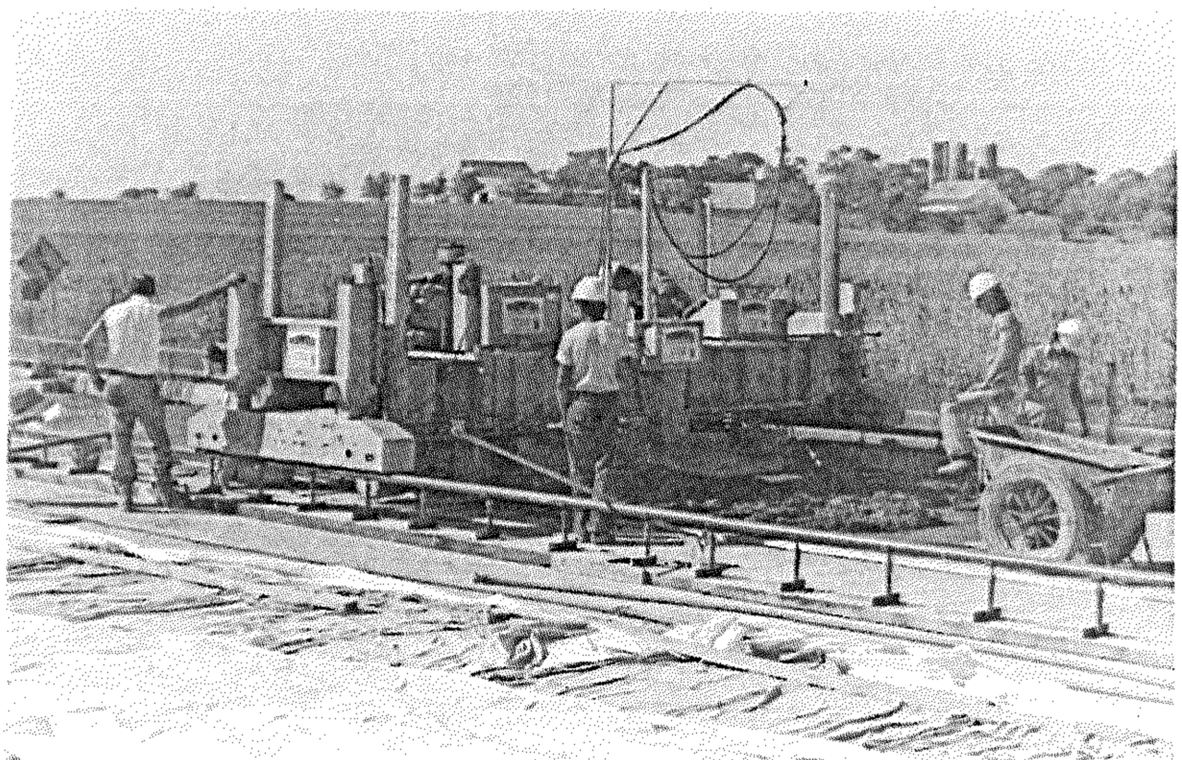

Fig. 1.2 Second Course Consolidation Using A Vibratory Screed.

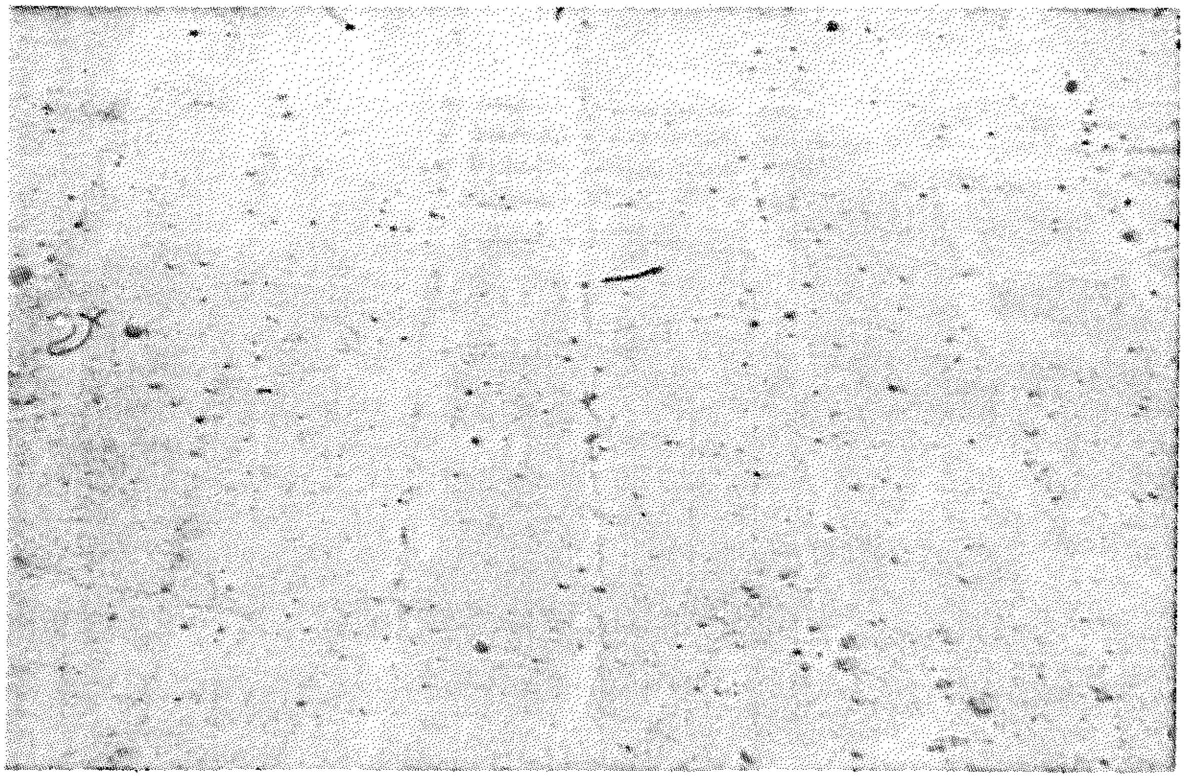

Fig. 1.3 Longitudinal Cracks over the Reinforcement within the First Course of a Deck.

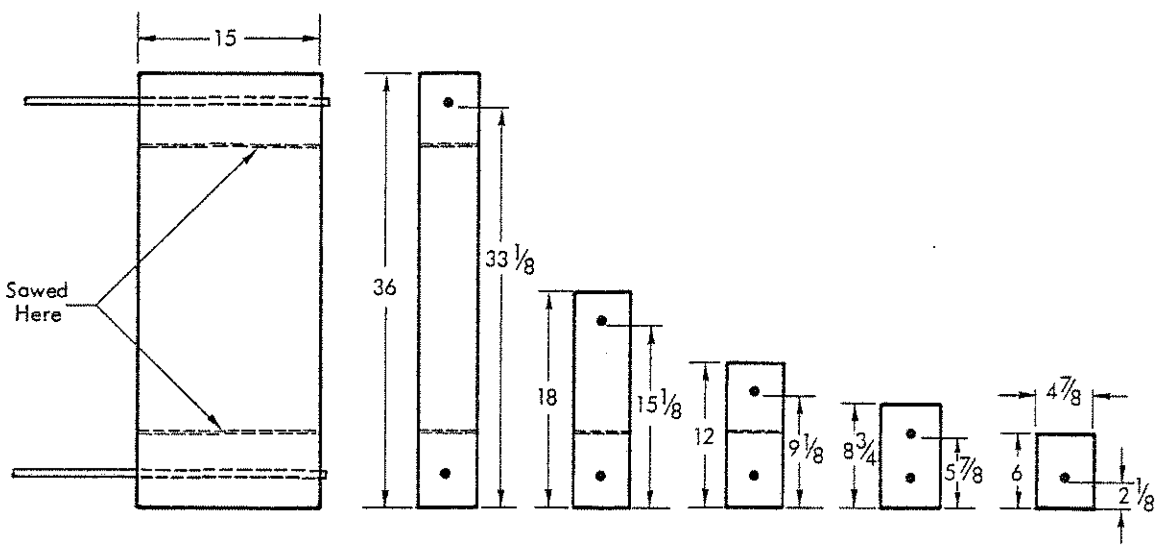

Fig. 1.4 Pullout Specimens Used by Menzel (27).

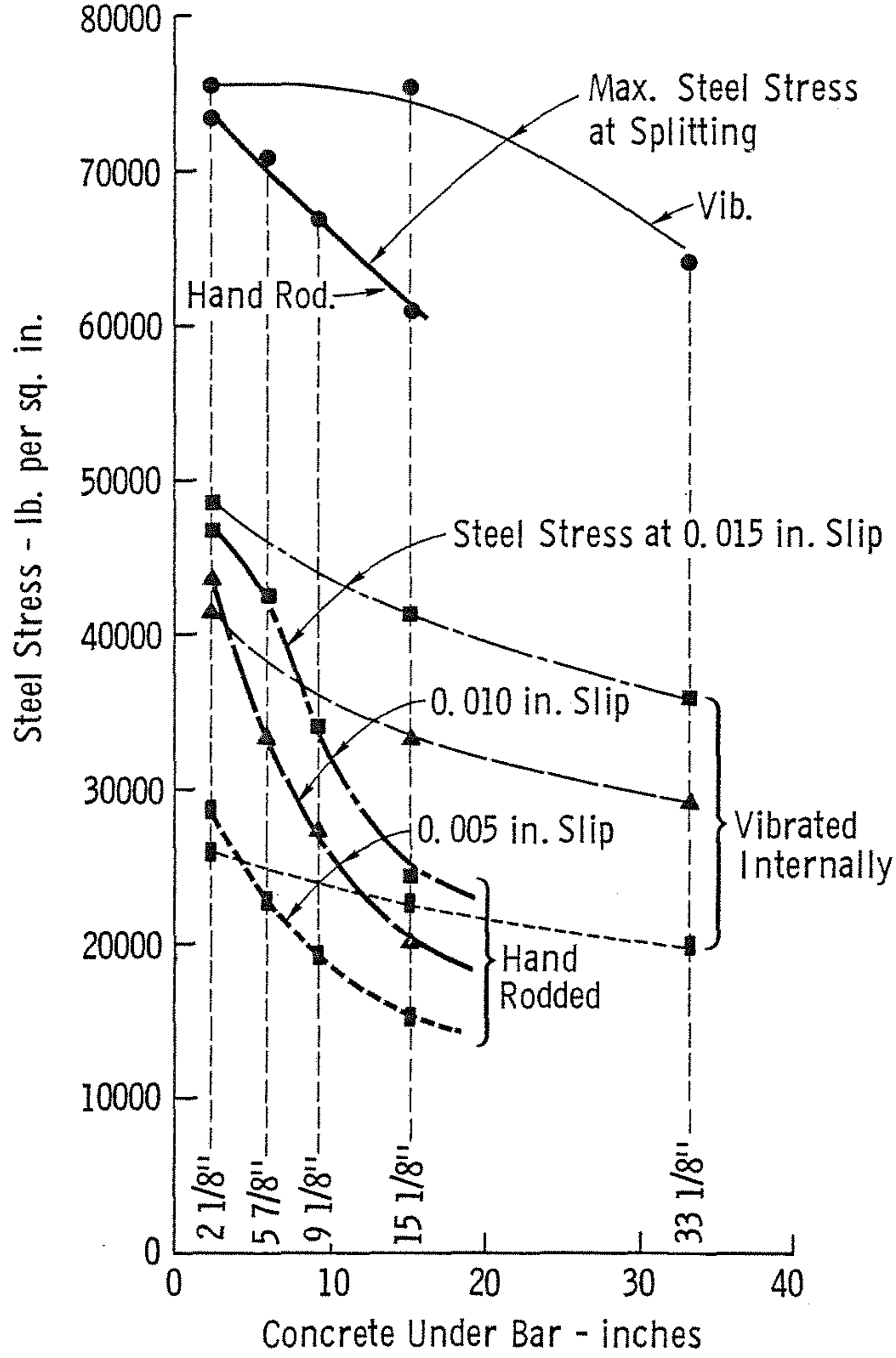

Fig. 1.5 Steel Stresses for Vibrated and Hand Rodded Concrete (27).

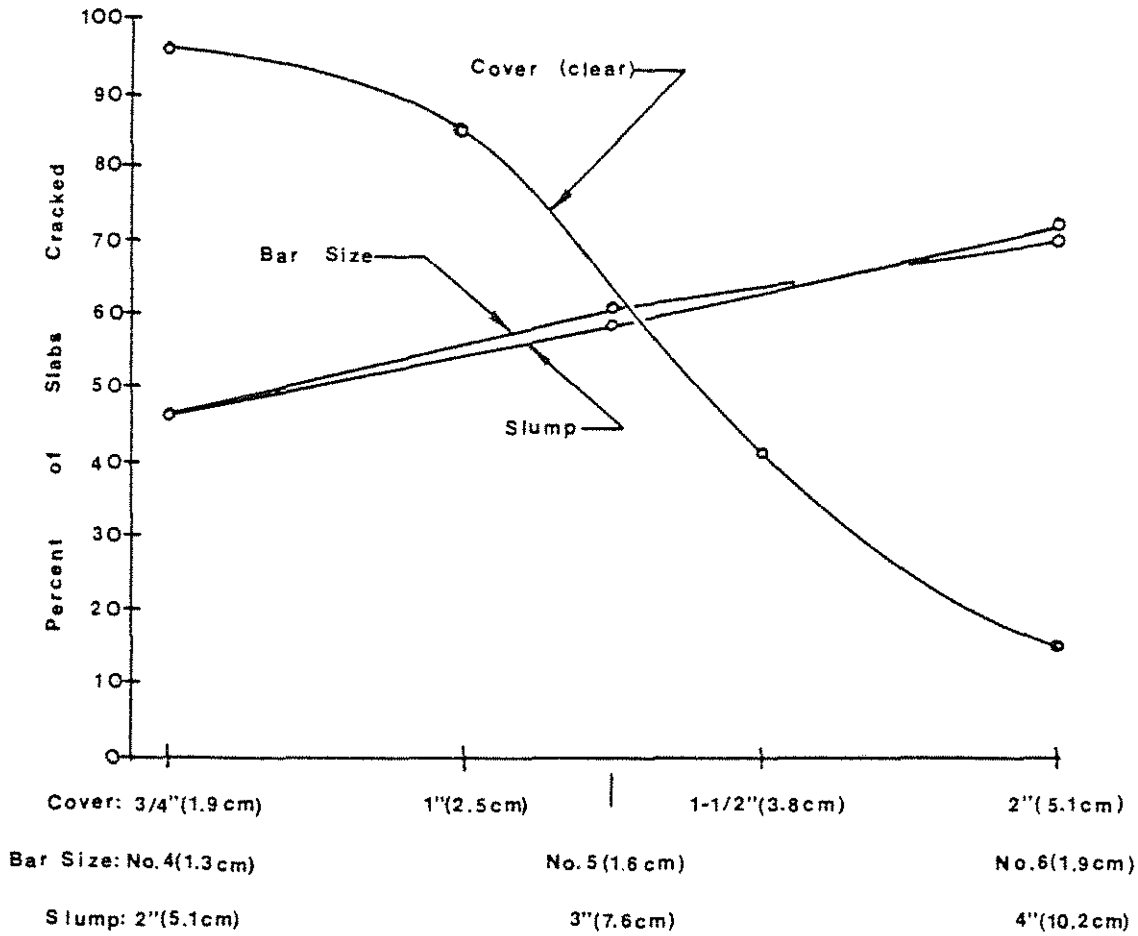

Fig. 1.6 Cracking As A Function of Bar Size, Slump, and Cover (16).

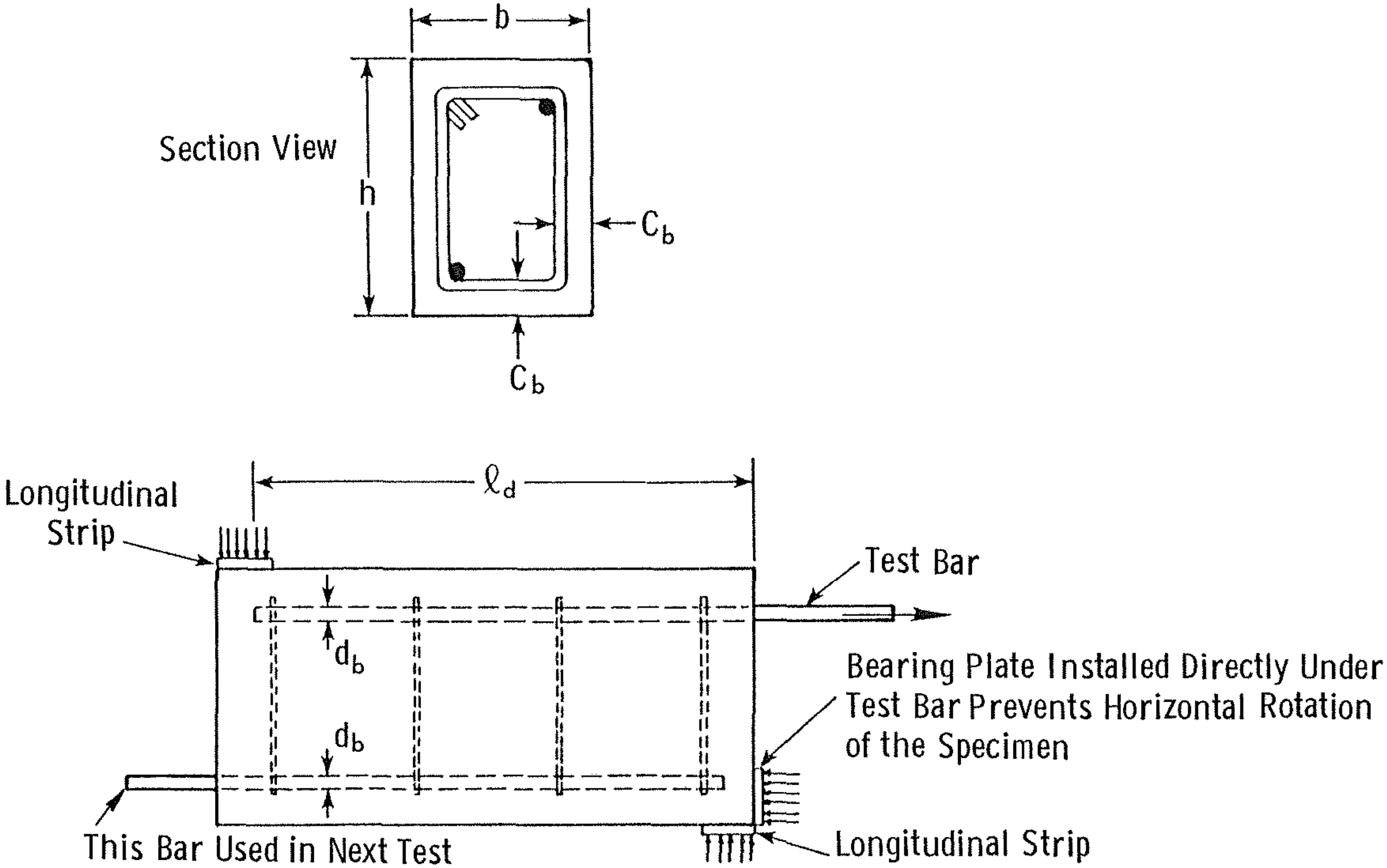

Fig. 1.7 Pullout Specimens Used by the C.U.R. (12).

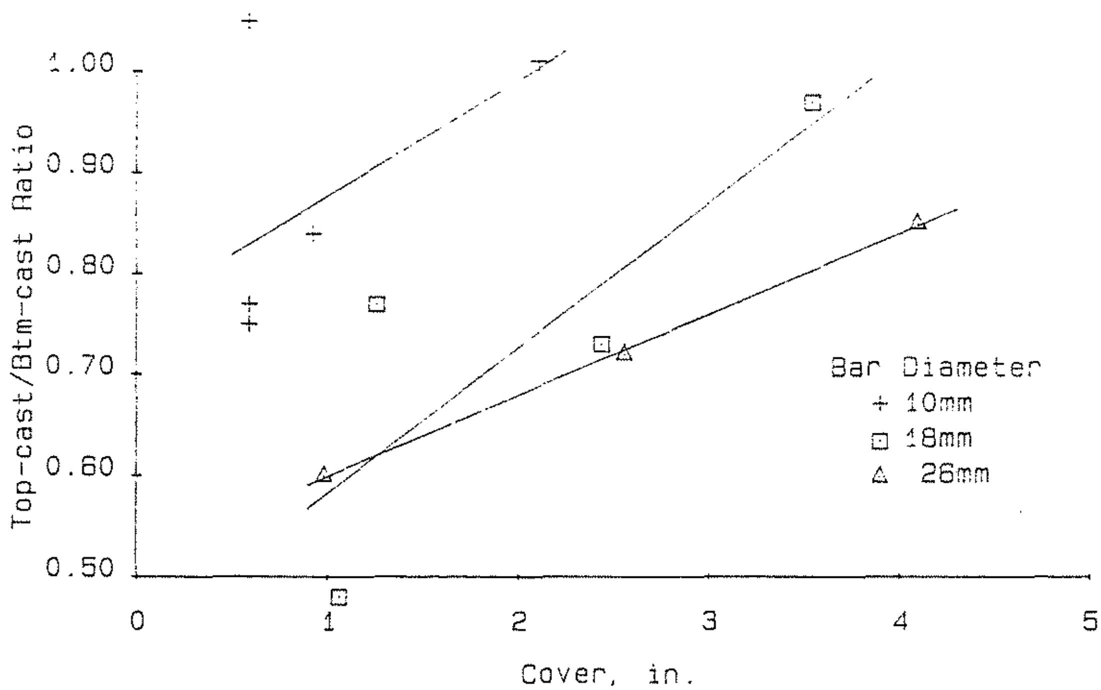

Fig. 1.8 Ratio of Top-Cast to Bottom-Cast Bar Bond Strength versus Cover (15).

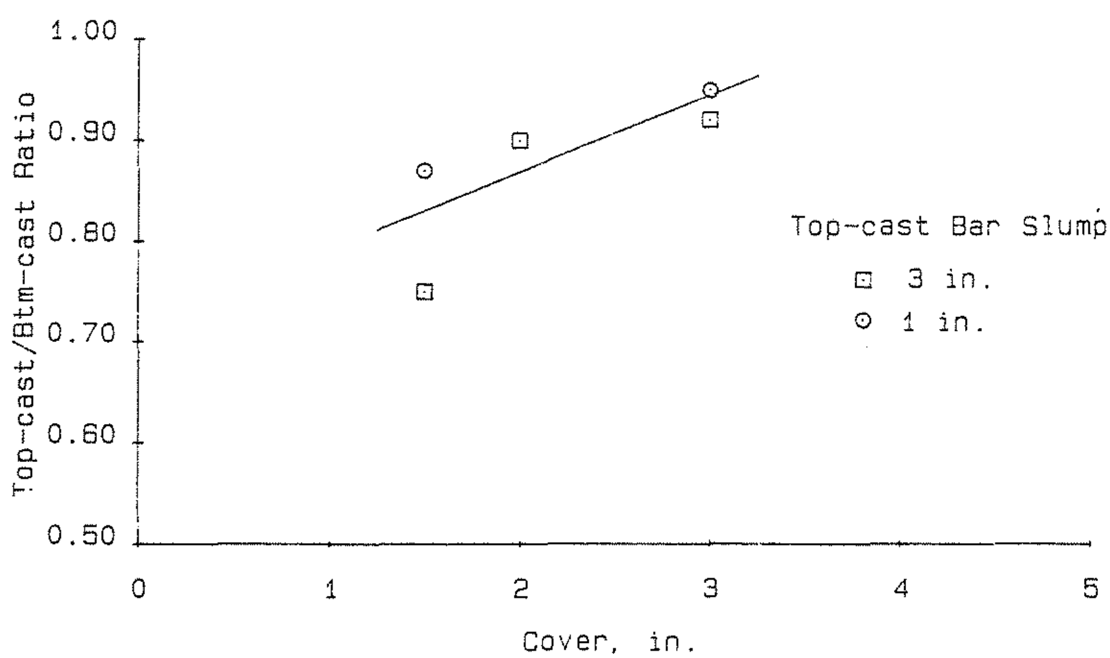

Fig. 1.9 Ratio of Top-Cast to Bottom-Cast Bar Bond Strength versus Cover (19).

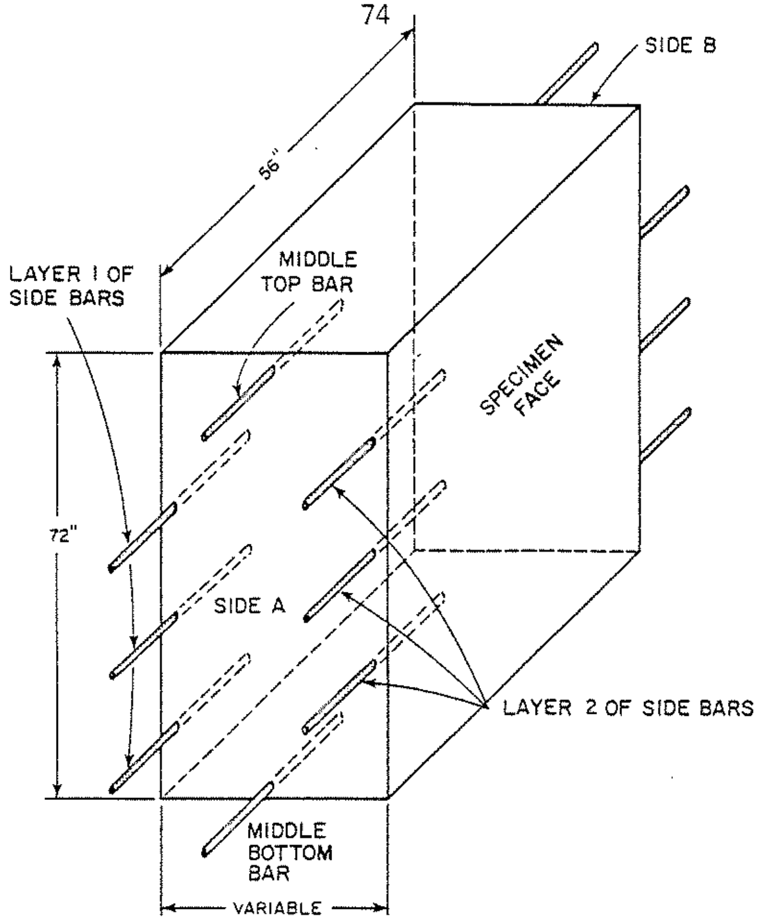

Fig. 1.10 Wall Specimens Used by Luke, et al (25).

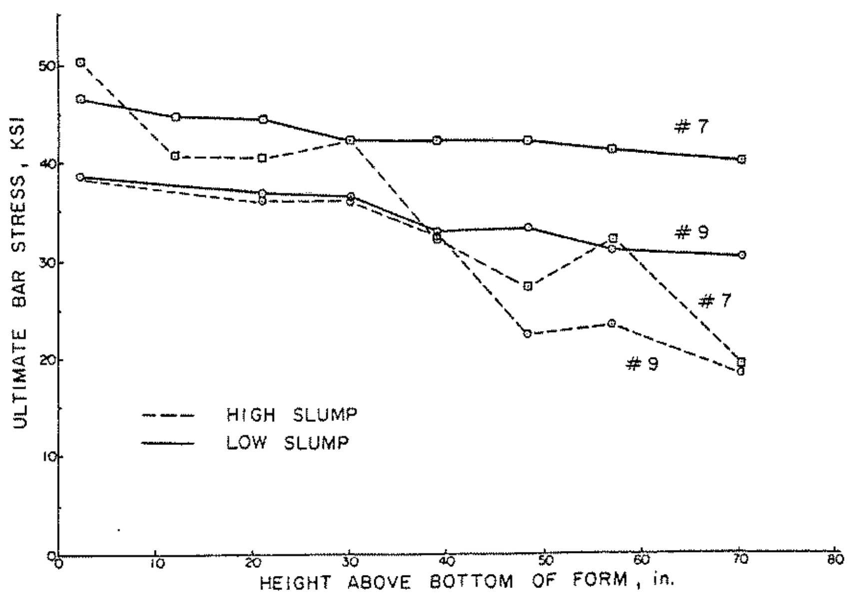

Fig. 1.11 Bond Strength As A Function of Bar Location Within A Wall Specimen (25).

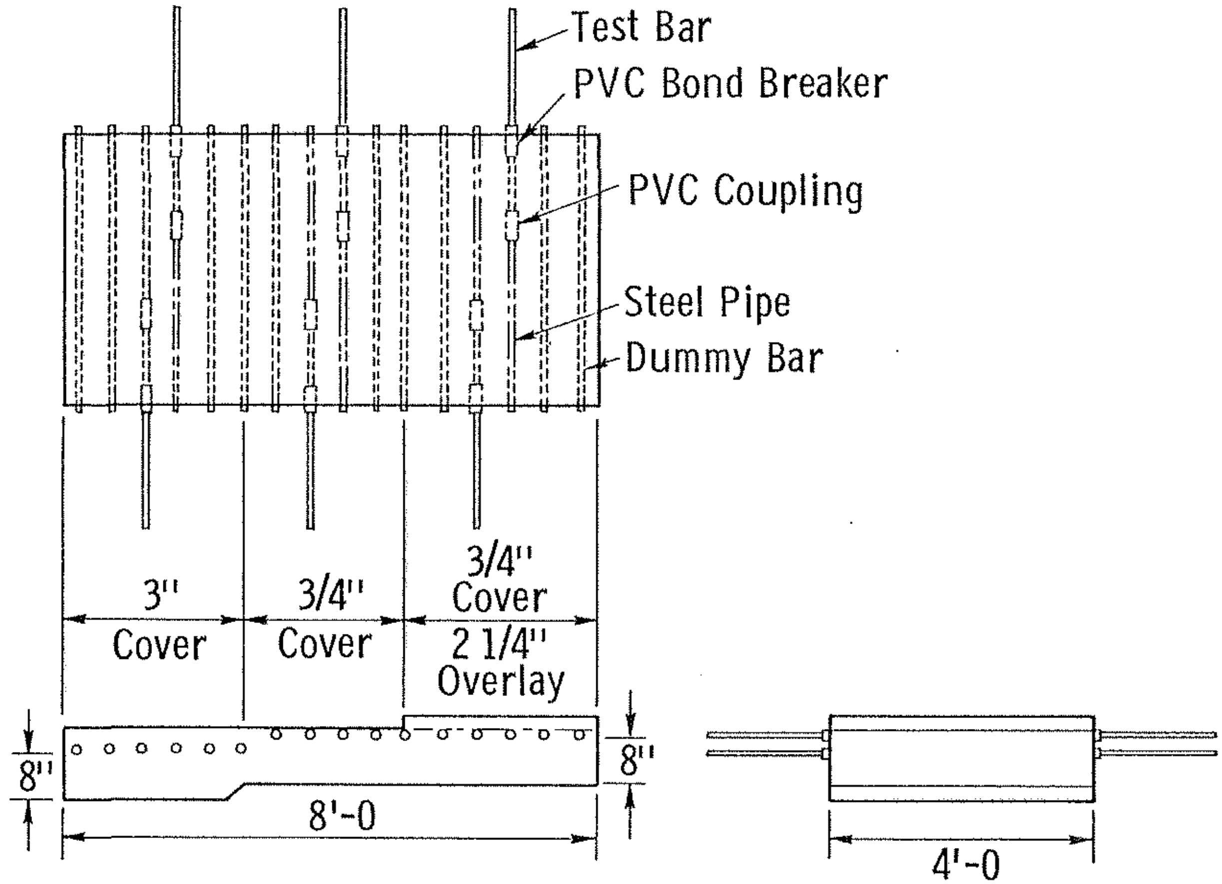

Fig. 2.1 Shallow Slab.

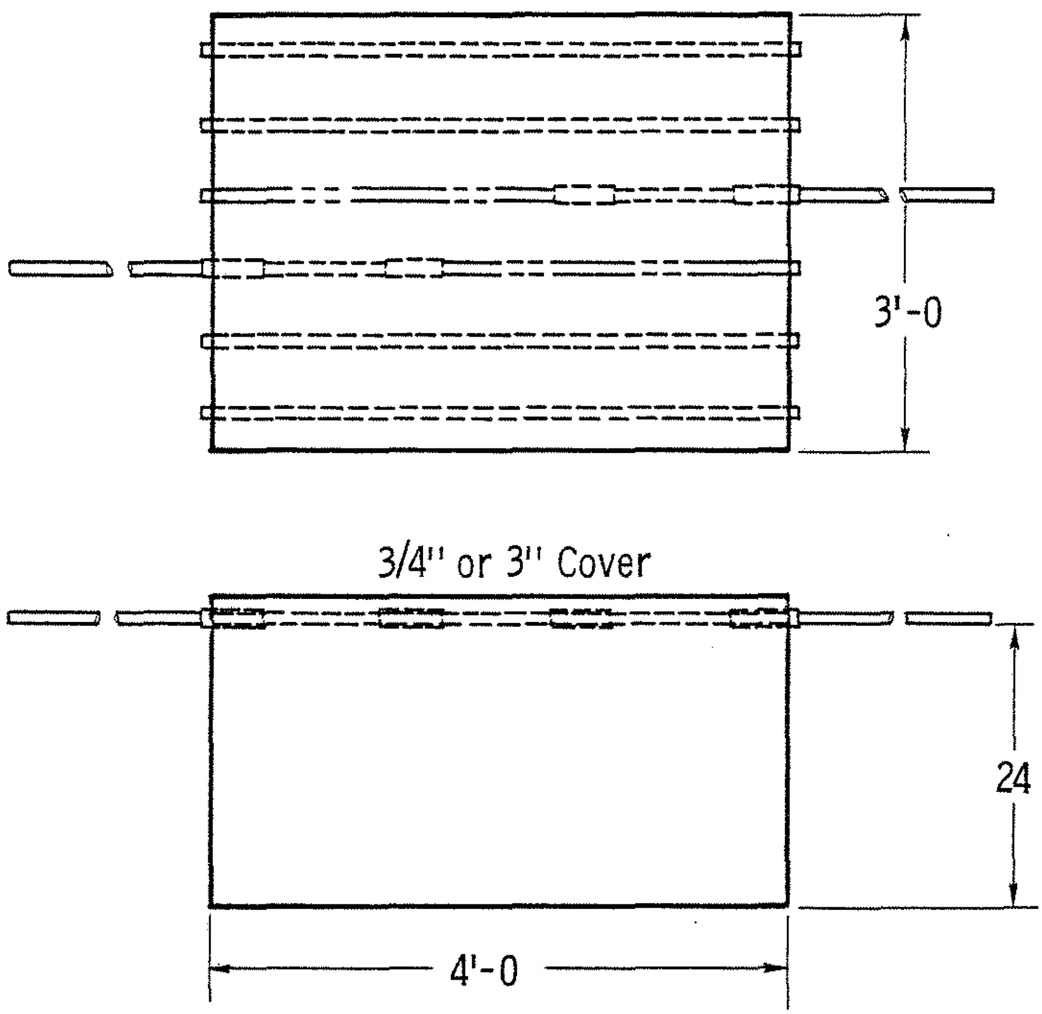

Fig. 2.2 Deep Slab

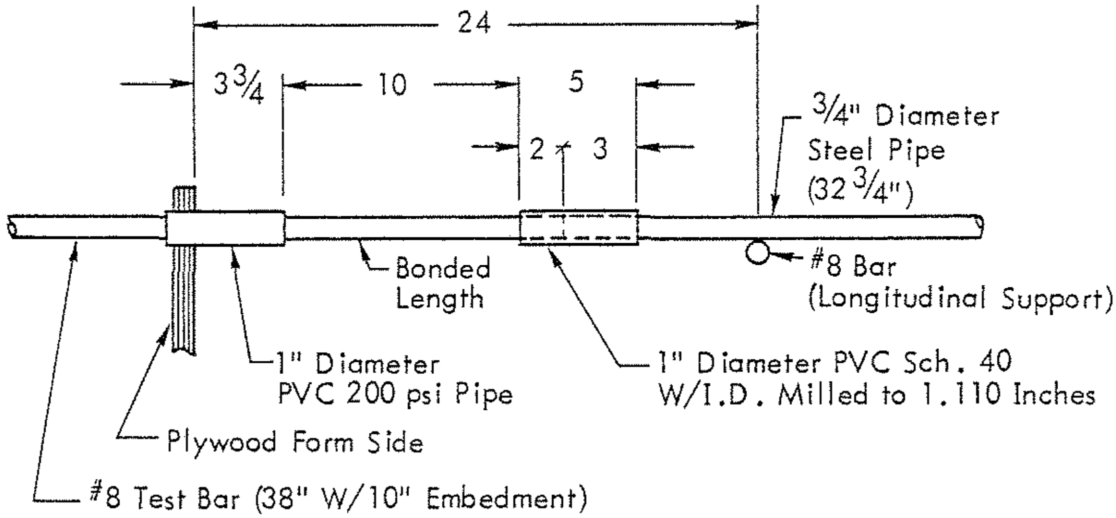

#8 Test Bar Installation

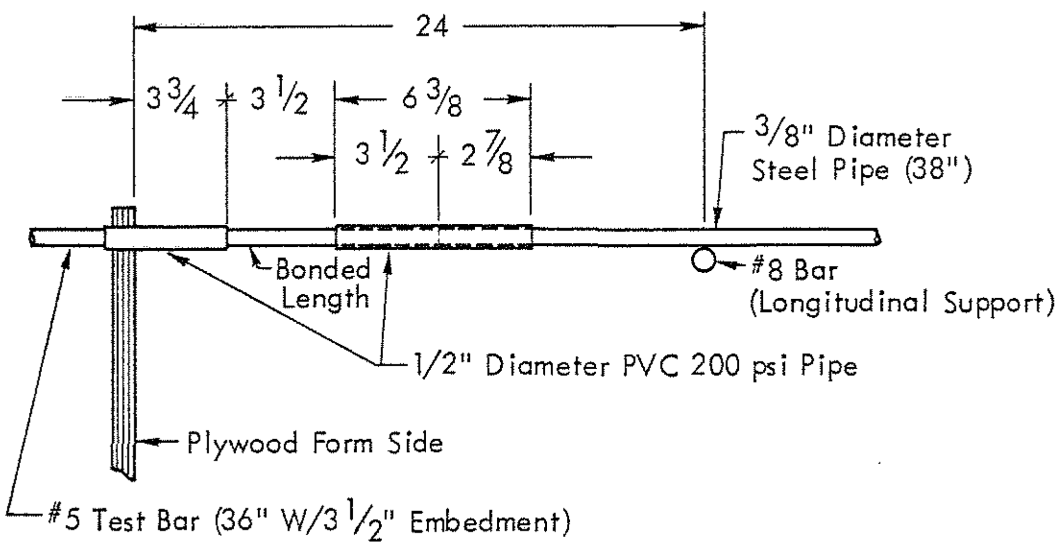

#5 Test Bar Installation

Fig. 2.3 Test Bar Installation.

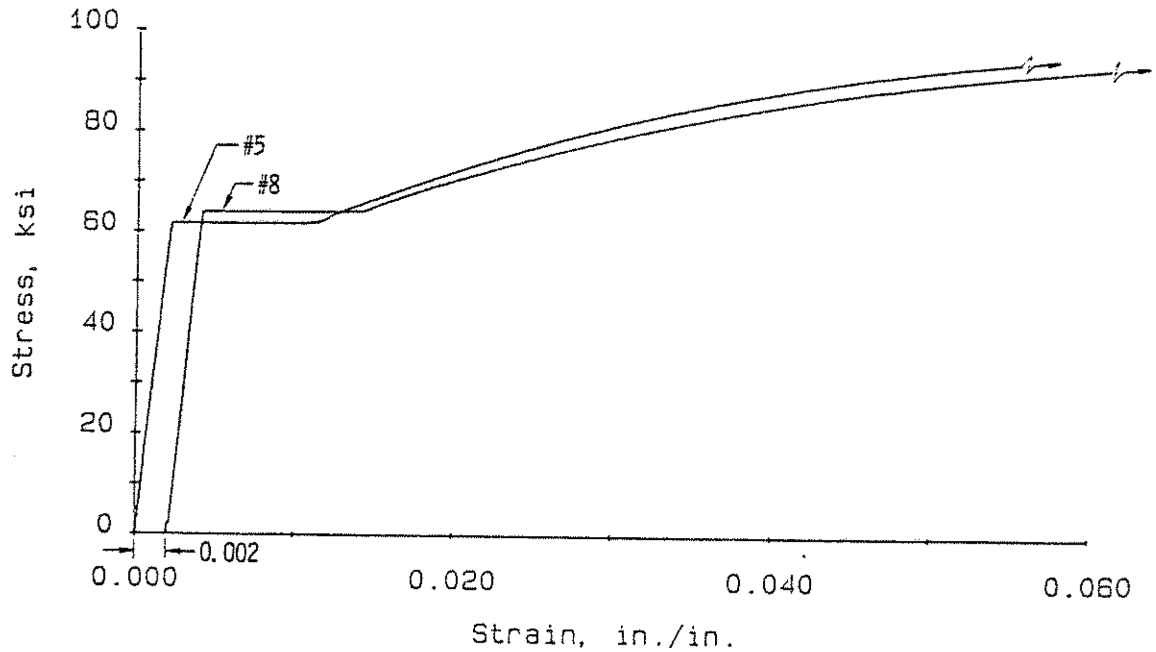

Fig. 2.4 Stress-Strain Curves for Test Bars.

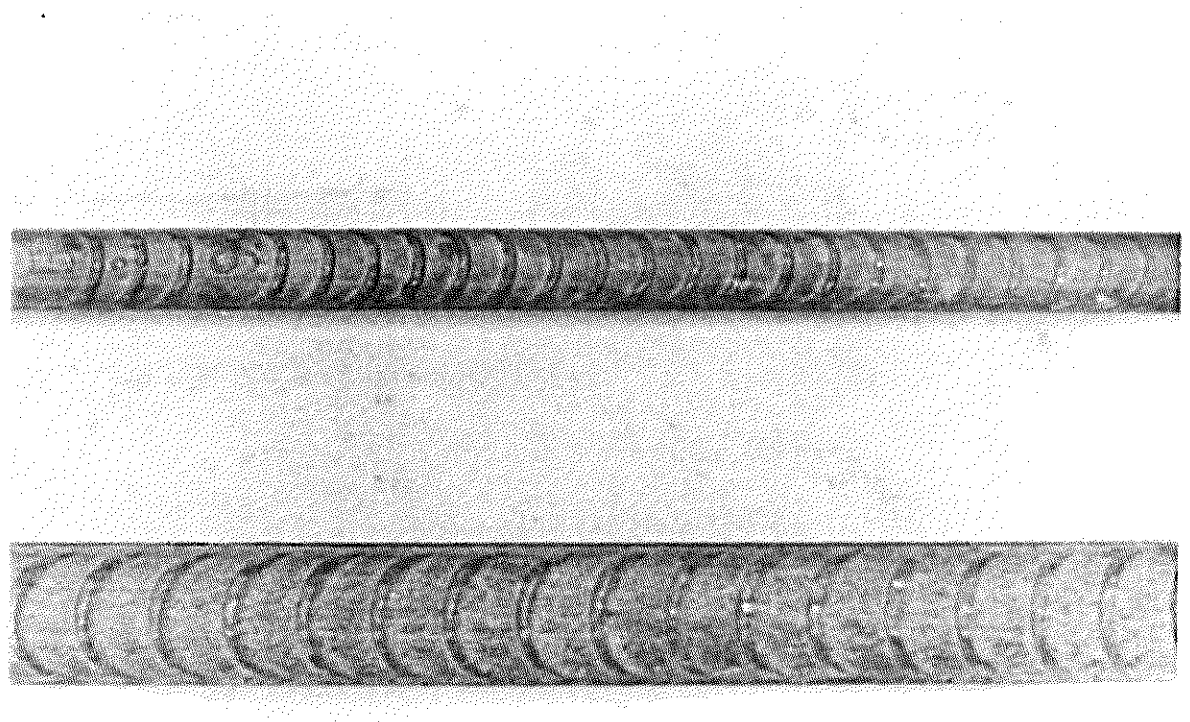

Fig. 2.5 Test Bar Deformation Patterns.

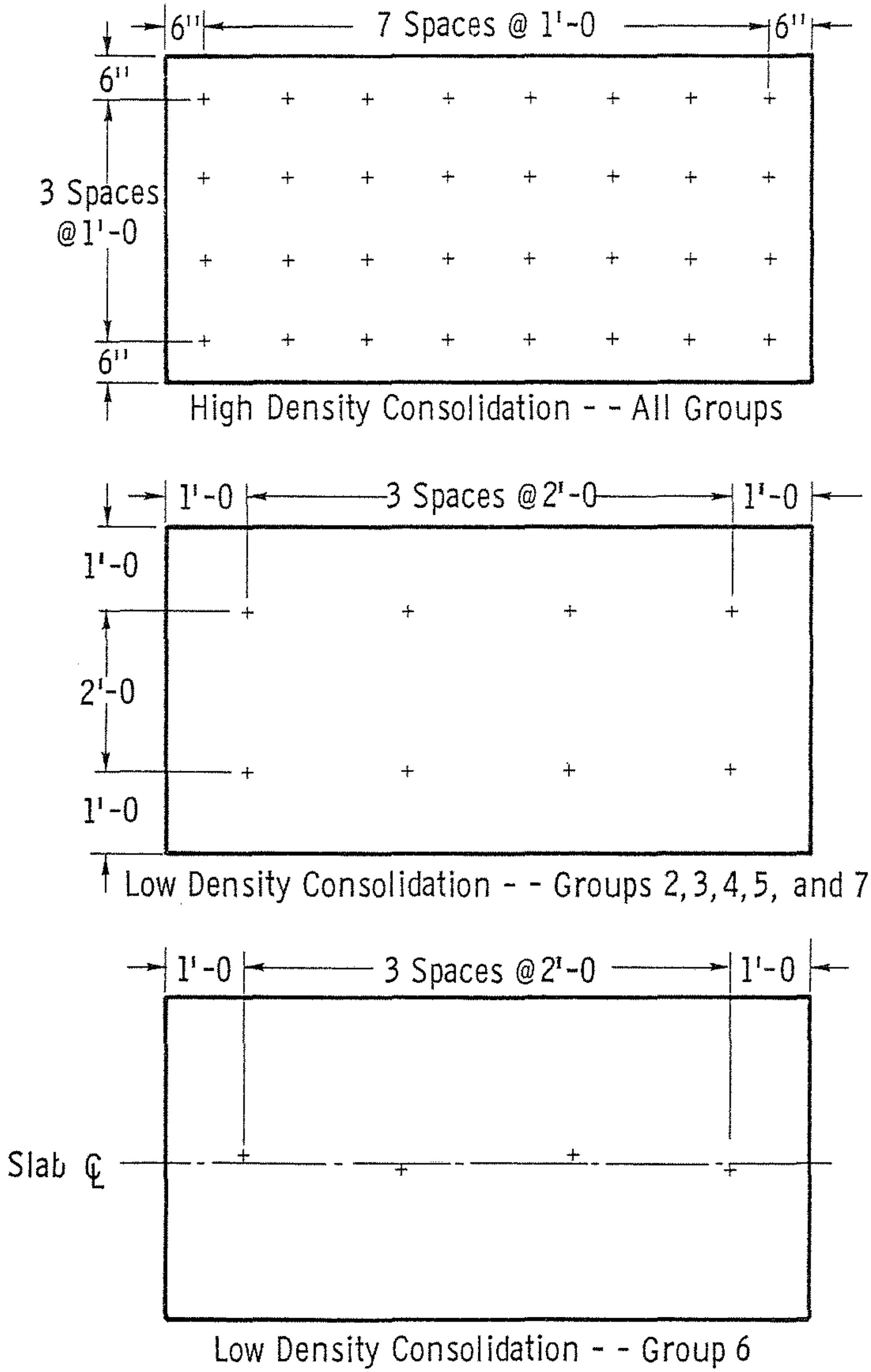

Fig. 2.6 Vibrator Insertion Patterns for Shallow Slabs.

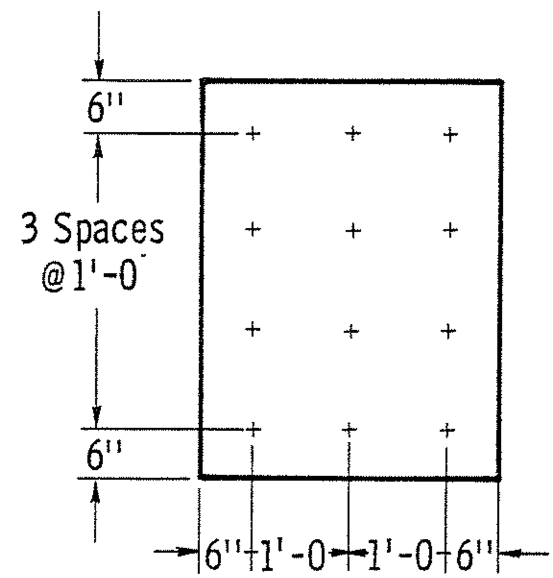

Fig. 2.7 Vibrator Insertion Pattern for Deep Slabs.

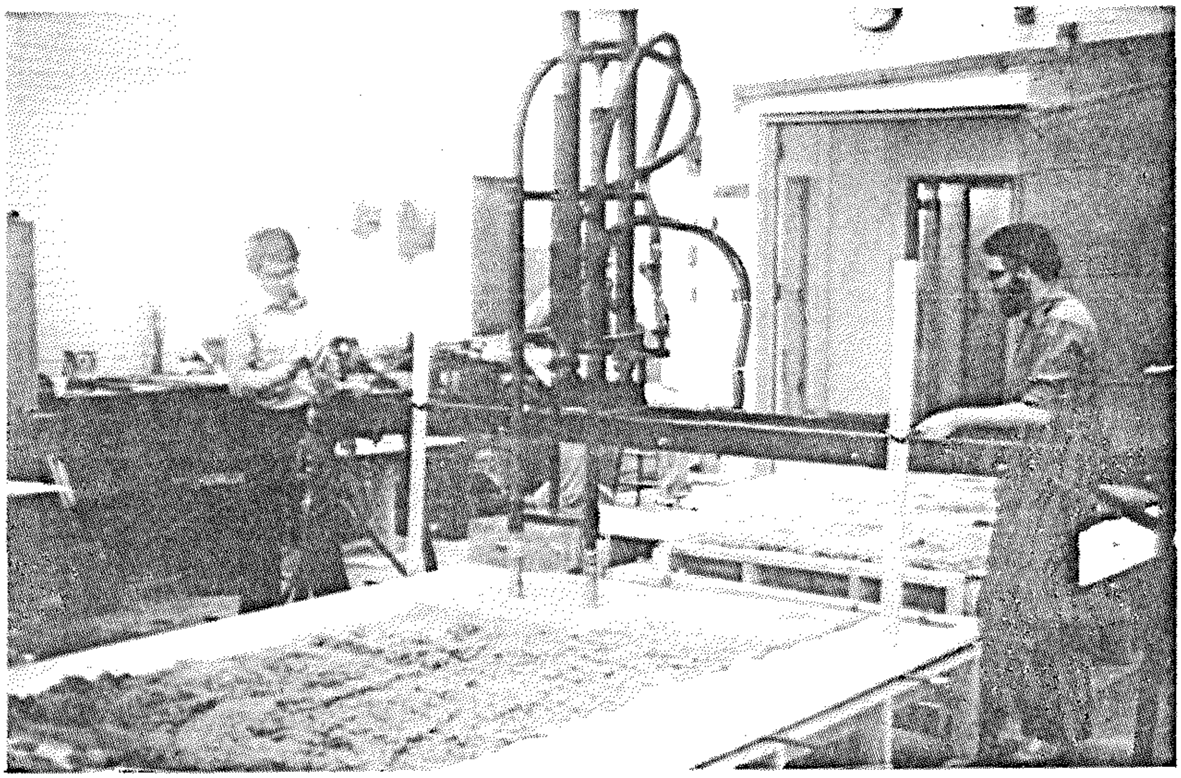

Fig. 2.8 Slab Consolidation.

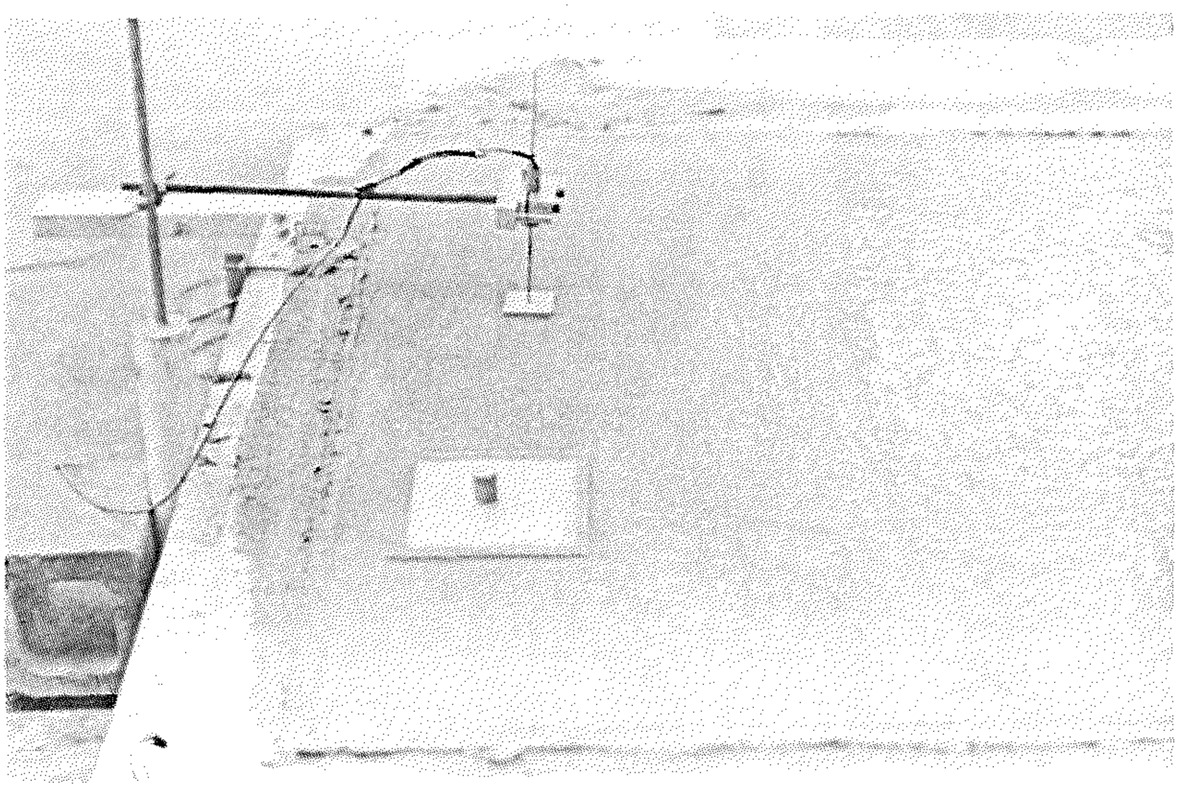

Fig. 2.9 Slab Bleed and Settlement Test Set-Up.

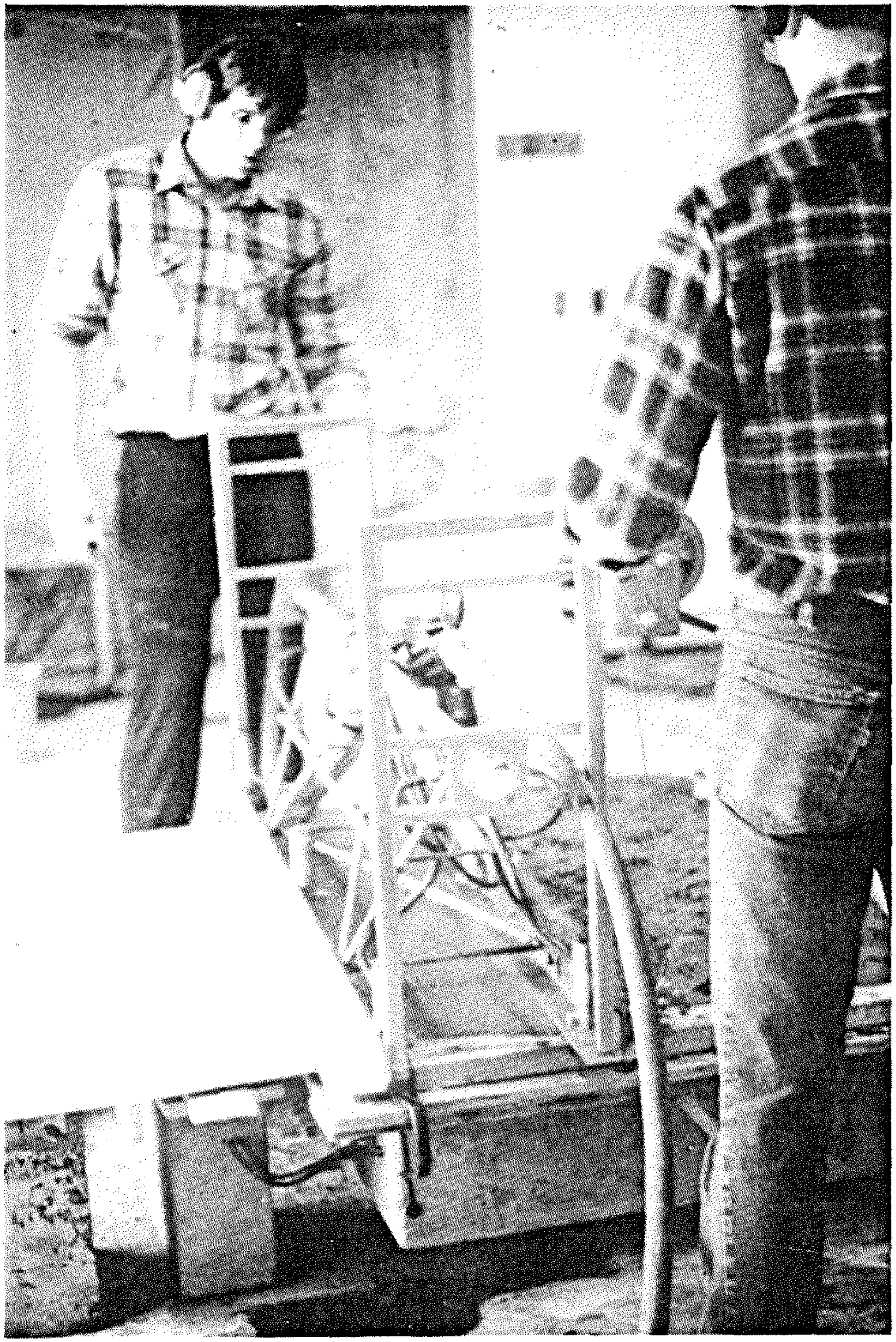

Fig. 2.10 Overlay Consolidation Using Vibratory Screed.

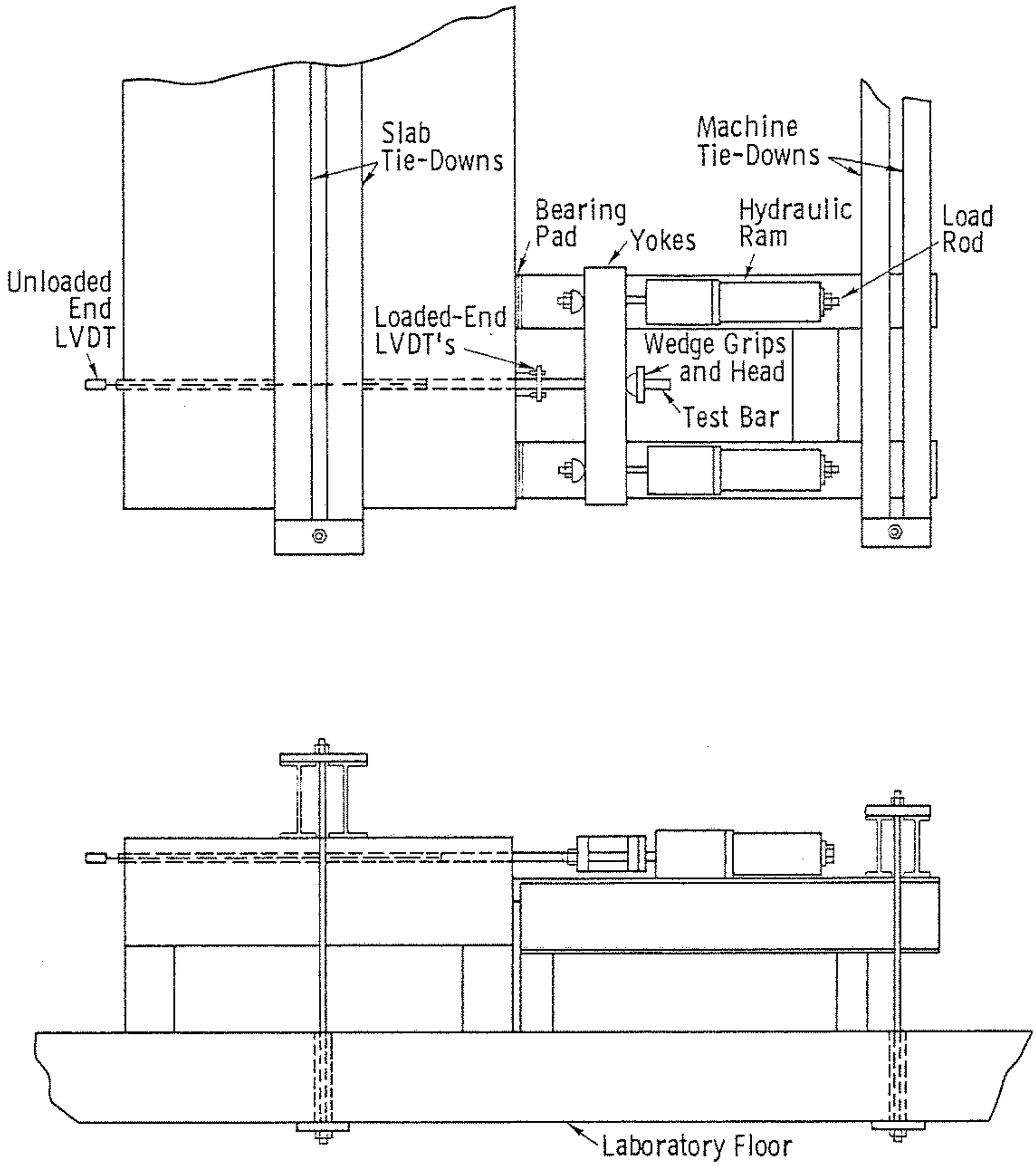

Fig. 2.11 Schematic of Bond Test.

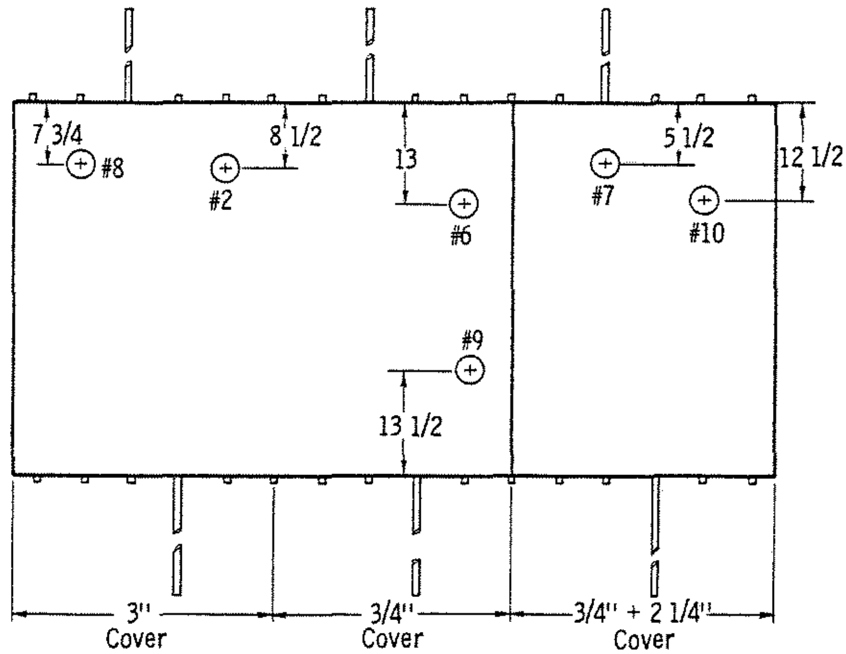

Fig. 2.12 a) Location of Cores Taken from Group 6.
2, 6, and 7--High Density Consolidation.
7, 8, 9, and 10--Low Density Consolidation.

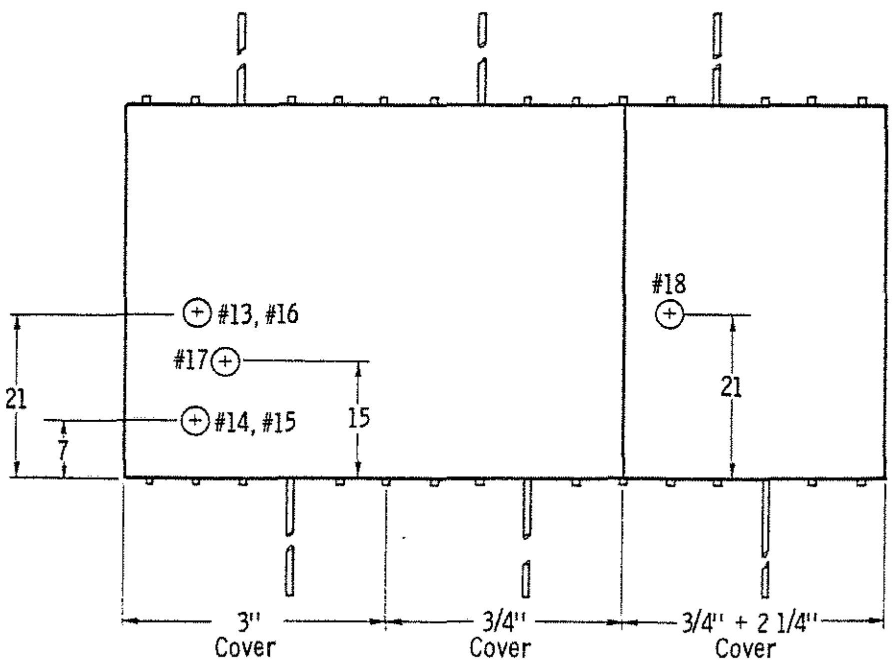

Fig. 2.12 b) Location of Cores Taken from Group 7.
13 and 14--High Density Consolidation.
15, 16, 17, and 18--Low Density Consolidation.

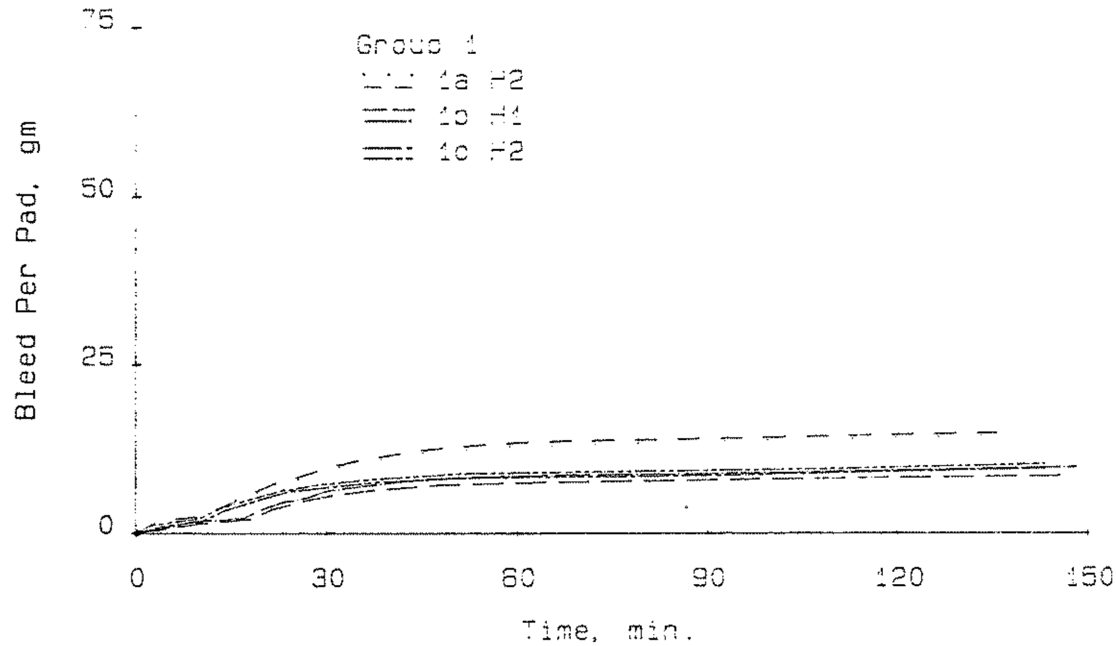

Fig. 2.13 Bleed Test Curves for Group I Slabs.

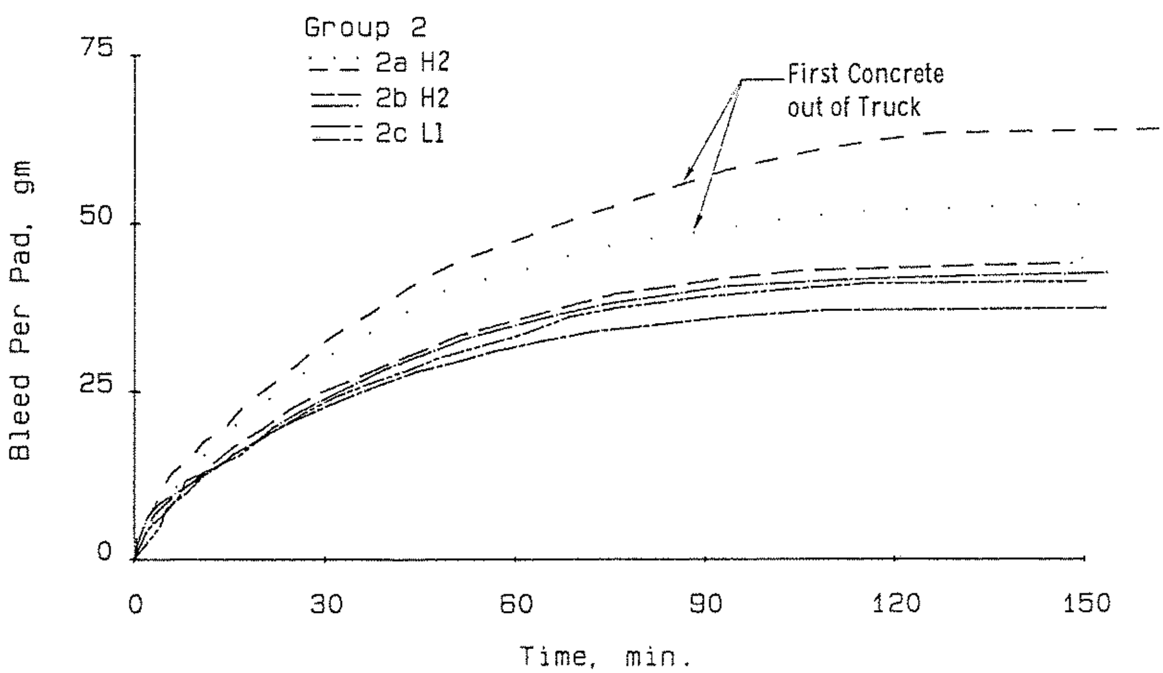

Fig. 2.14 Bleed Test Curves for Group 2 Slabs.

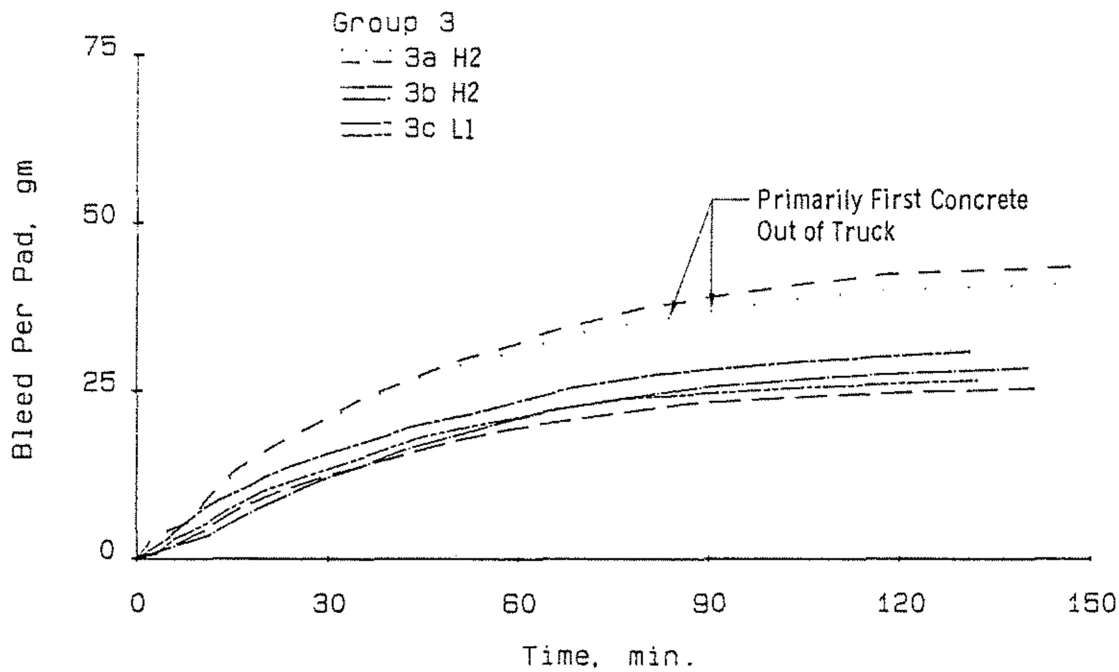

Fig. 2.15 Bleed Test Curves for Group 3 Slabs.

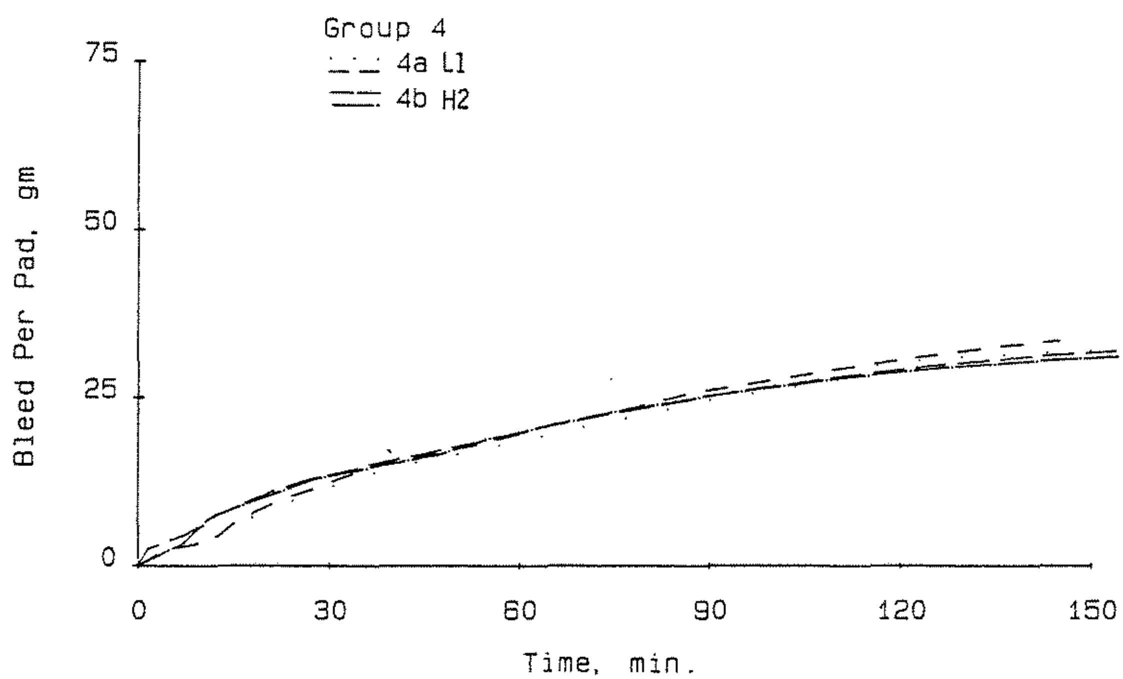

Fig. 2.16 Bleed Test Curves for Group 4 Slabs.

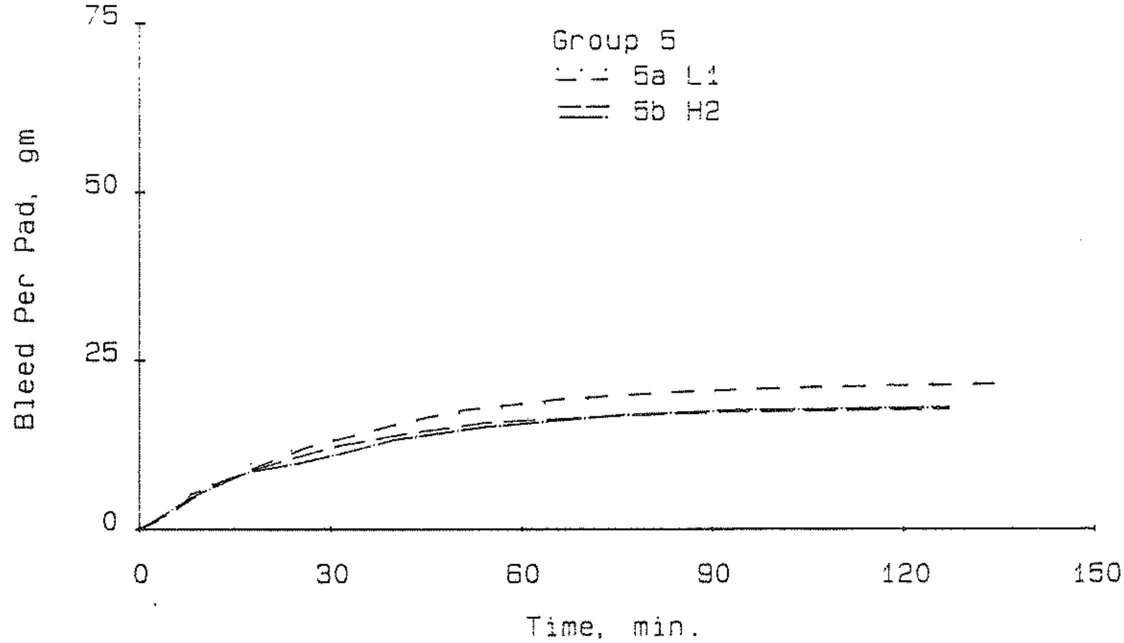

Fig. 2.17 Bleed Test Curves for Group 5 Slabs.

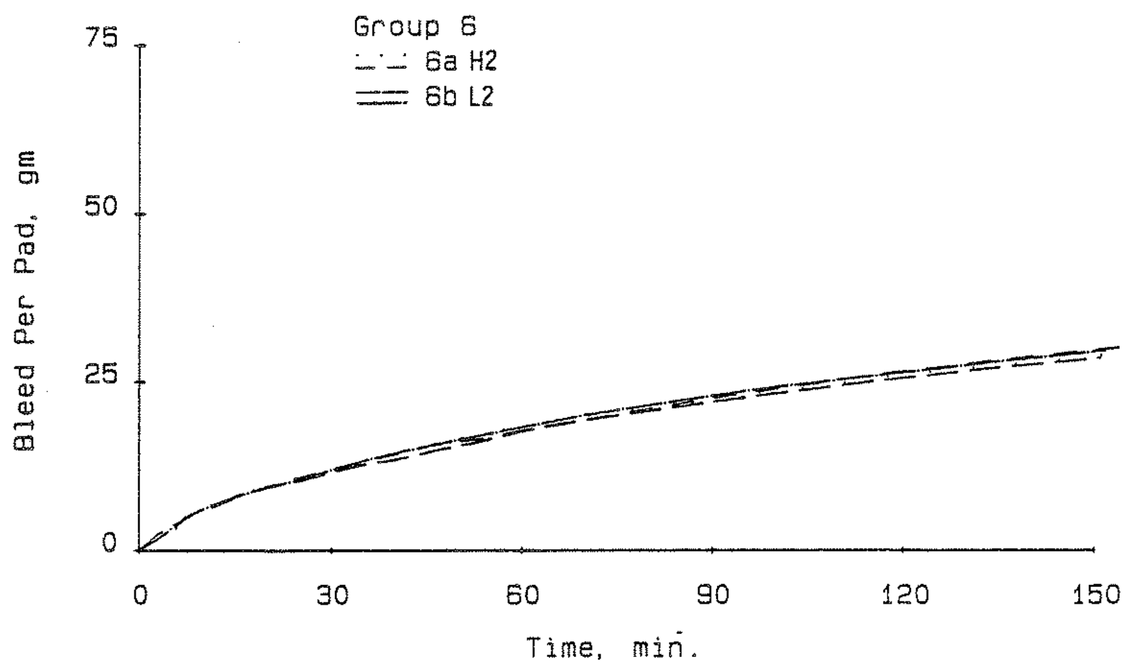

Fig. 2.18 Bleed Test Curves for Group 6 Slabs.

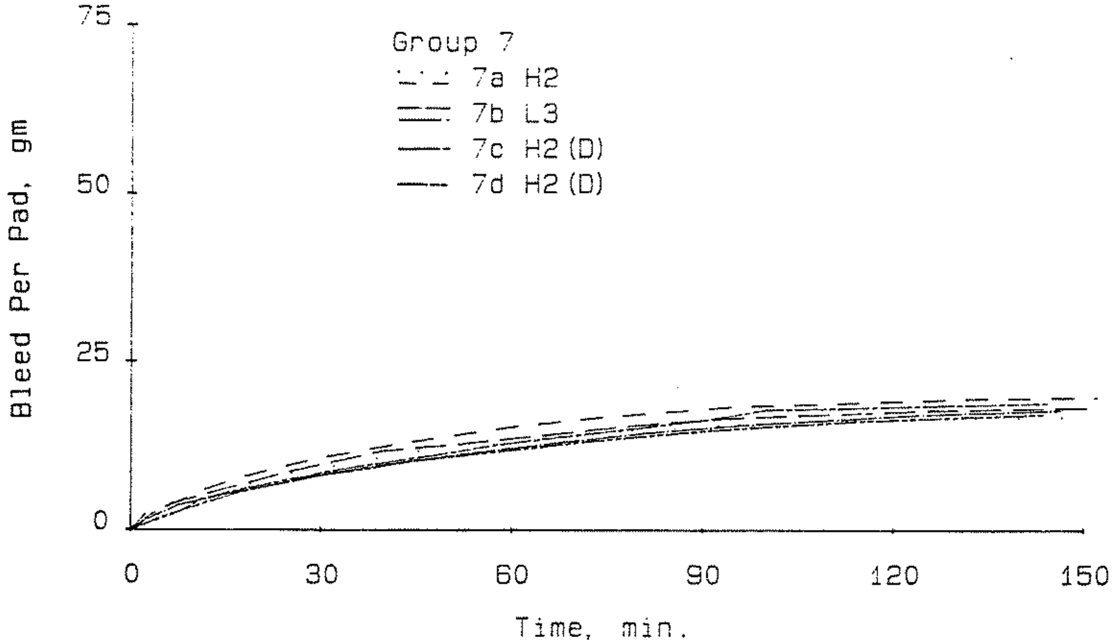

Fig. 2.19 Bleed Test Curves for Group 7 Slabs.

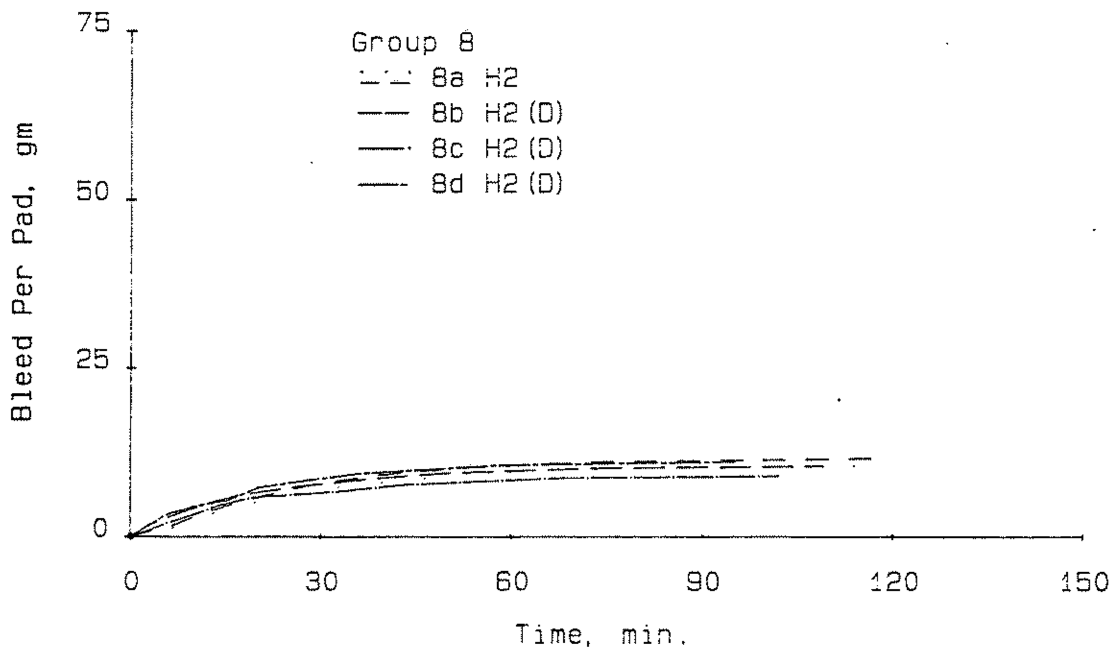

Fig. 2.20 Bleed Test Curves for Group 8 Slabs.

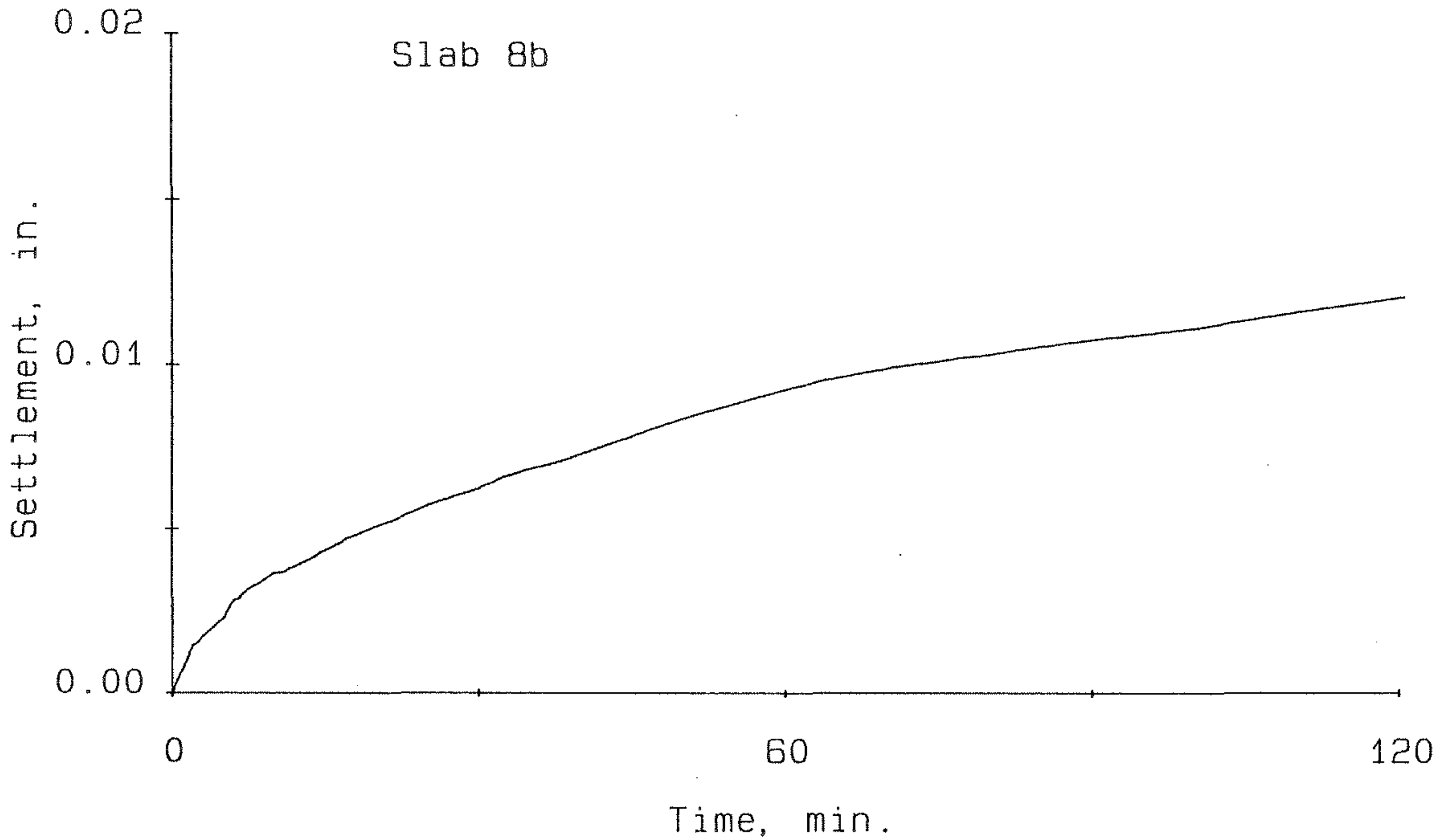

Fig. 2.21 Settlement As A Function of Time for Slab 8b.

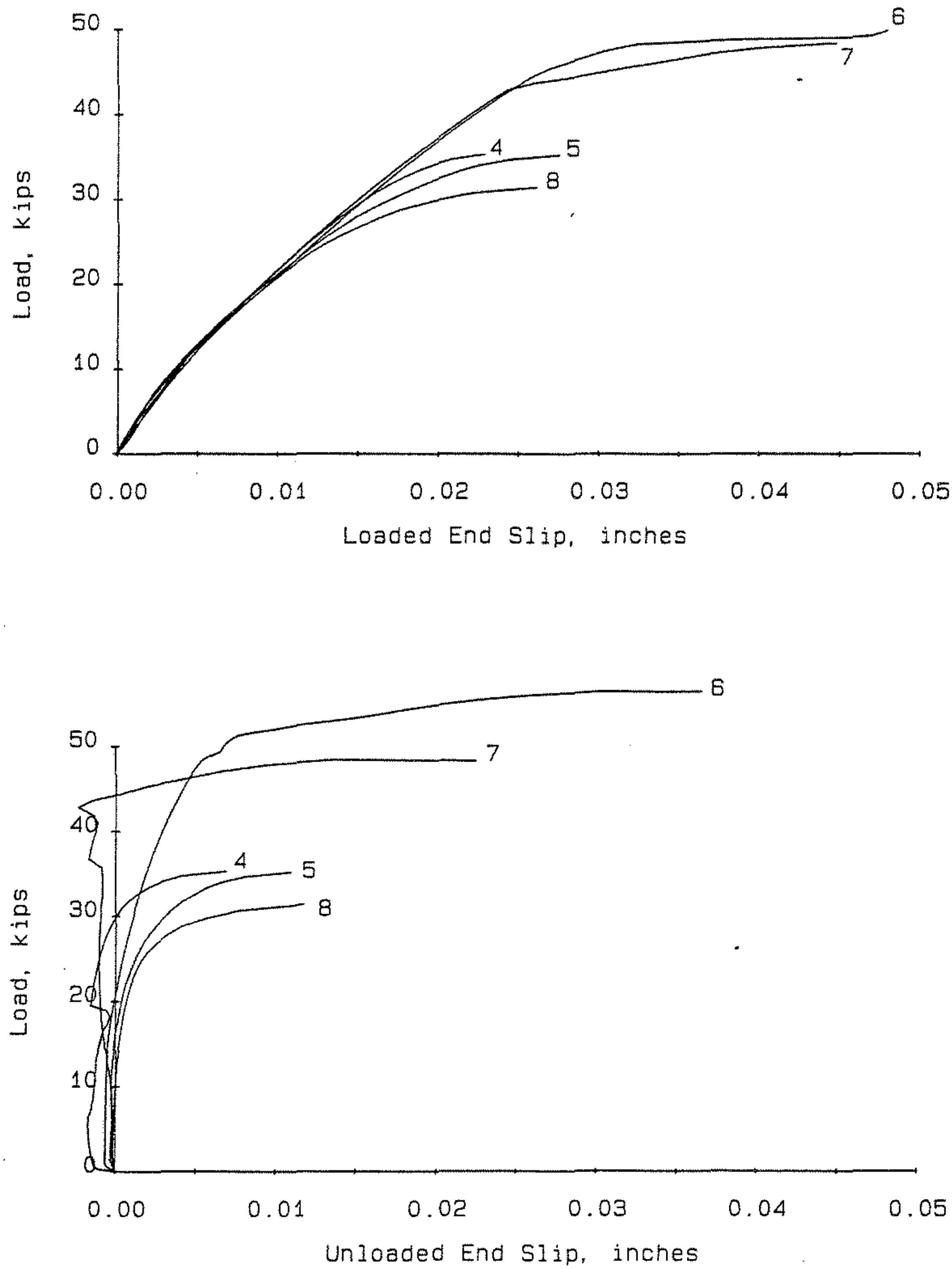

Fig. 2.22 Load-Slip Curves for Slab Ic.

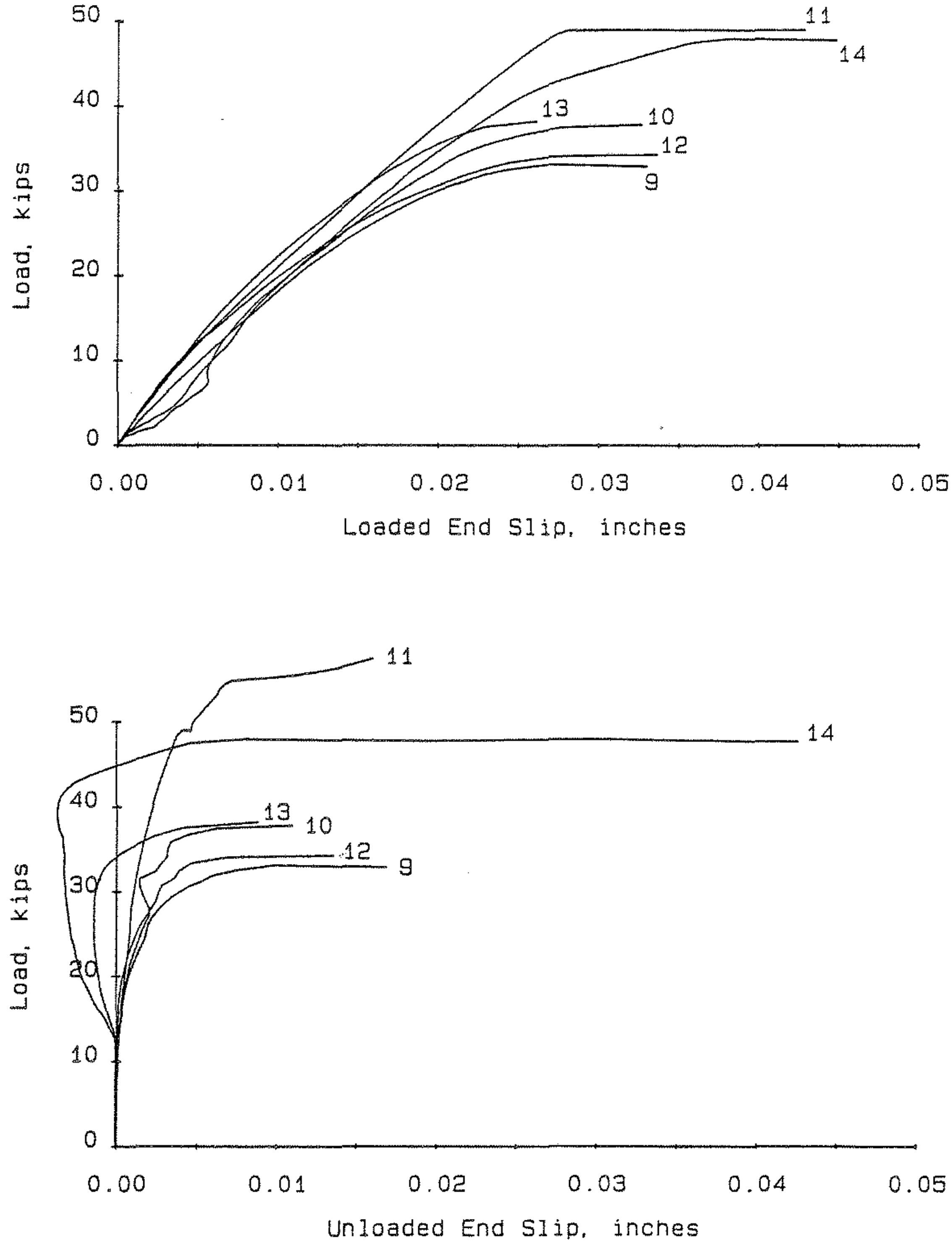

Fig. 2.23 Load-Slip Curves for Slab Ib.

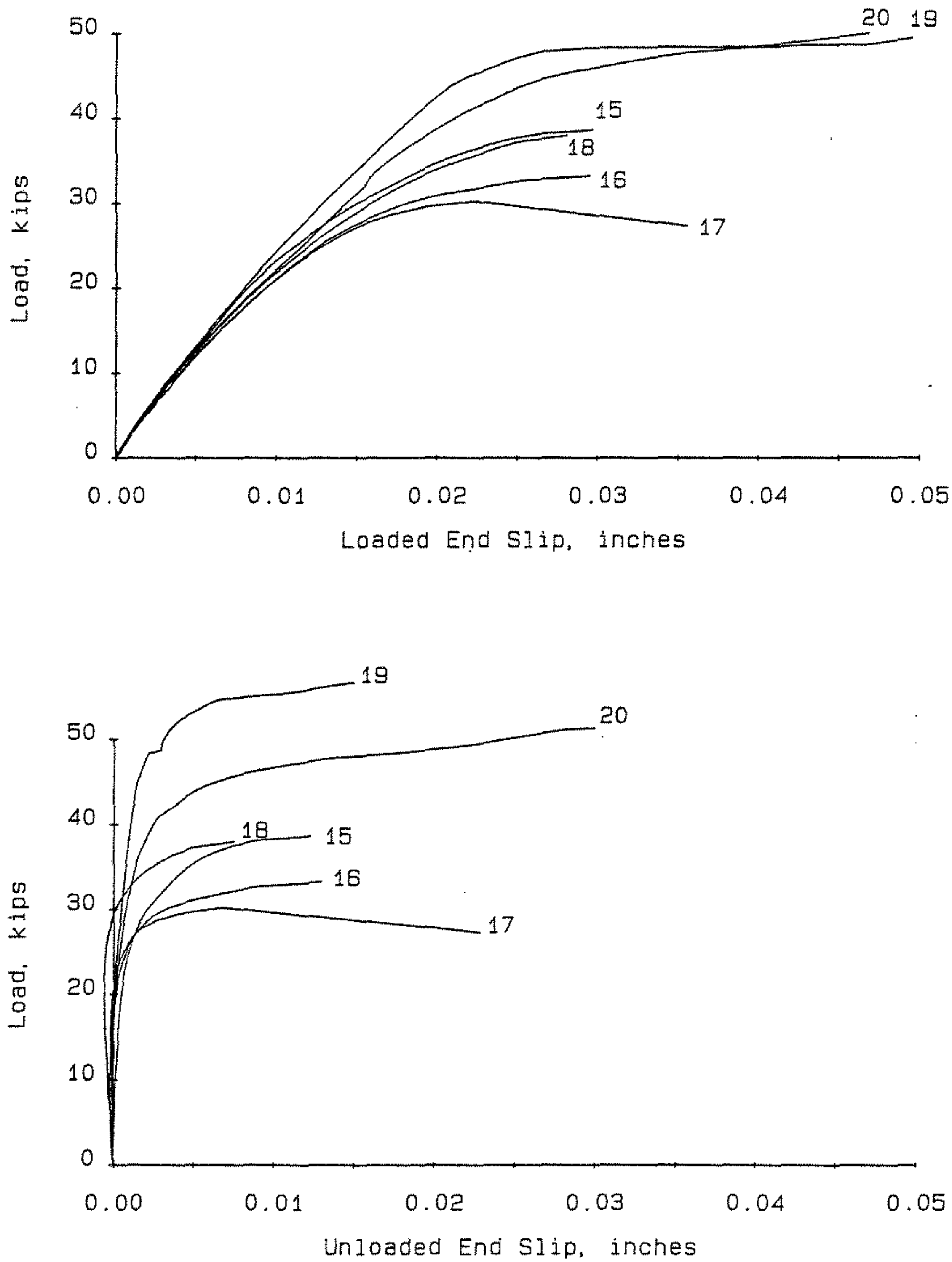

Fig. 2.24 Load-slip Curves for Slab Ia.

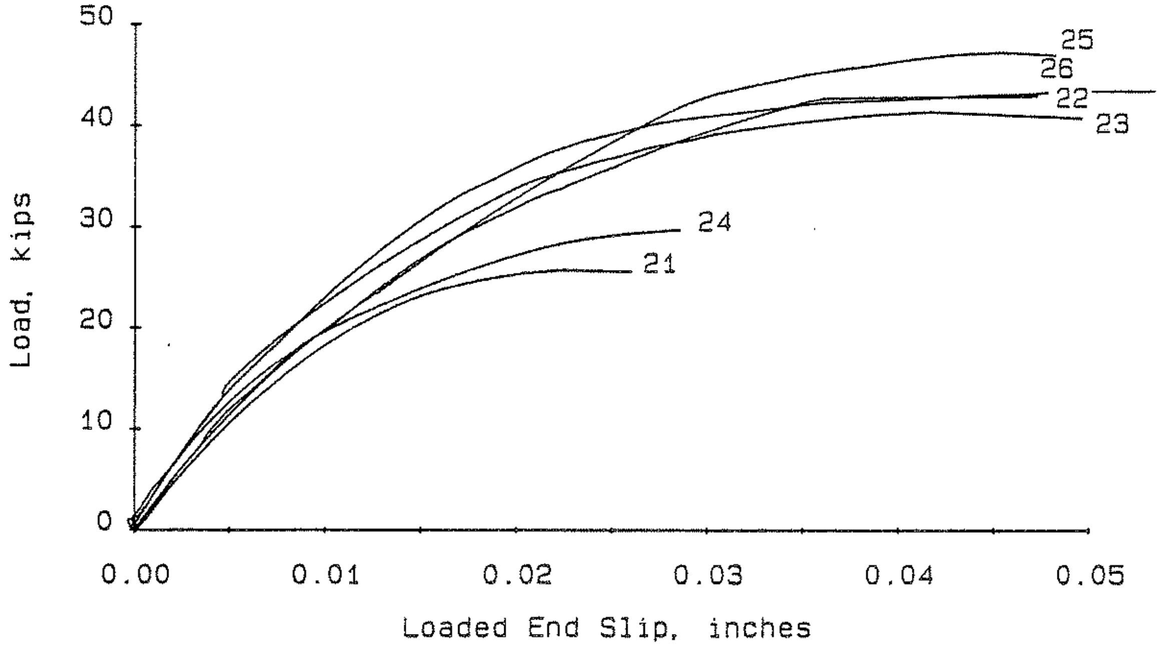

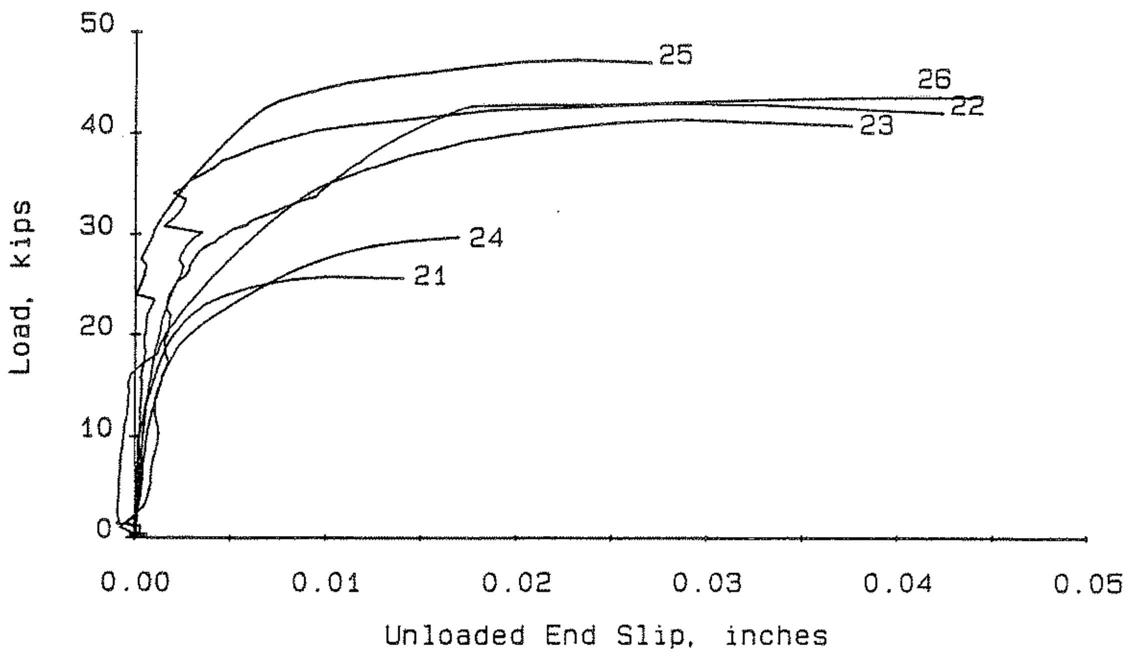

Fig. 2.25 Load-Slip Curves for Slab 3a.

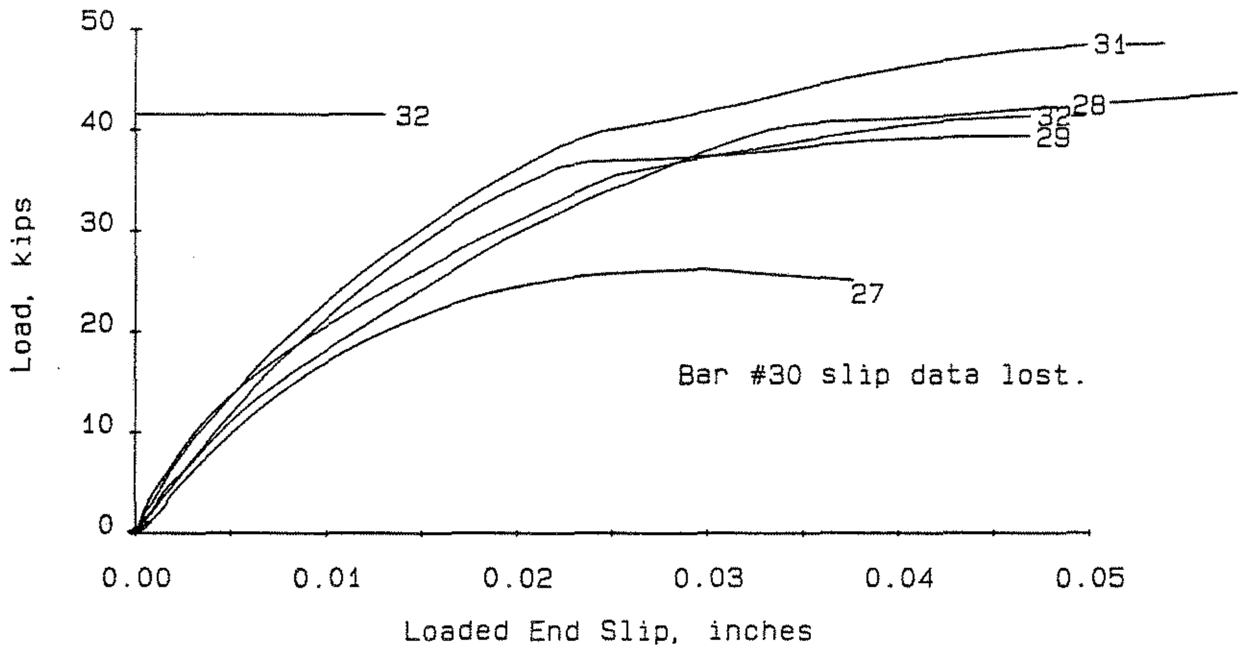

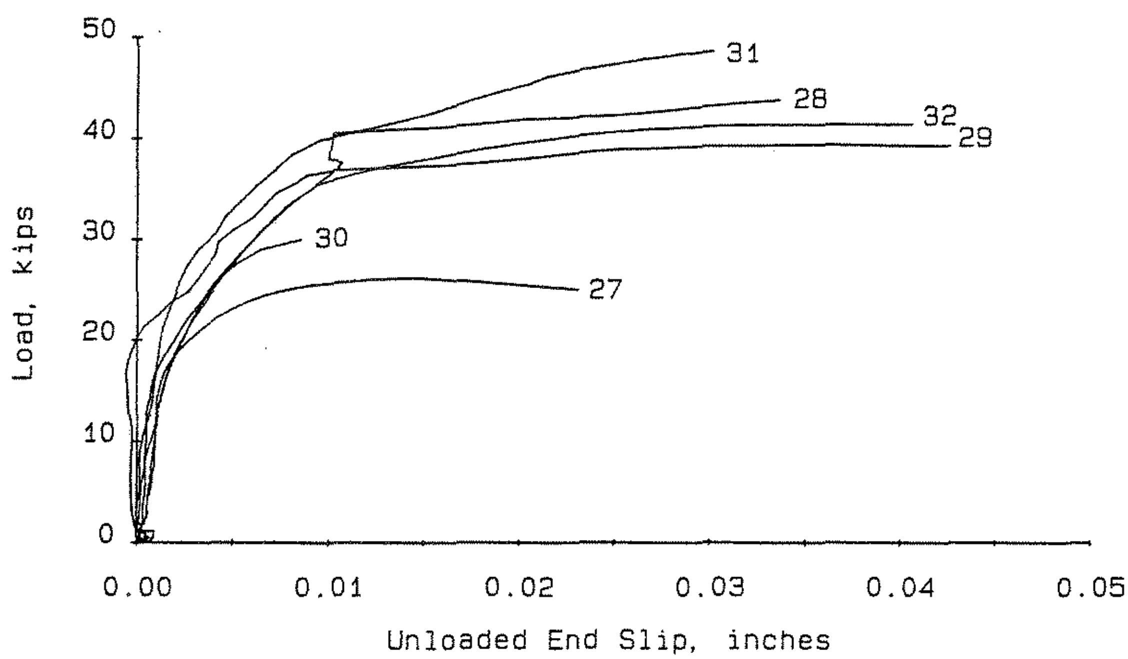

Fig. 2.26 Load-Slip Curves for Slab 3c.

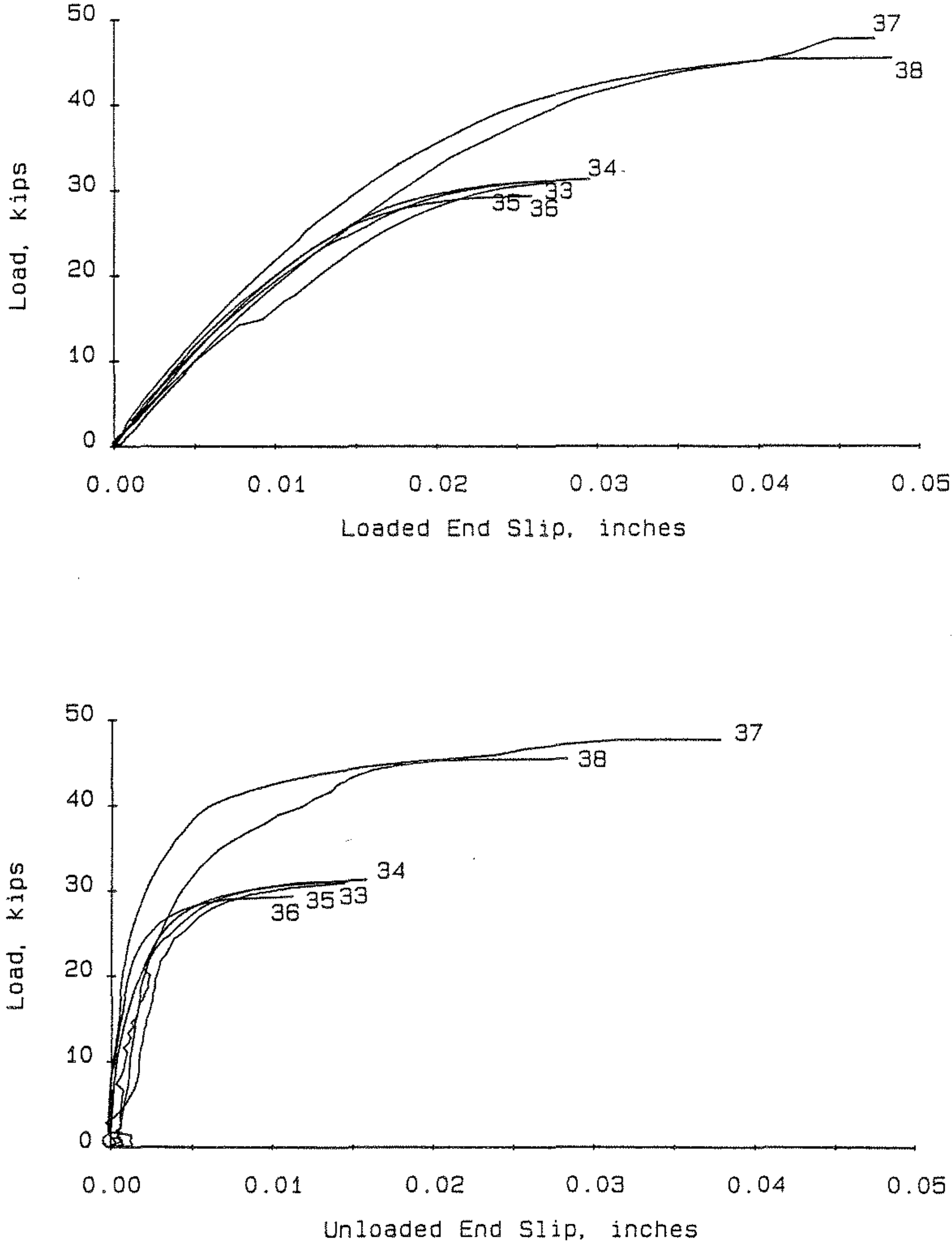

Fig. 2.27 Load-Slip Curves for Slab 3b.

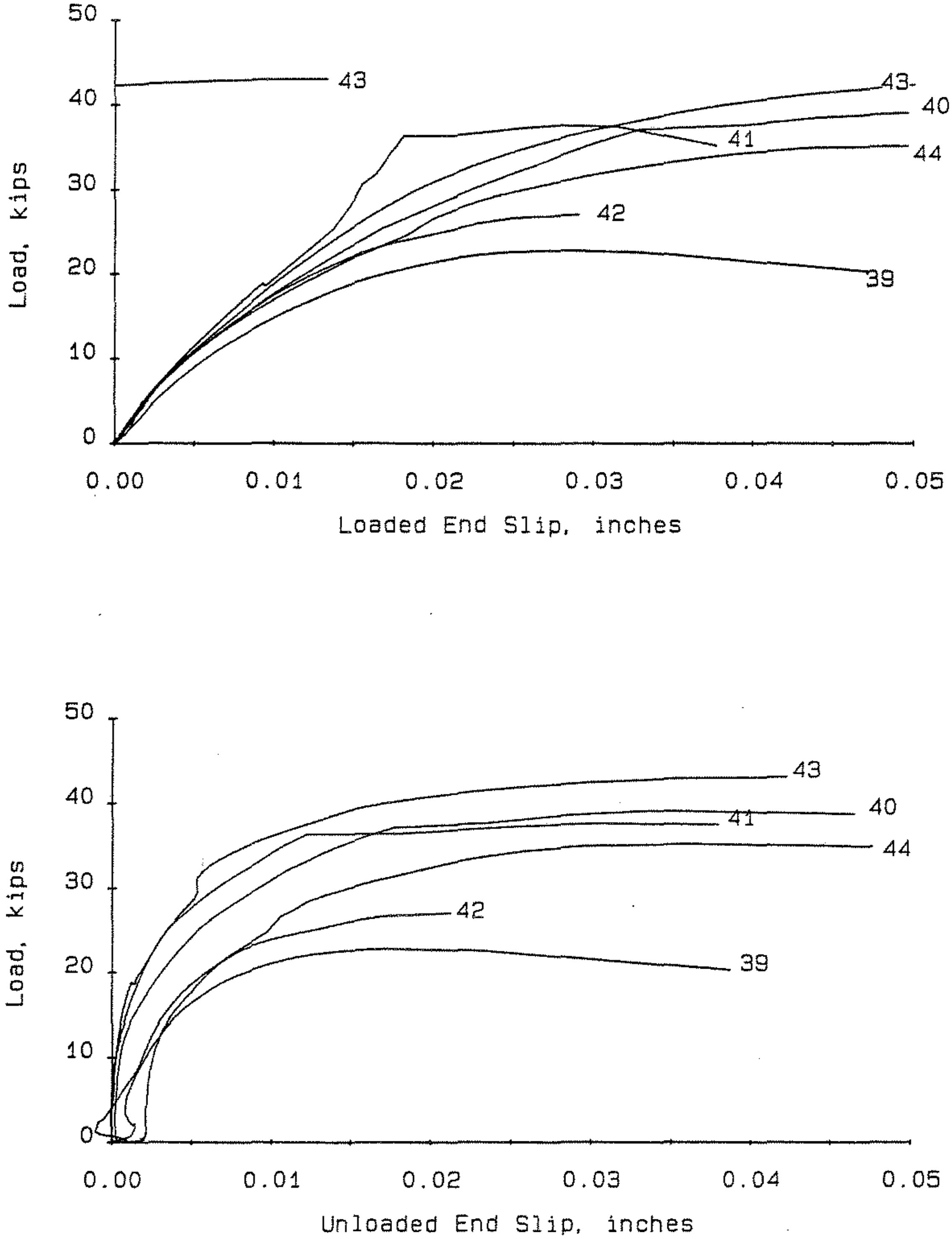

Fig. 2.28 Load-Slip Curves for Slab 2c.

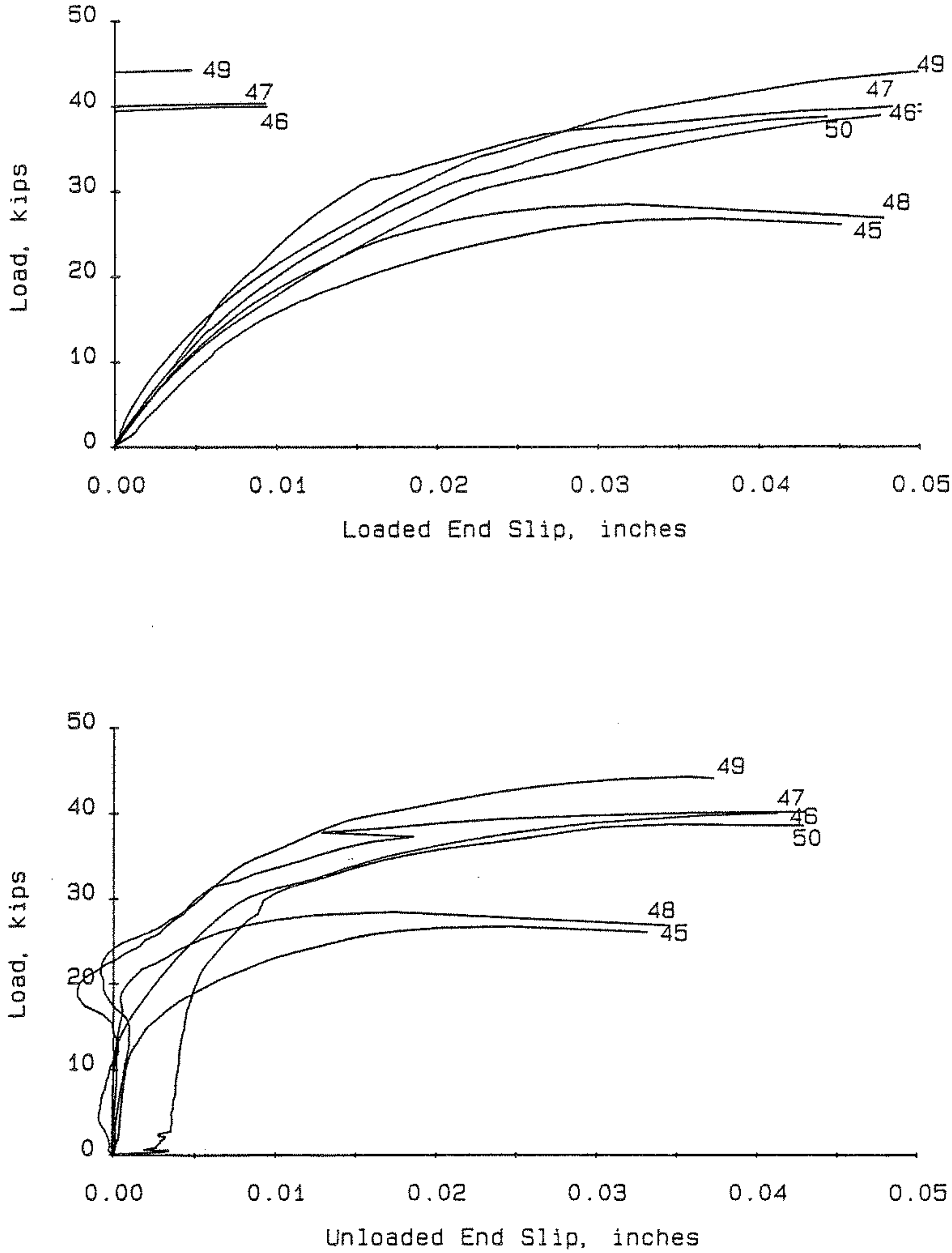

Fig. 2.29 Load-Slip Curves for Slab 2b.

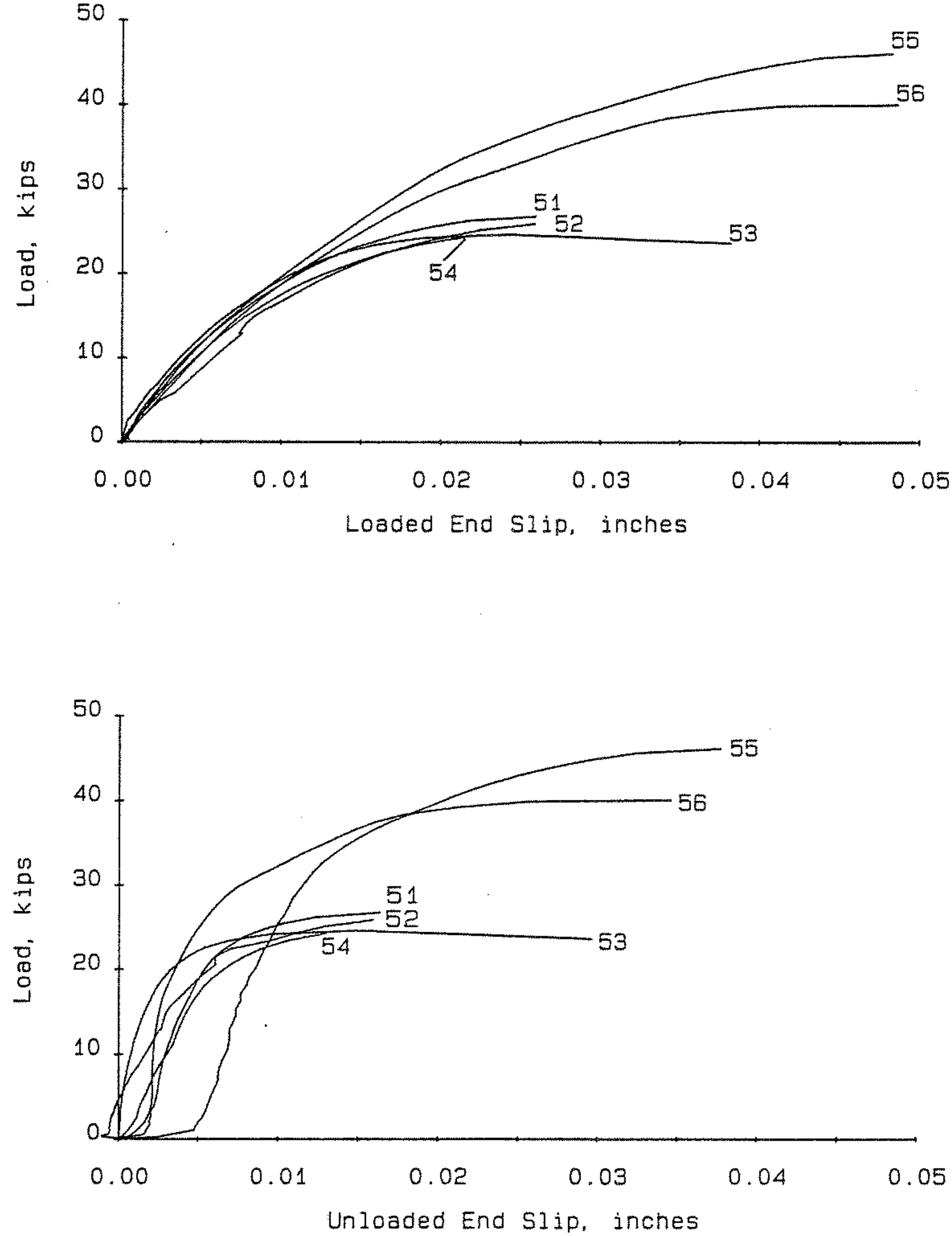

Fig. 2.30 Load-Slip Curves for Slab 2a.

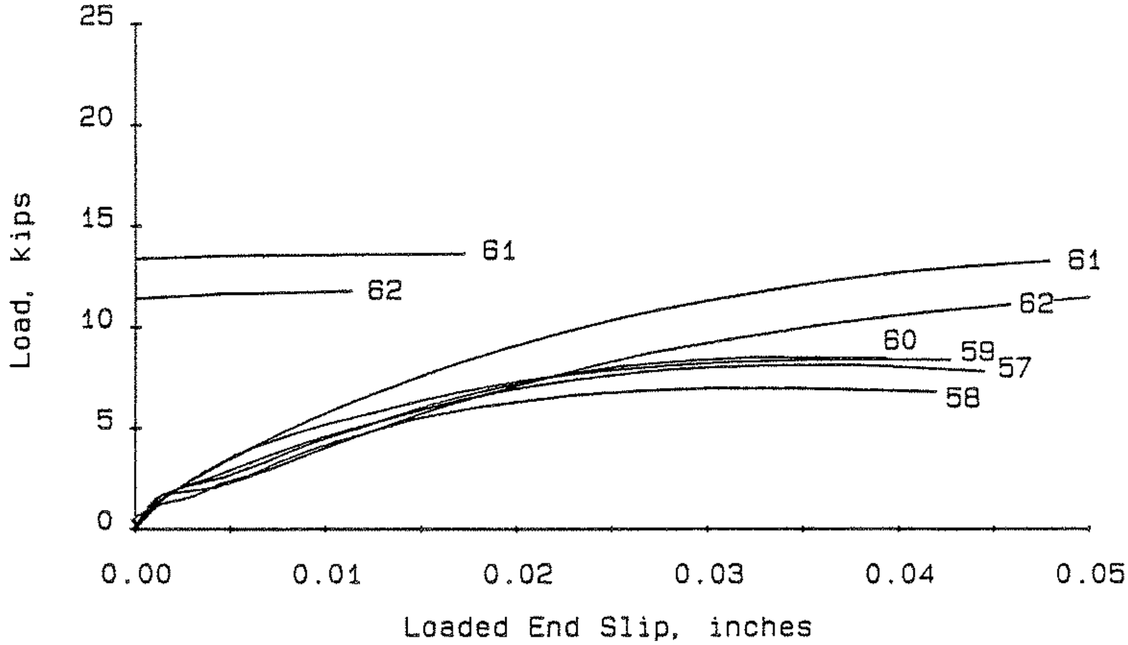

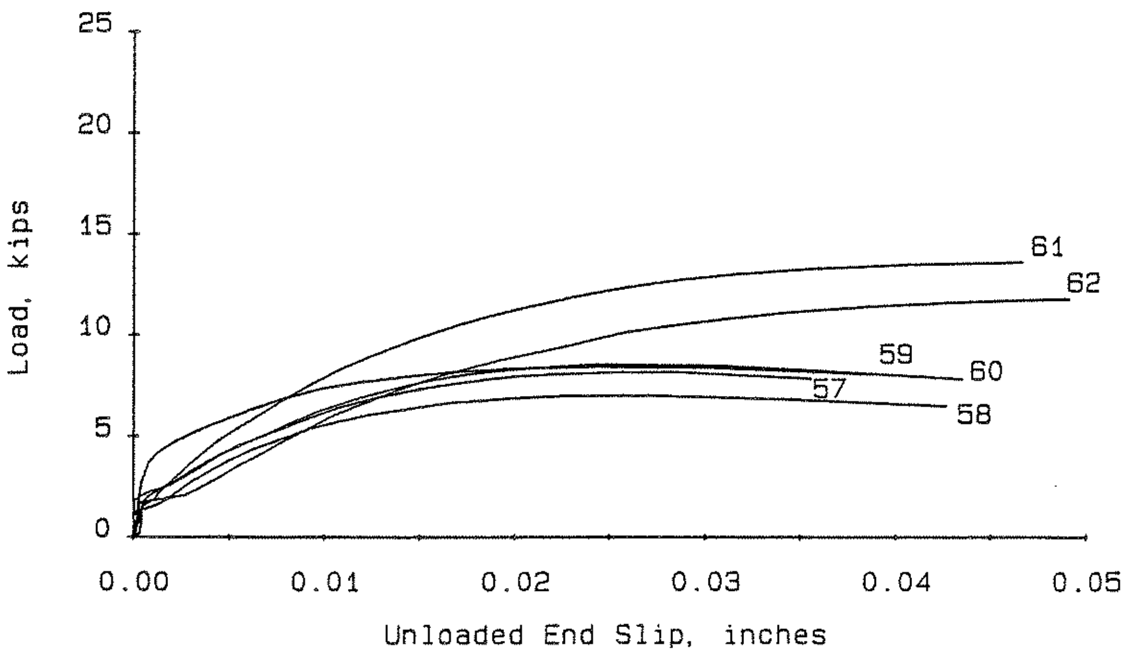

Fig. 2.31 Load-Slip Curves for Slab 4b.

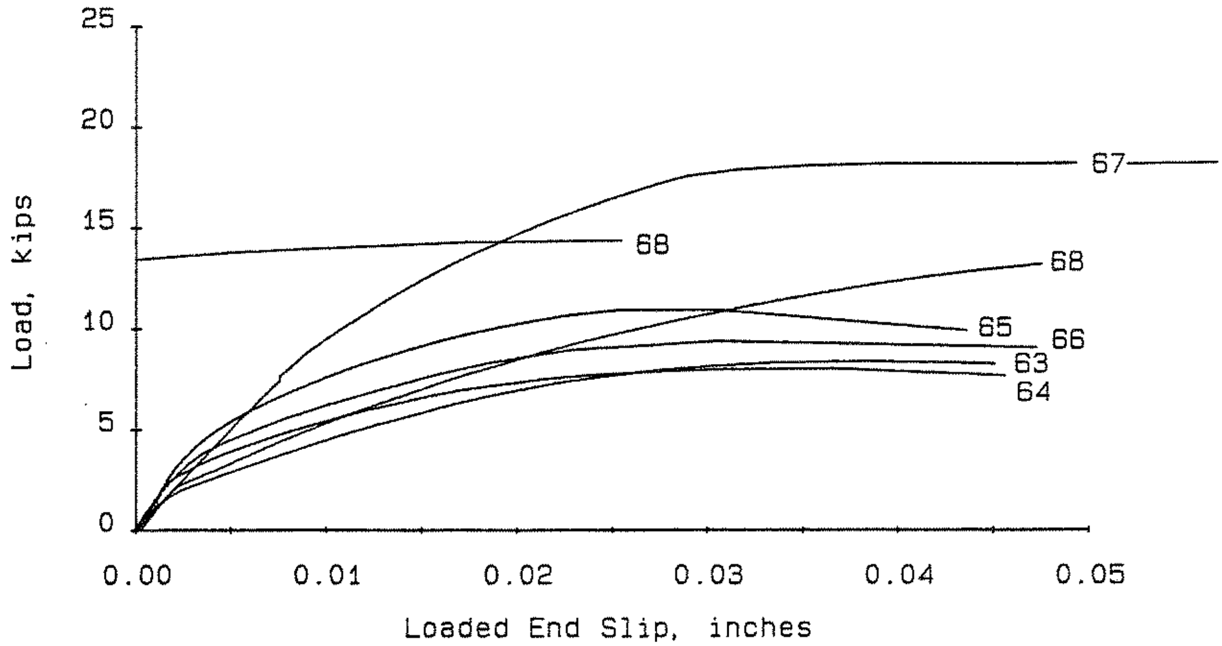

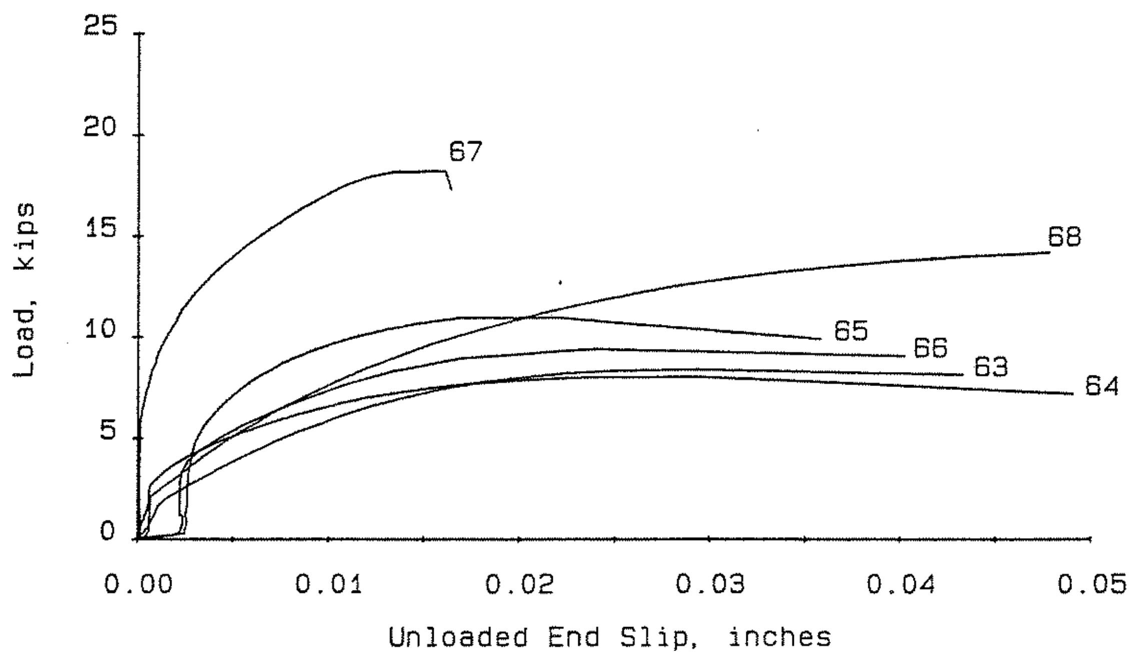

Fig. 2.32 Load-Slip Curves for Slab 4a.

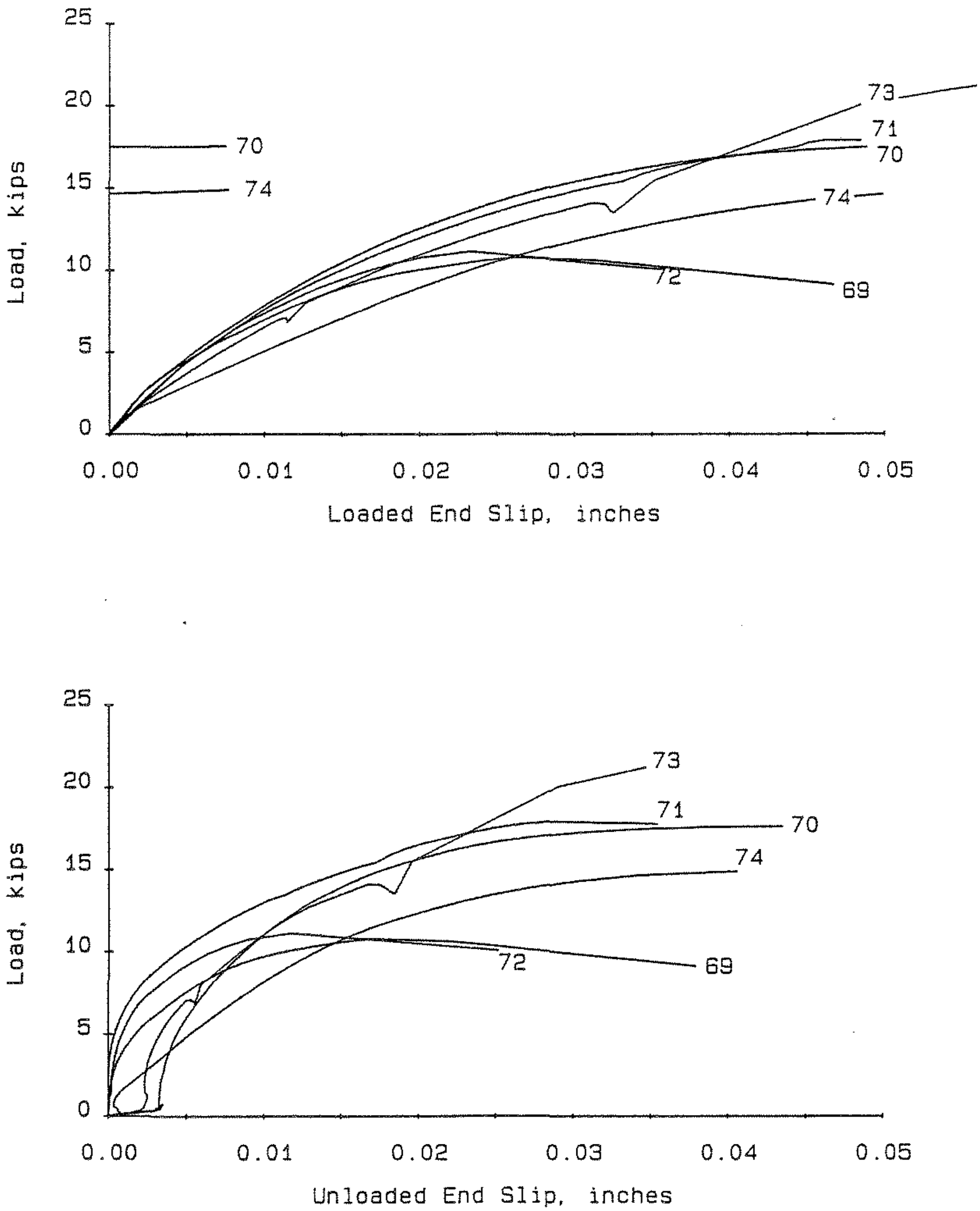

Fig. 2.33 Load-Slip Curves for Slab 5b.

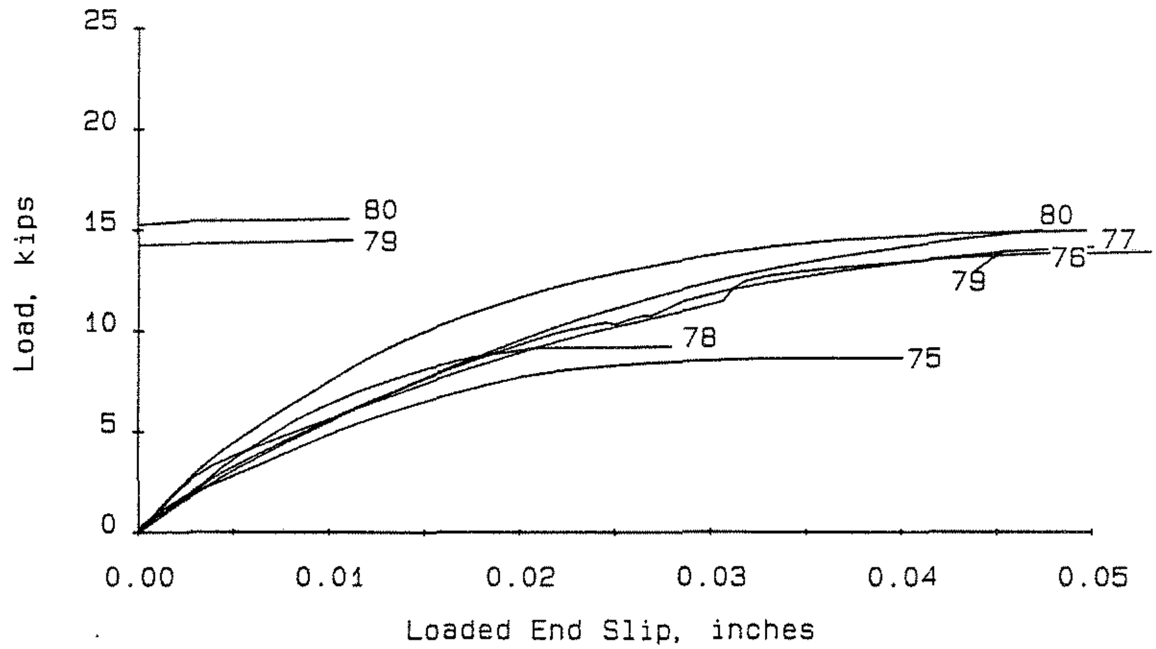

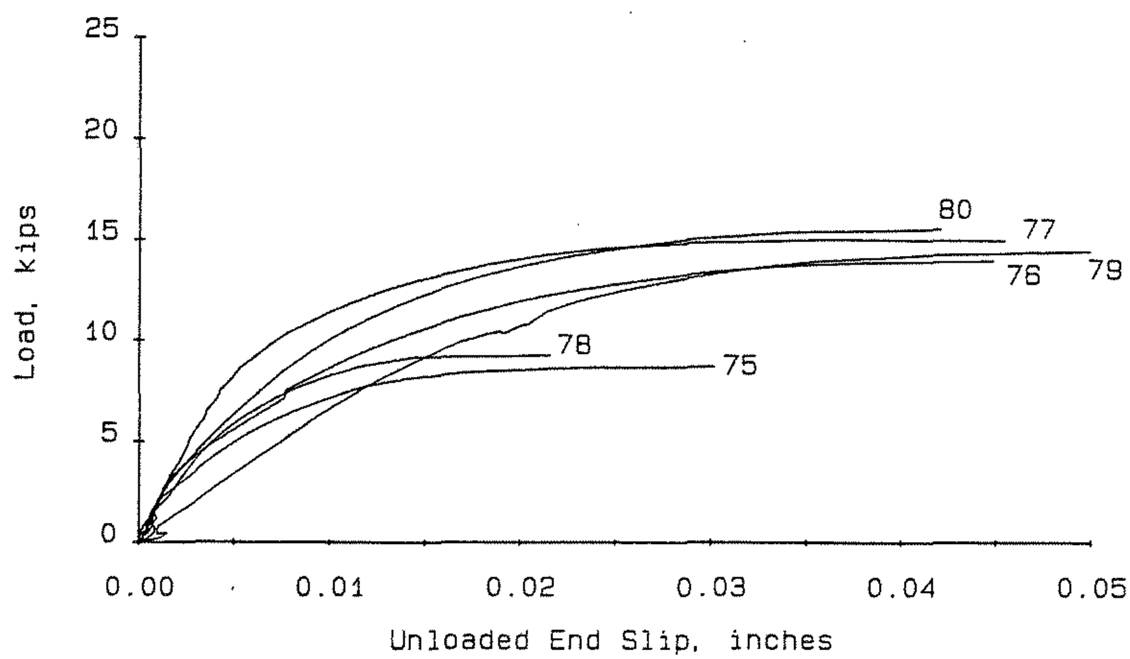

Fig. 2.34 Load-Slip Curves for Slab 5a.

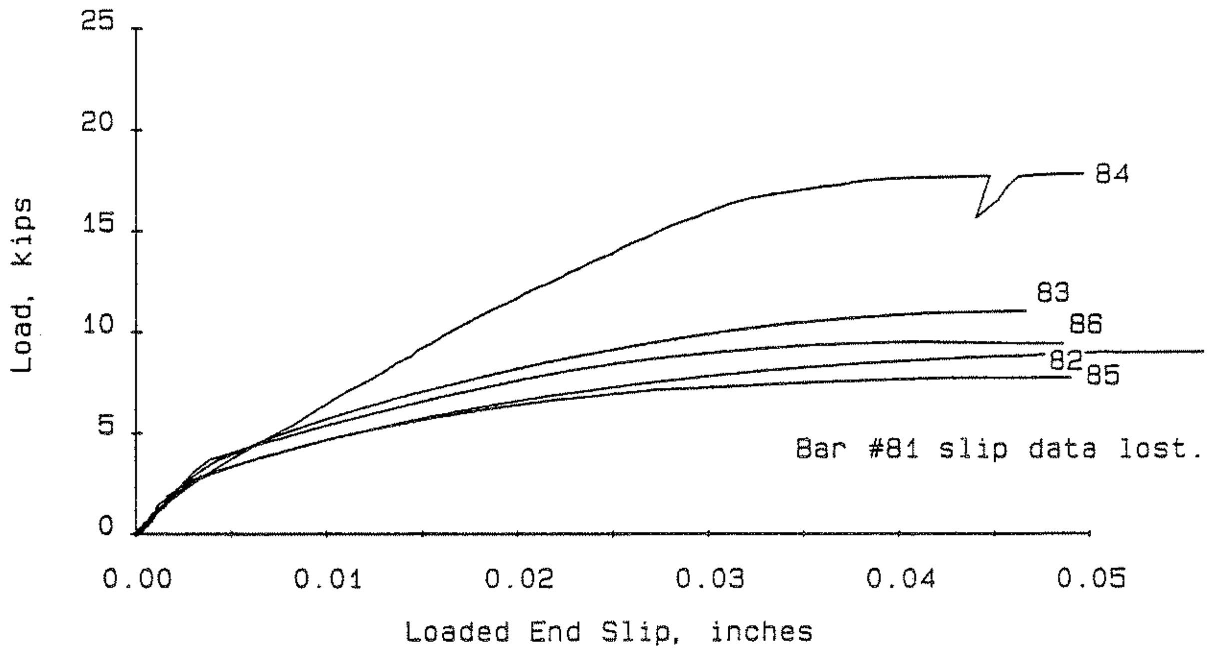

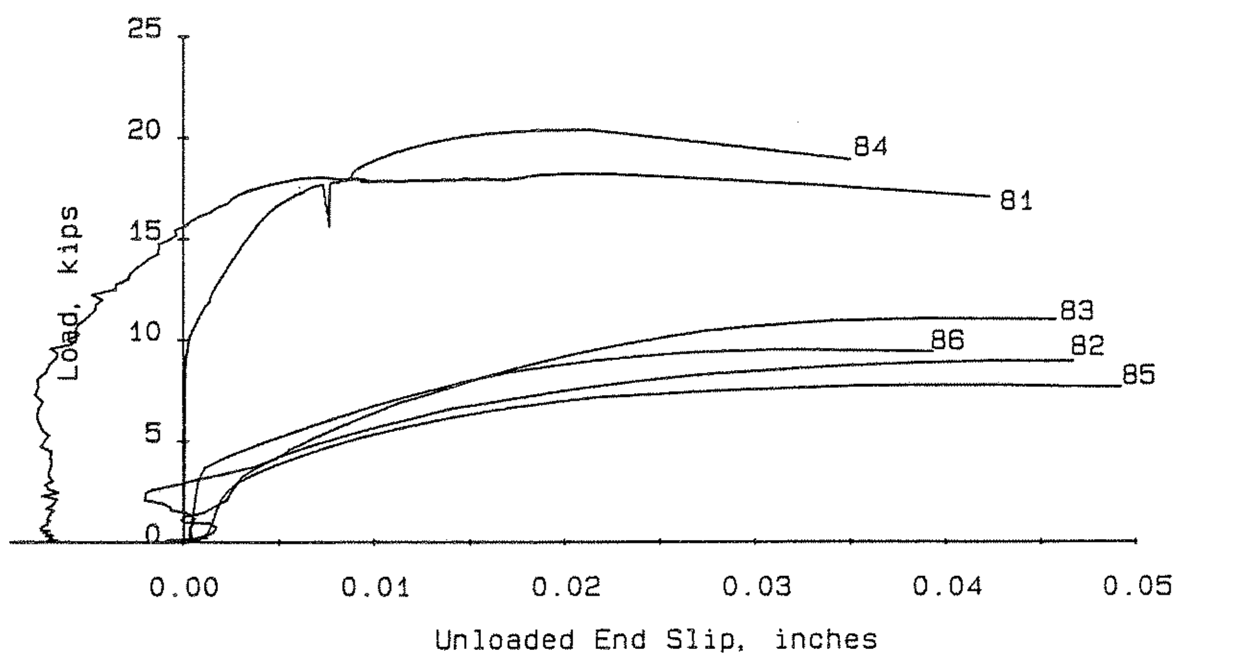

Fig. 2.35 Load-Slip Curves for Slab 6b.

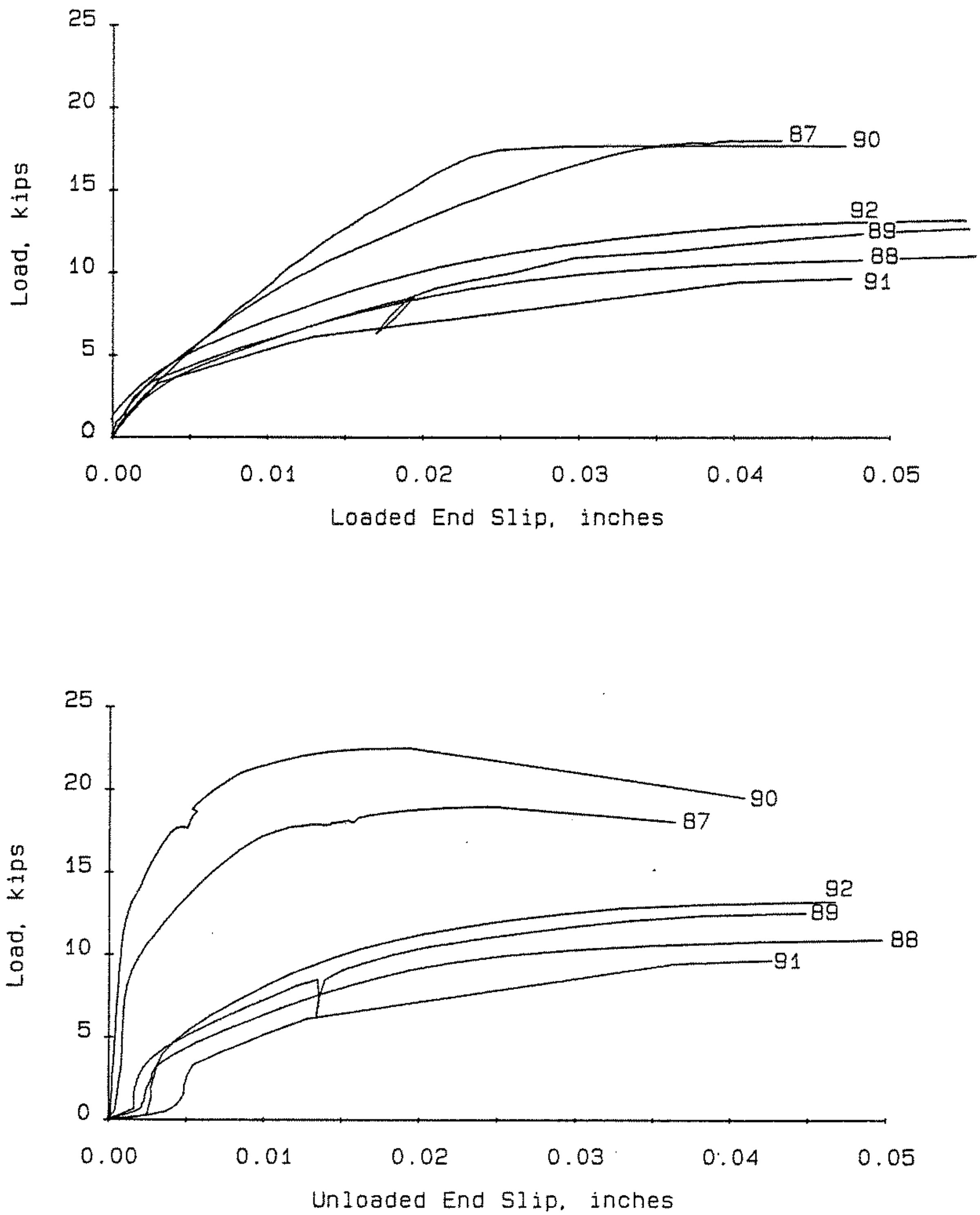

Fig. 2.36 Load-Slip Curves for Slab 6a.

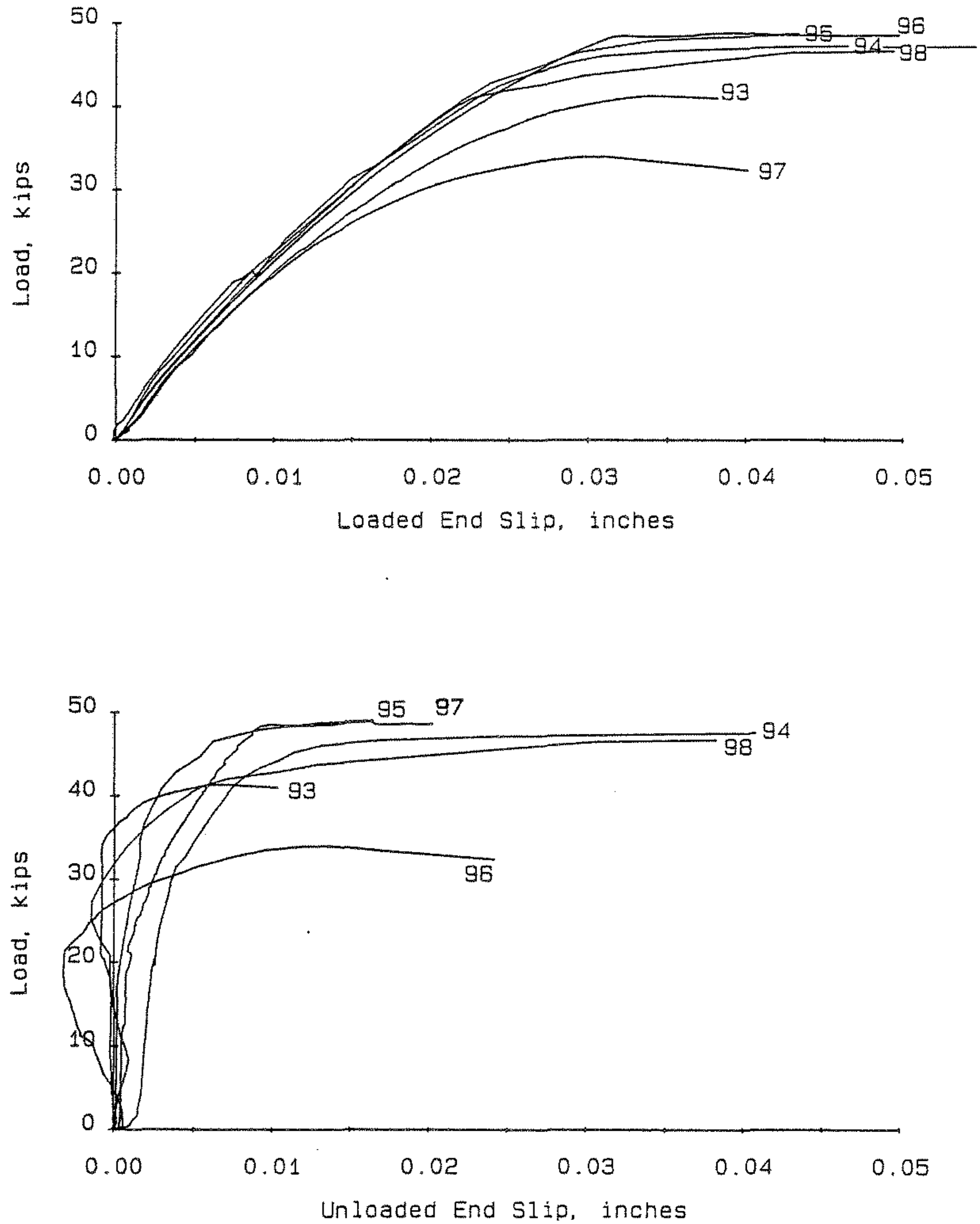

Fig. 2.37 Load-Slip Curves for Slab 7a.

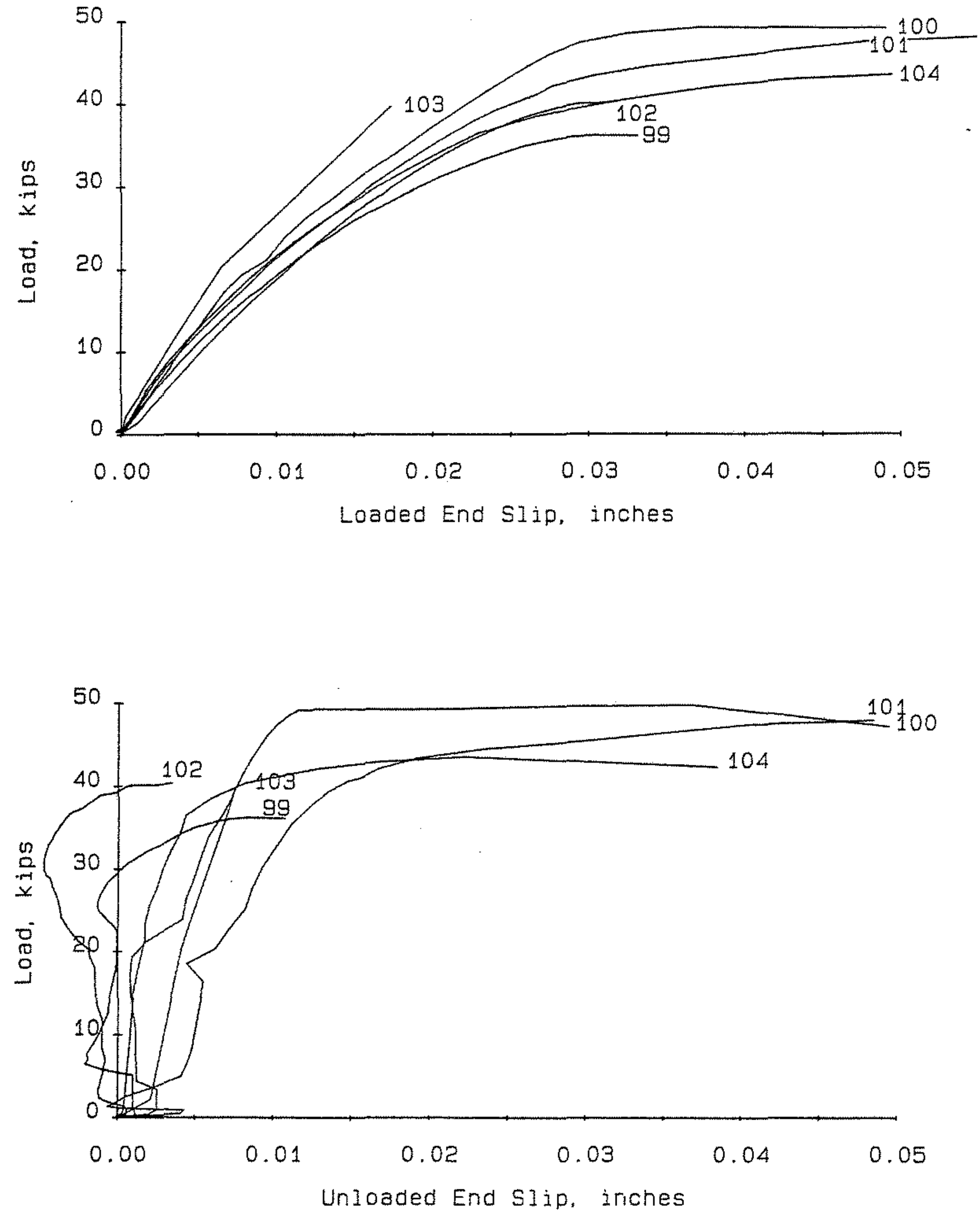

Fig. 2.38 Load-Slip Curves for Slab 7b.

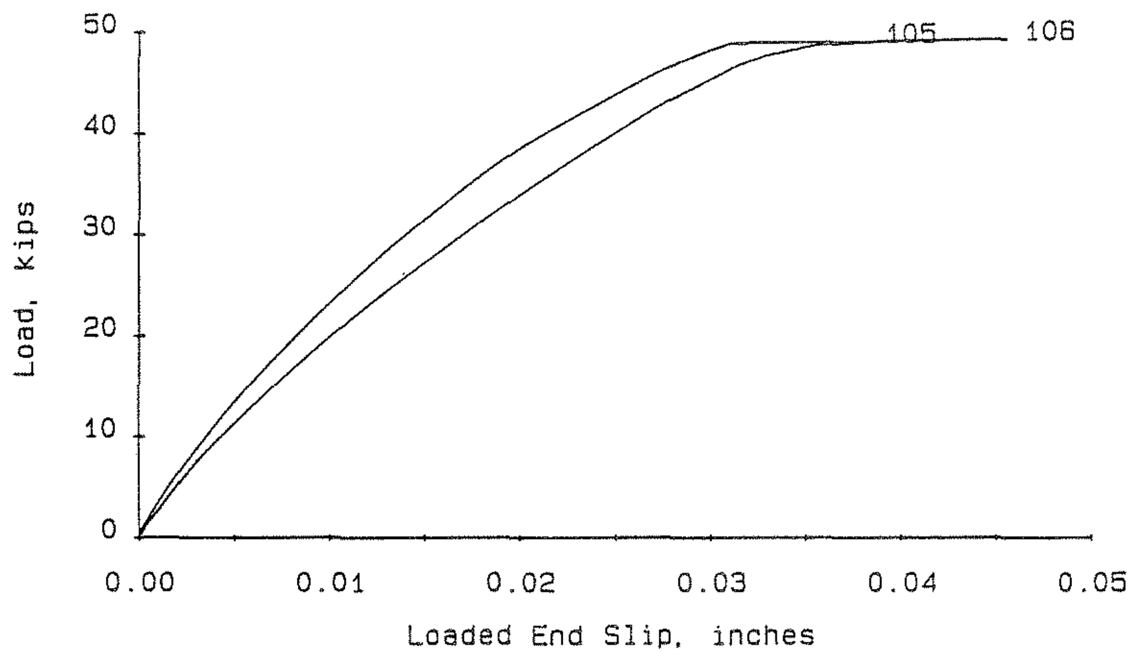

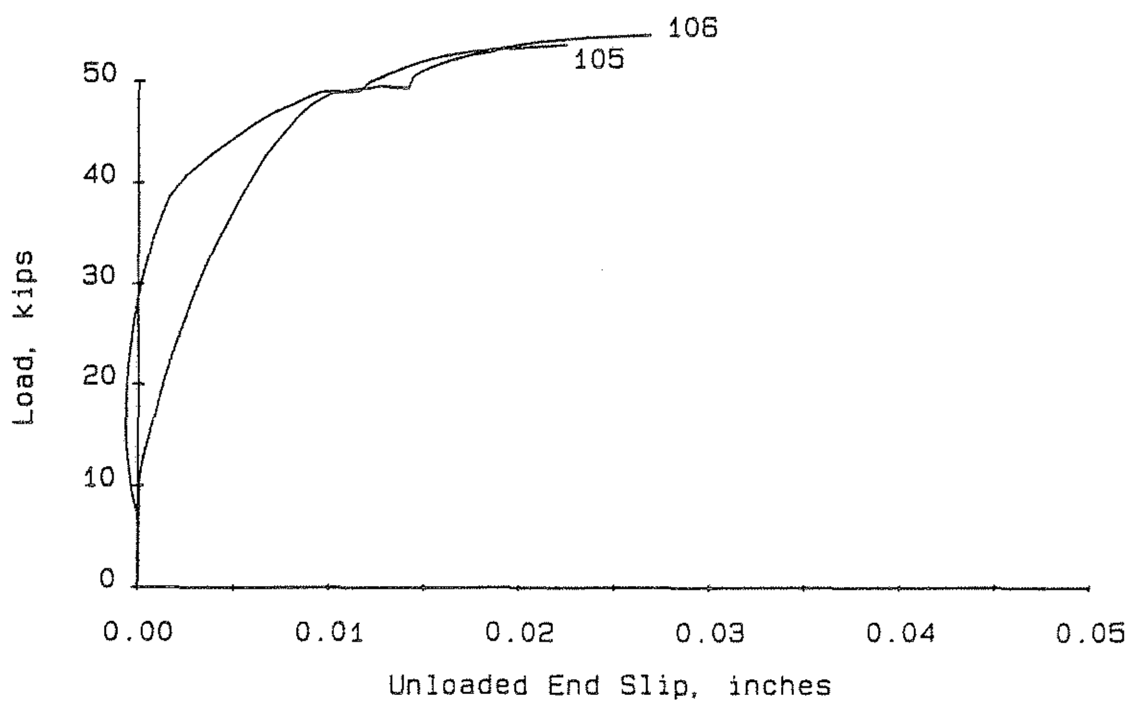

Fig. 2.39 Load-Slip Curves for Slab 7c.

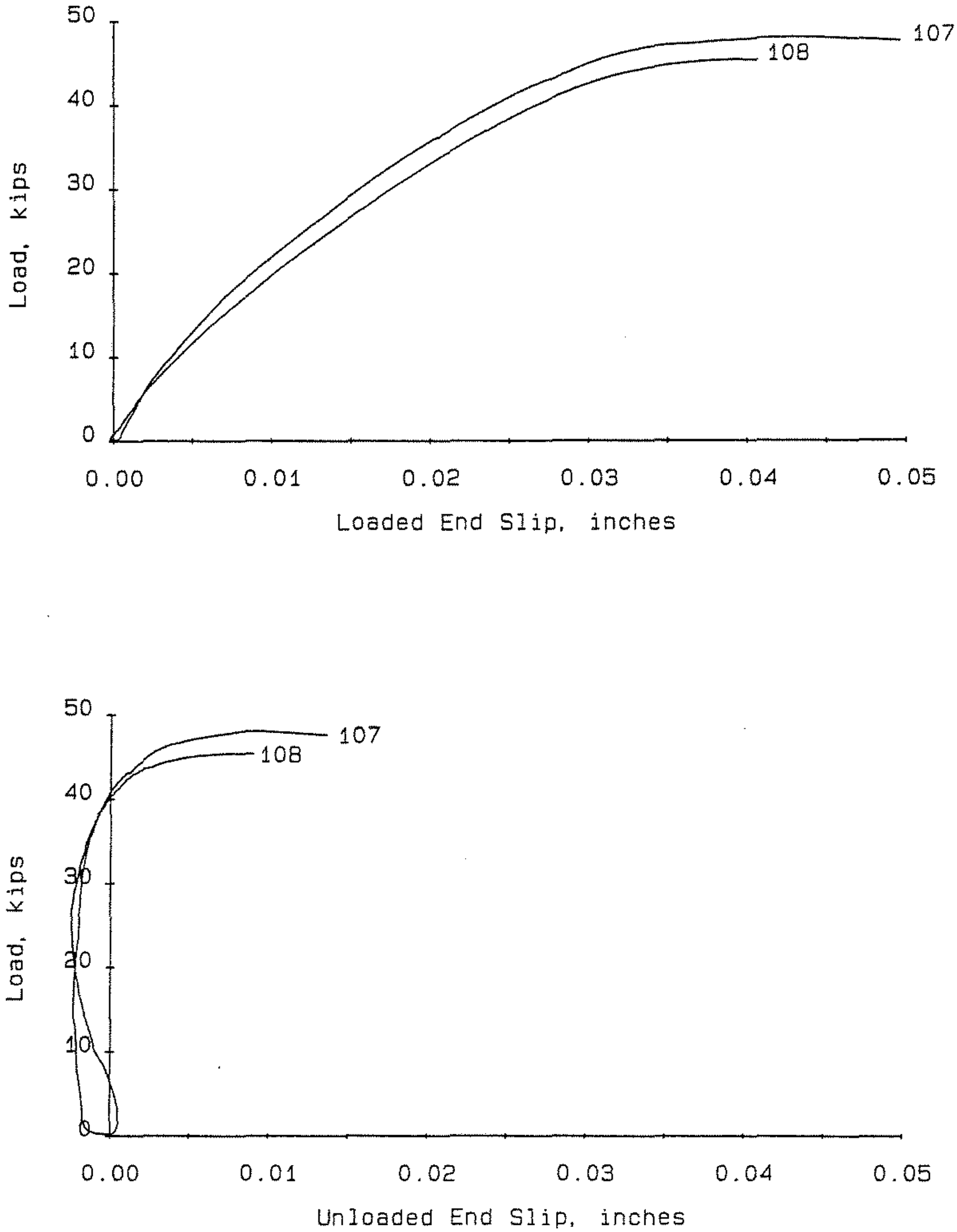

Fig. 2.40 Load-Slip Curves for Slab 7d.

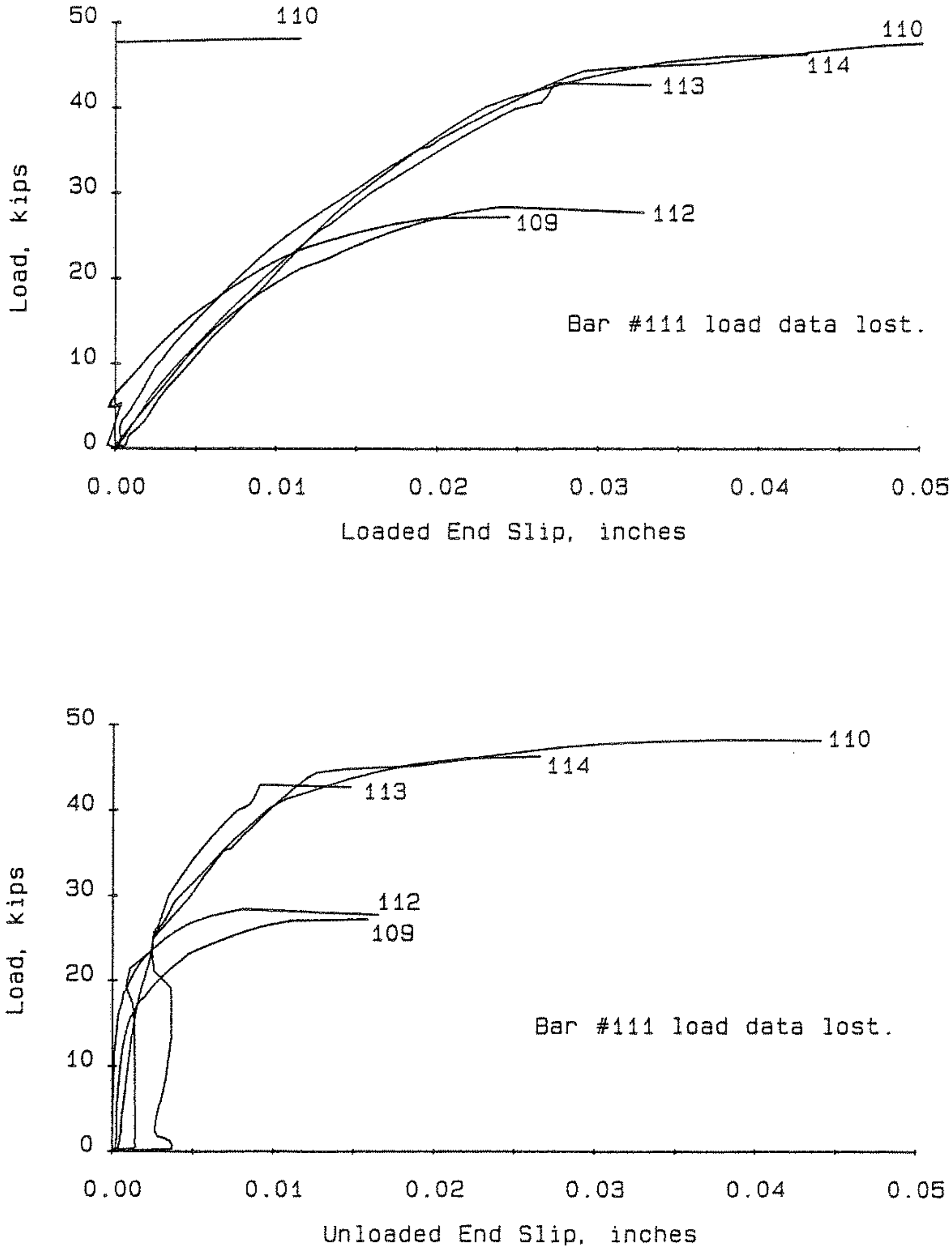

Fig. 2.41 Load-Slip Curves for Slab 8a.

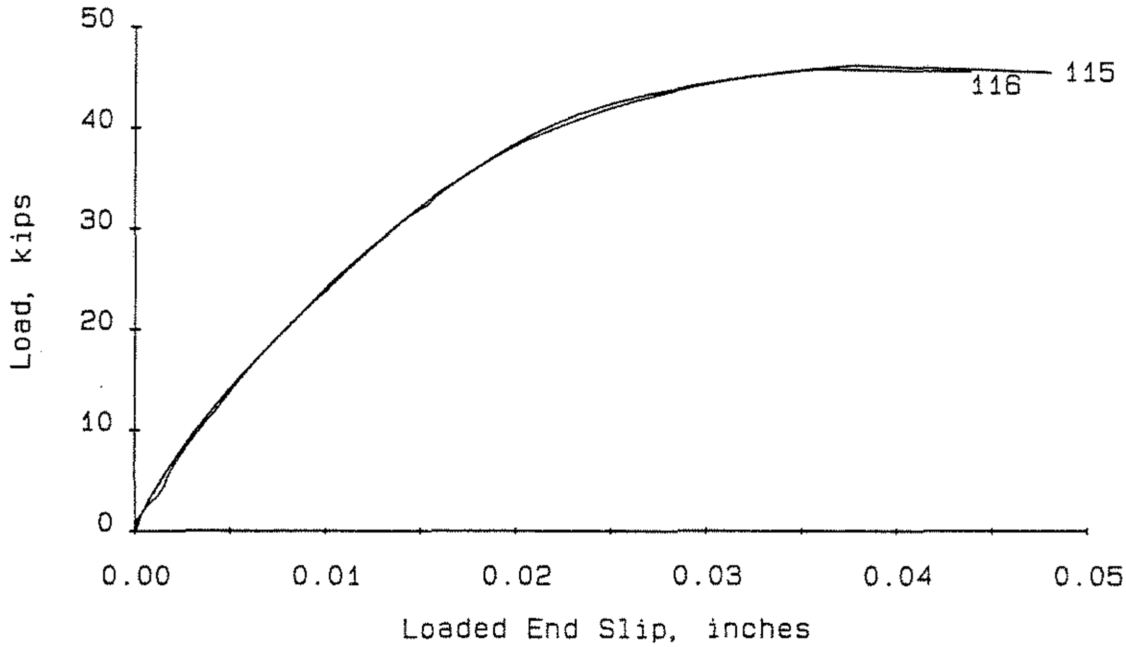

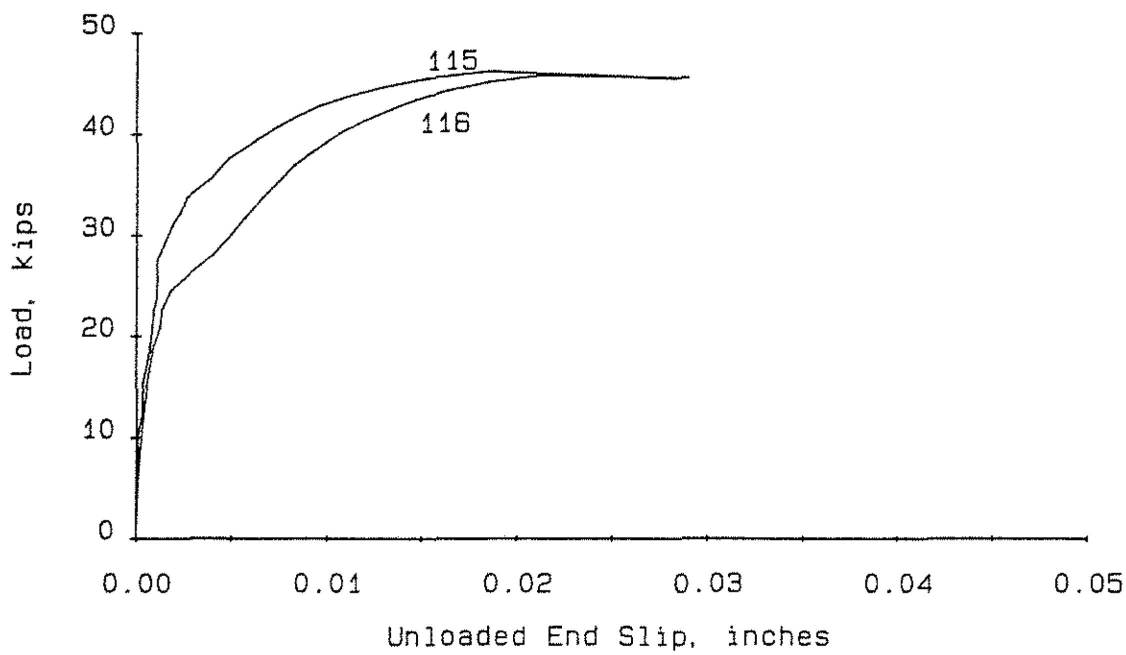

Fig. 2.42 Load-Slip Curves for Slab 8b.

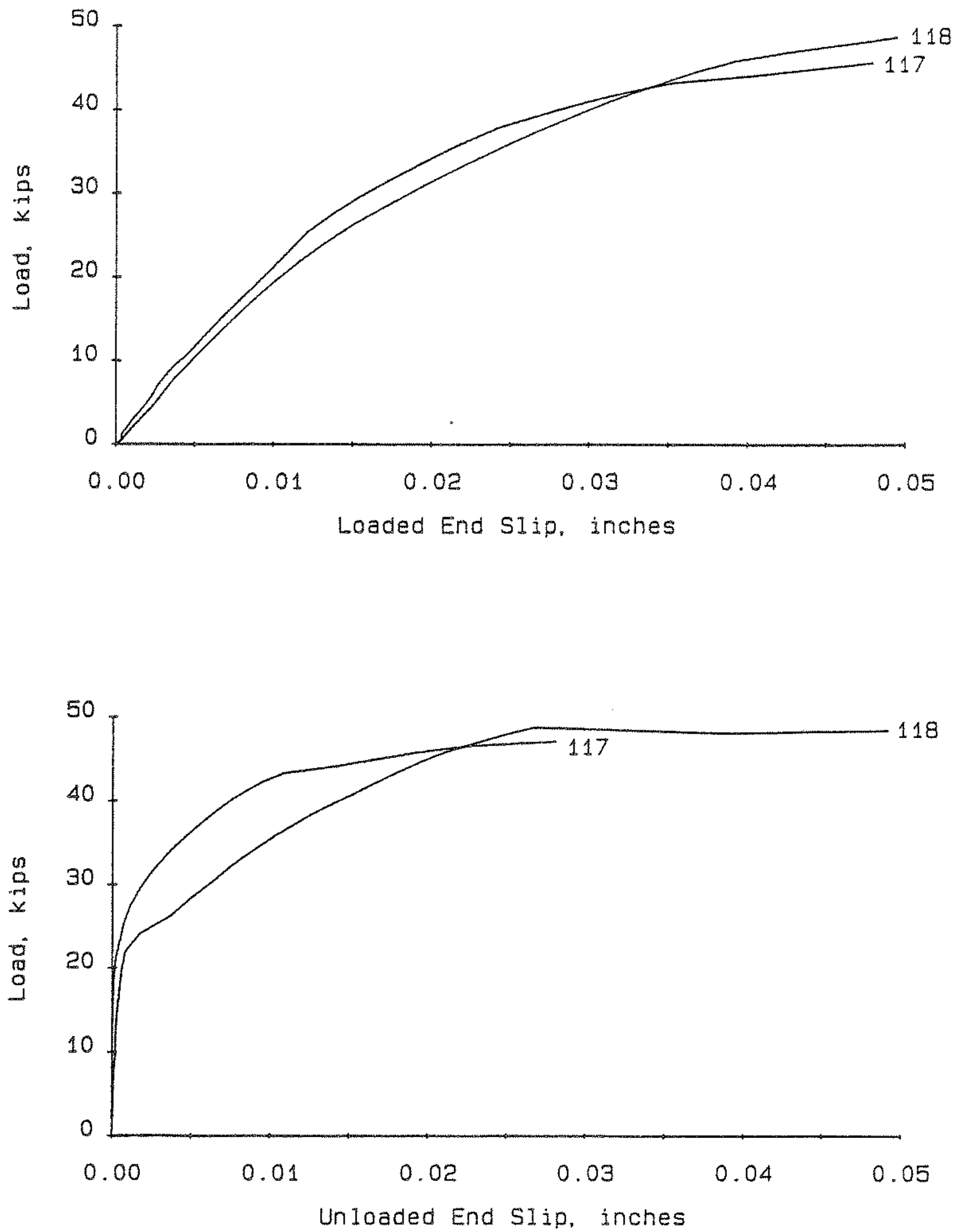

Fig. 2.43 Load-Slip Curves for Slab 8c.

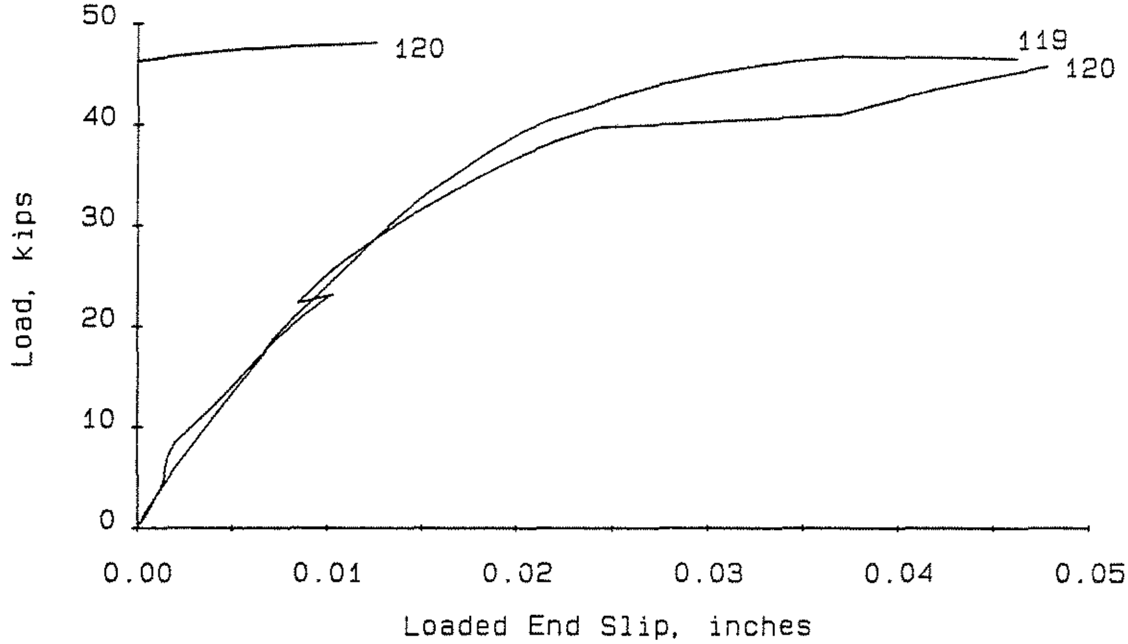

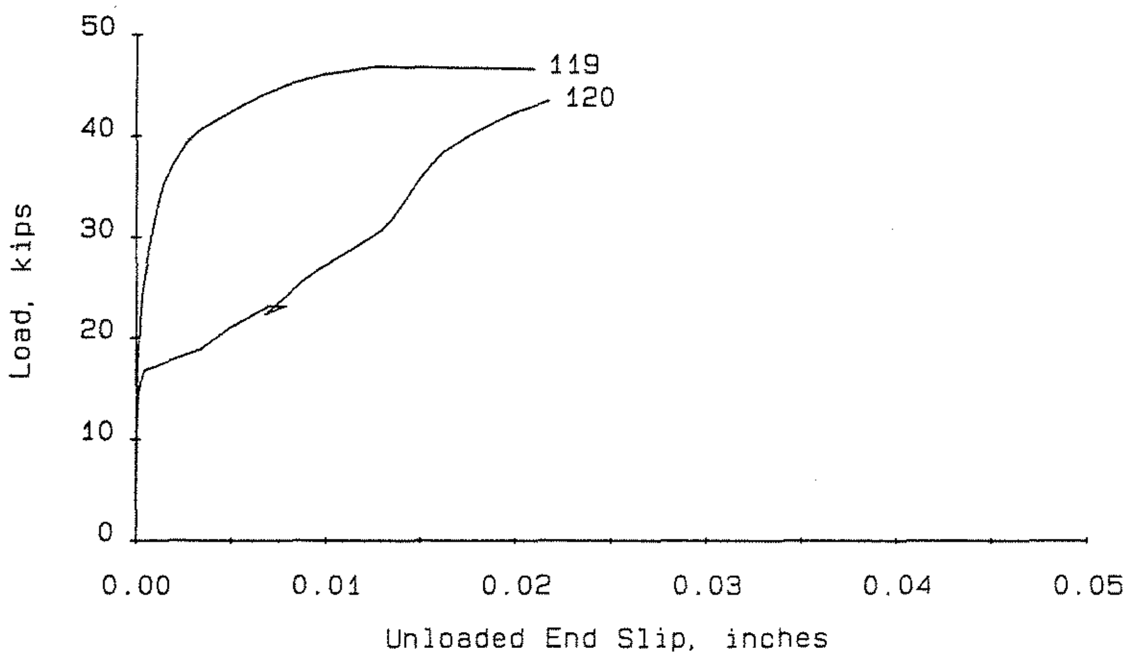

Fig. 2.44 Load-Slip Curves for Slab 8d.

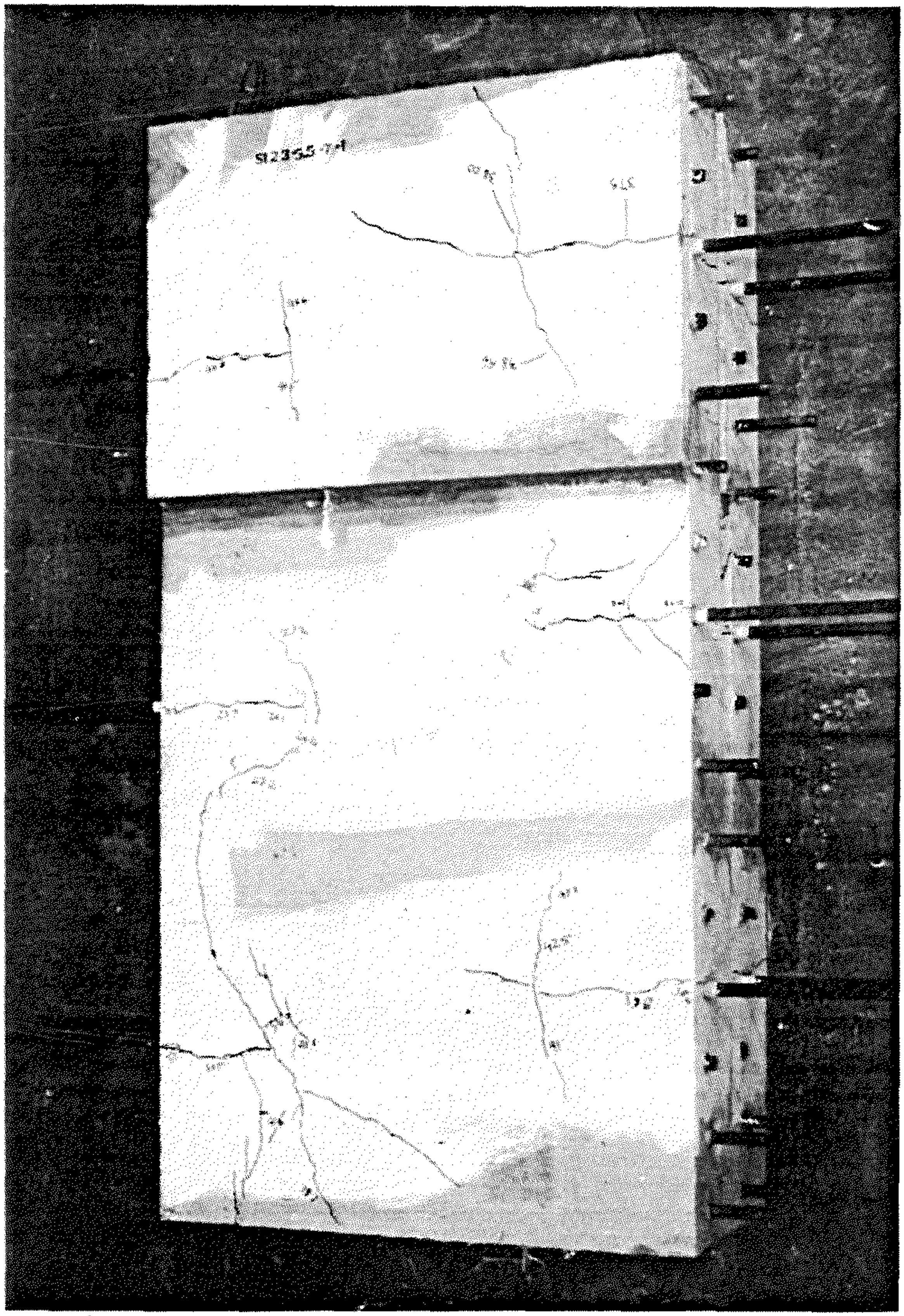

Fig. 2.45 Shallow Slab with #8 Test Bars After Test.

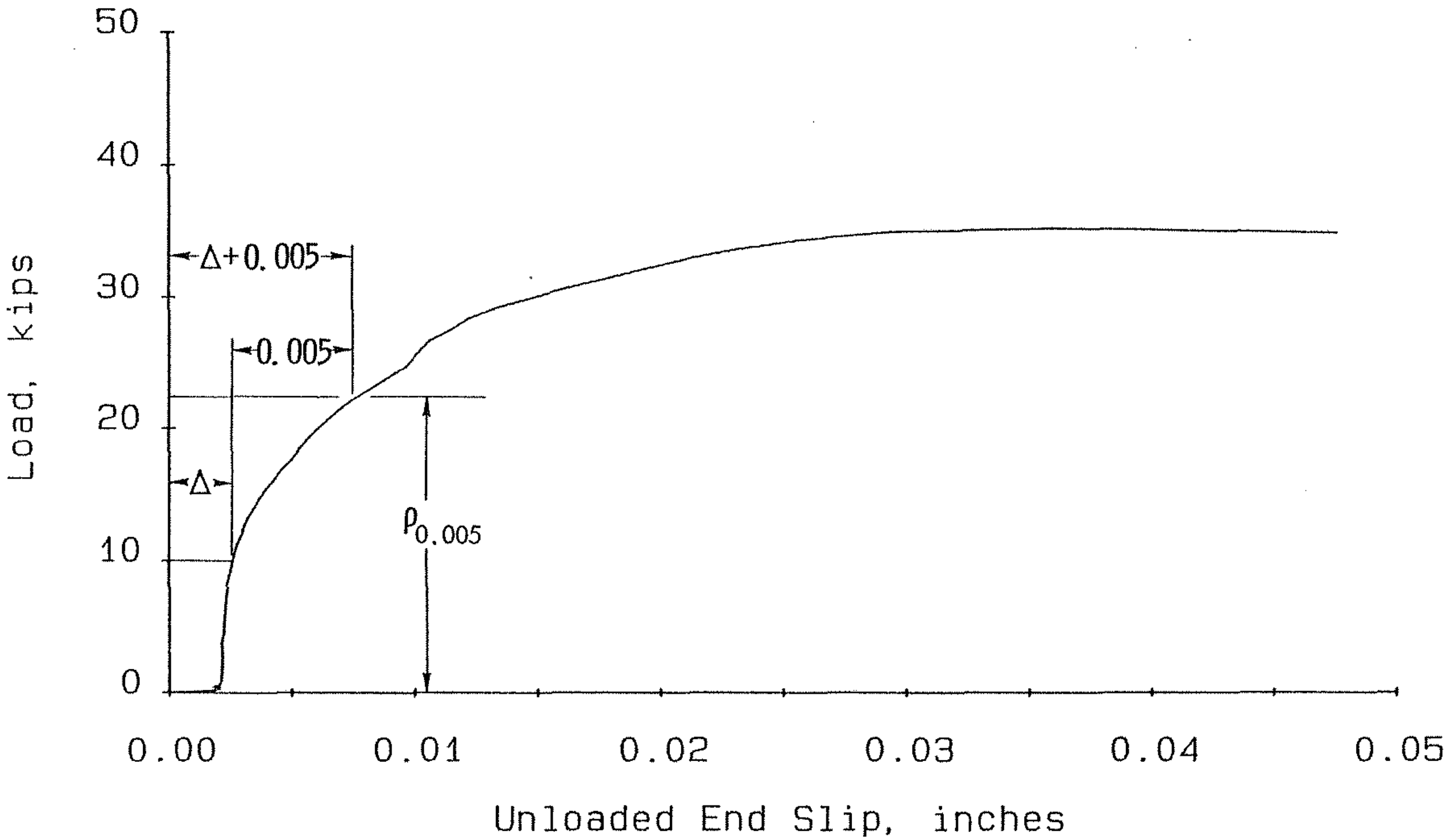

Fig. 3.1 Slip Correction Procedure--#8 Bar.

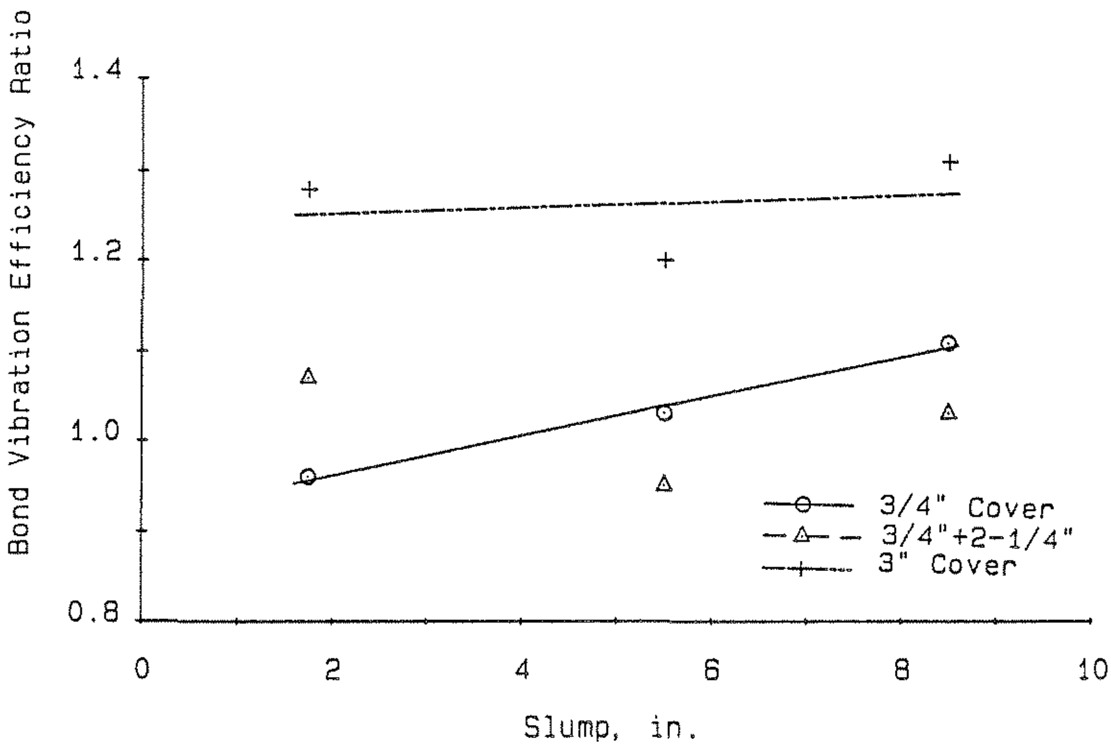

Fig. 3.2 Bond Vibration Efficiency Ratios at 0.005 Inch End Slip for #8 Bars Versus Slump (Groups 2, 3, and 7).

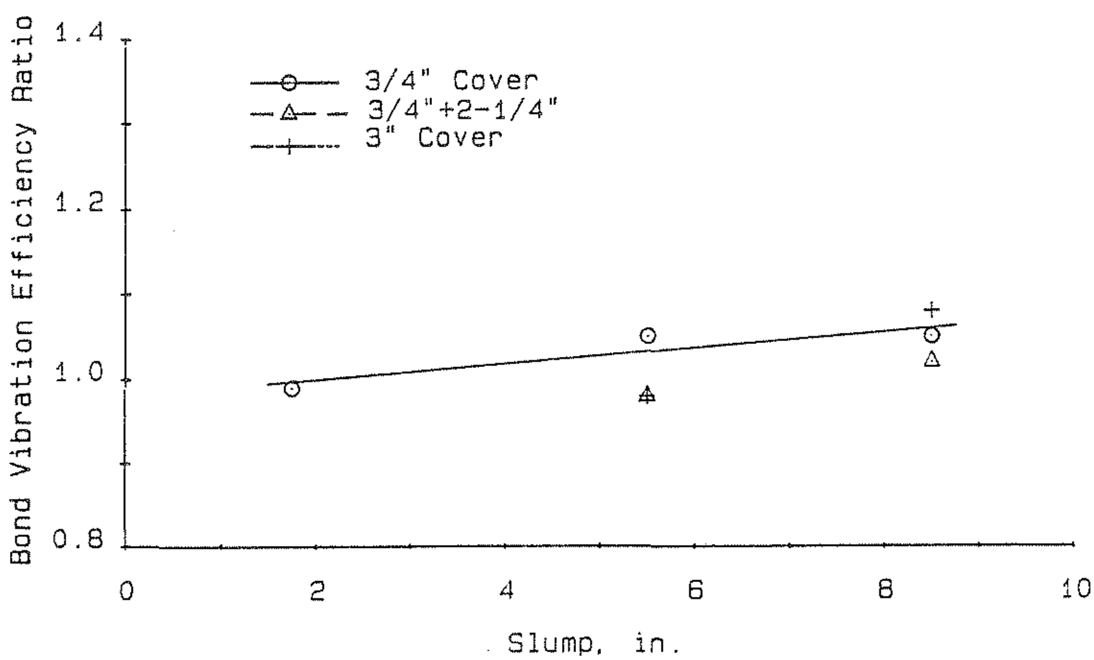

Fig. 3.3 Bond Vibration Efficiency Ratios at Ultimate Load for #8 Bars Versus Slump (Groups 2, 3, and 7).

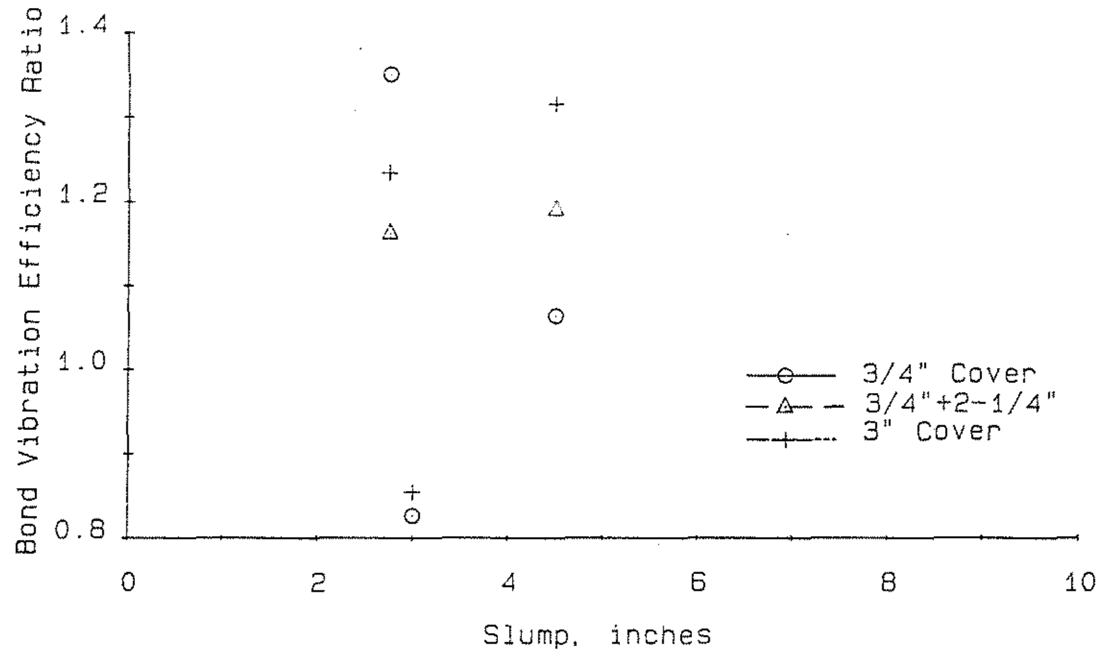

Fig. 3.4 Bond Vibration Efficienty Ratios at 0.010 Inch End Slip for #5 Bars Versus Slump (Groups 4, 5, and 6).

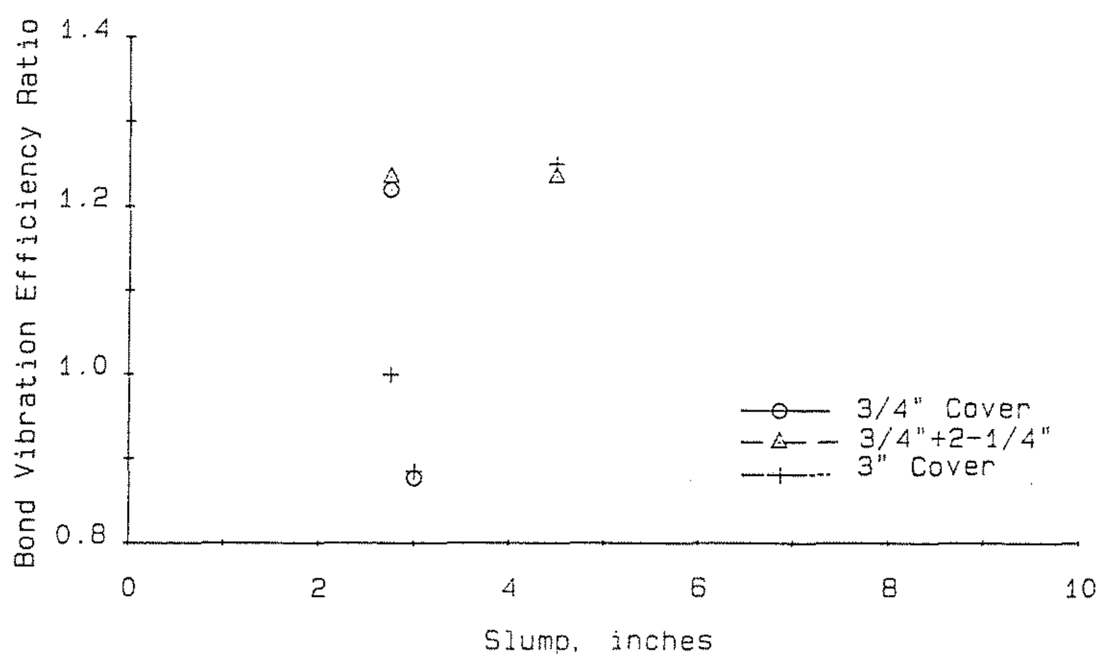

Fig. 3.5 Bond Vibration Efficiency Ratios at Ultimate Load for #5 Bars Versus Slump (Groups 4, 5, and 6).

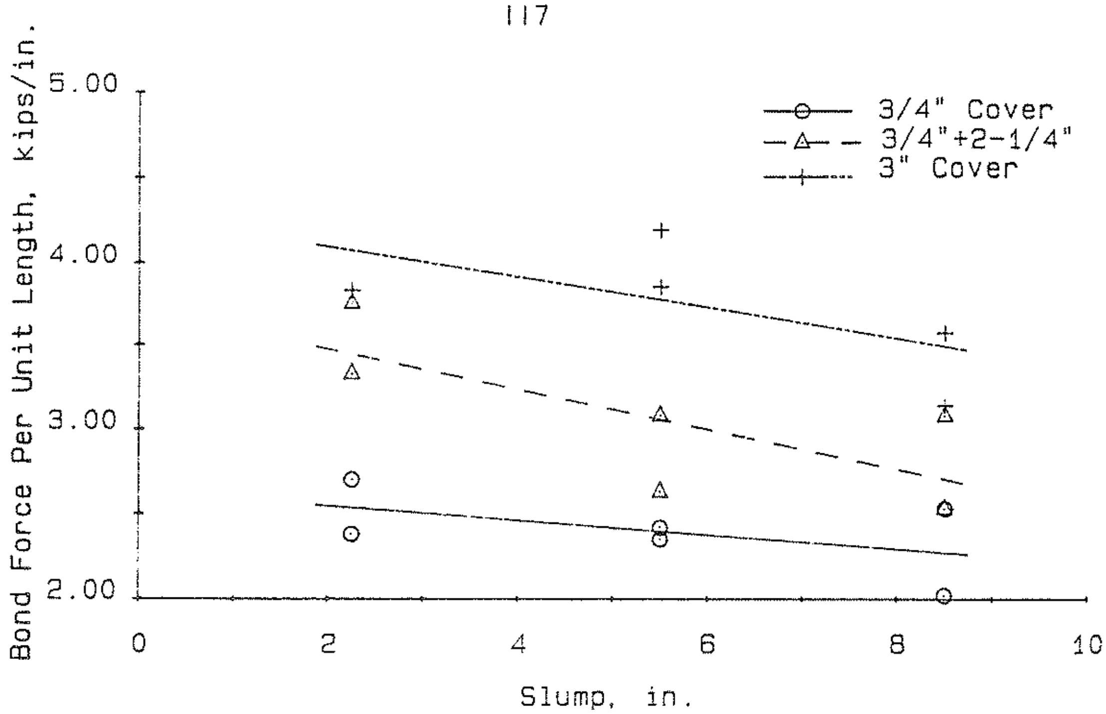

Fig. 3.6 Bond Forces Per Unit Length at 0.005 Inch End Slip for #8 Bars Versus Slump (Groups 2, 3, and 8).

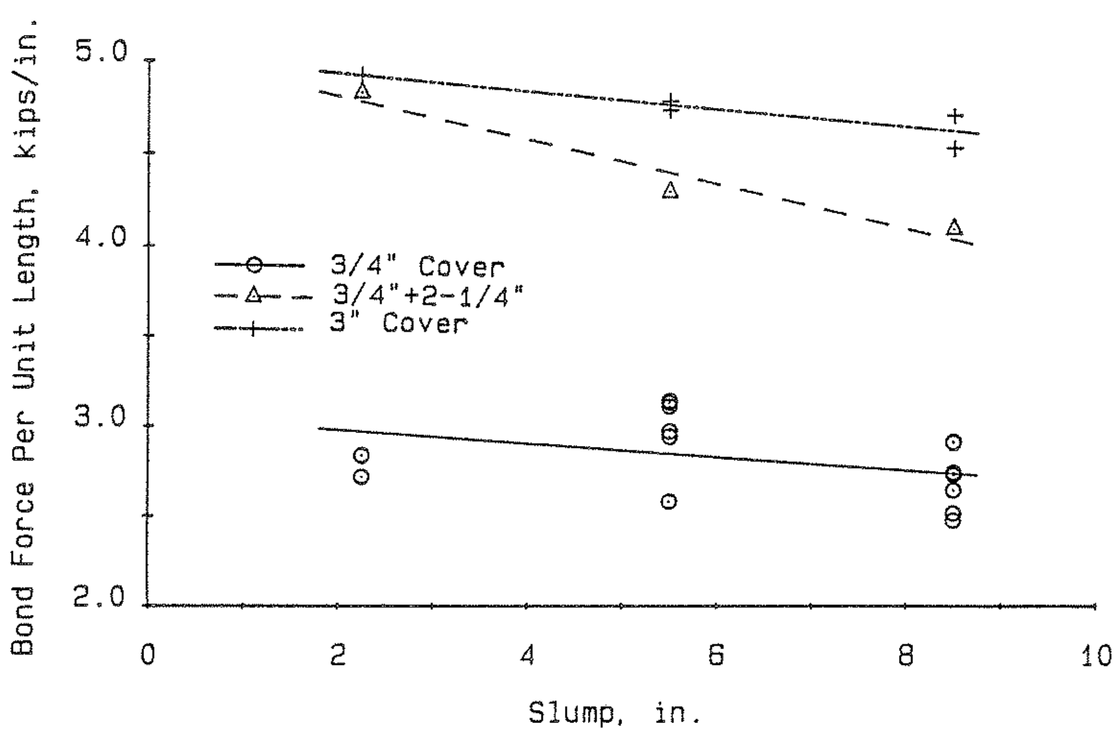

Fig. 3.7 Bond Forces Per Unit Length at Ultimate Load for #8 Bars Versus Slump (Groups 2, 3, and 8).

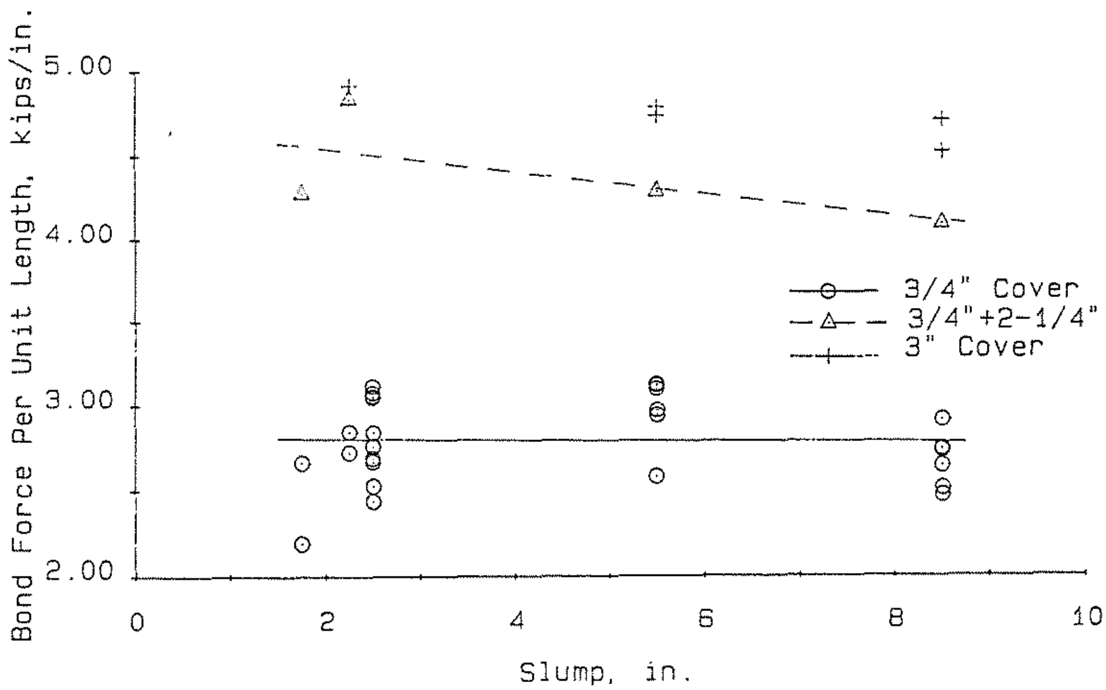

Fig. 3.8 Bond Forces Per Unit Length at Ultimate Load for #8 Bars Versus Slump (High Density Vibration Slabs from Groups 1, 2, 3, 7, and 8).

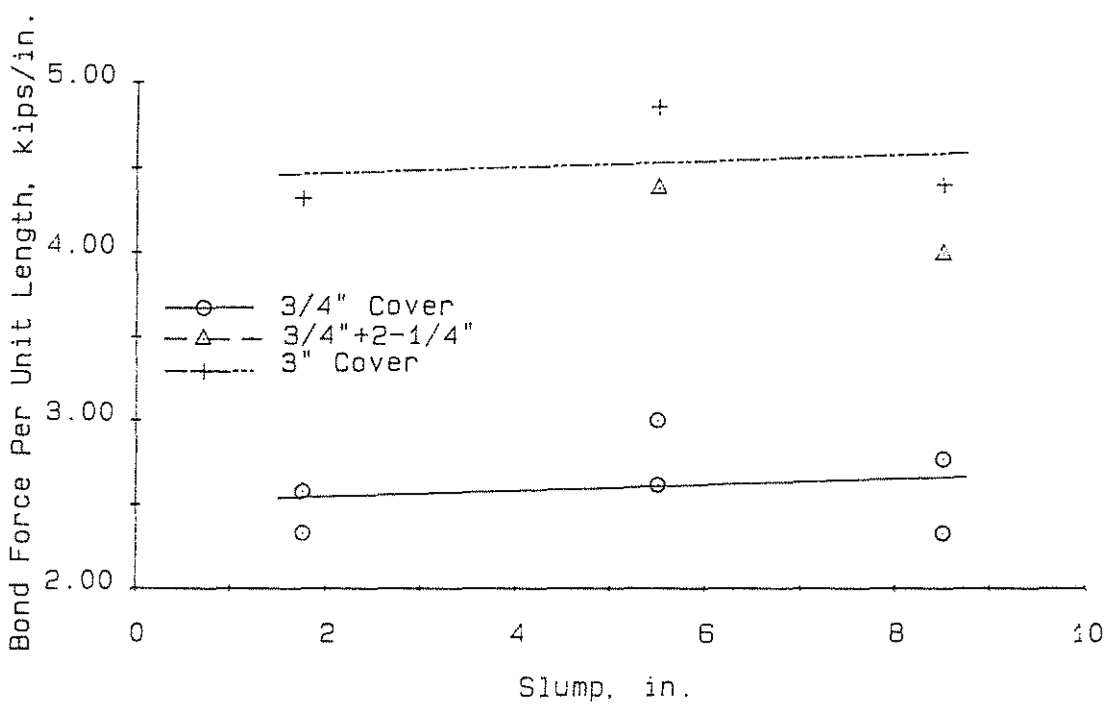

Fig. 3.9 Bond Forces Per Unit Length at Ultimate Load for #8 Bars Versus Slump (Low Density Vibration Slabs from Groups 2, 3, and 7).

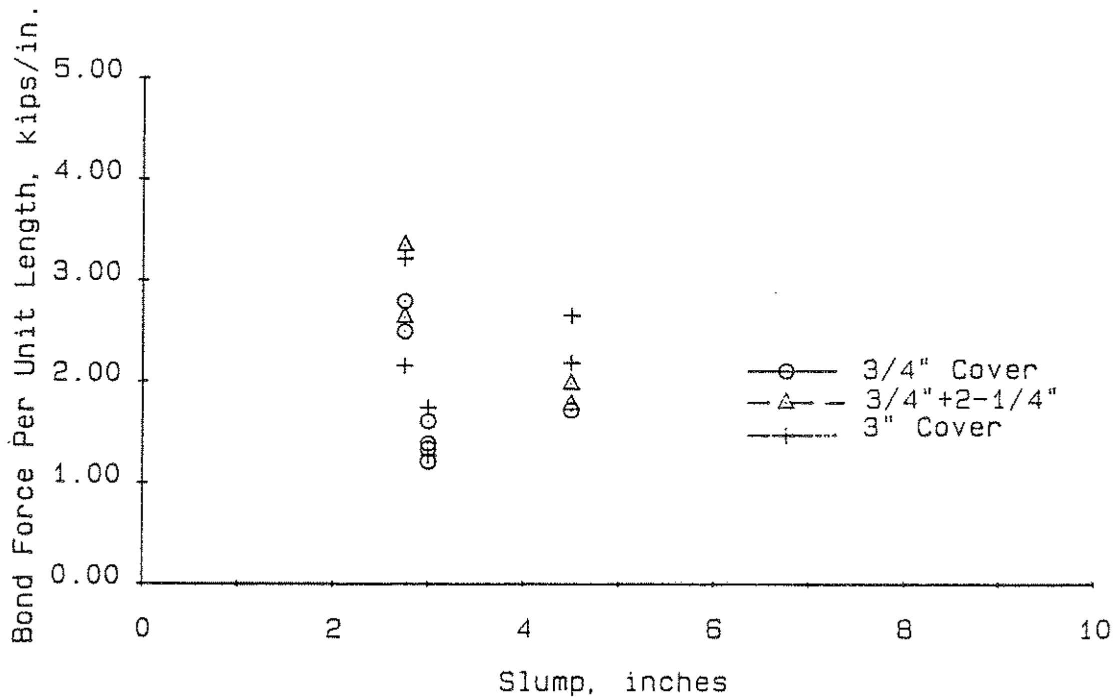

Fig. 3.10 Bond Forces Per Unit Length at 0.010 Inch End Slip for #5 Bars Versus Slump (High Density Vibration Slabs from Groups 4, 5, and 6).

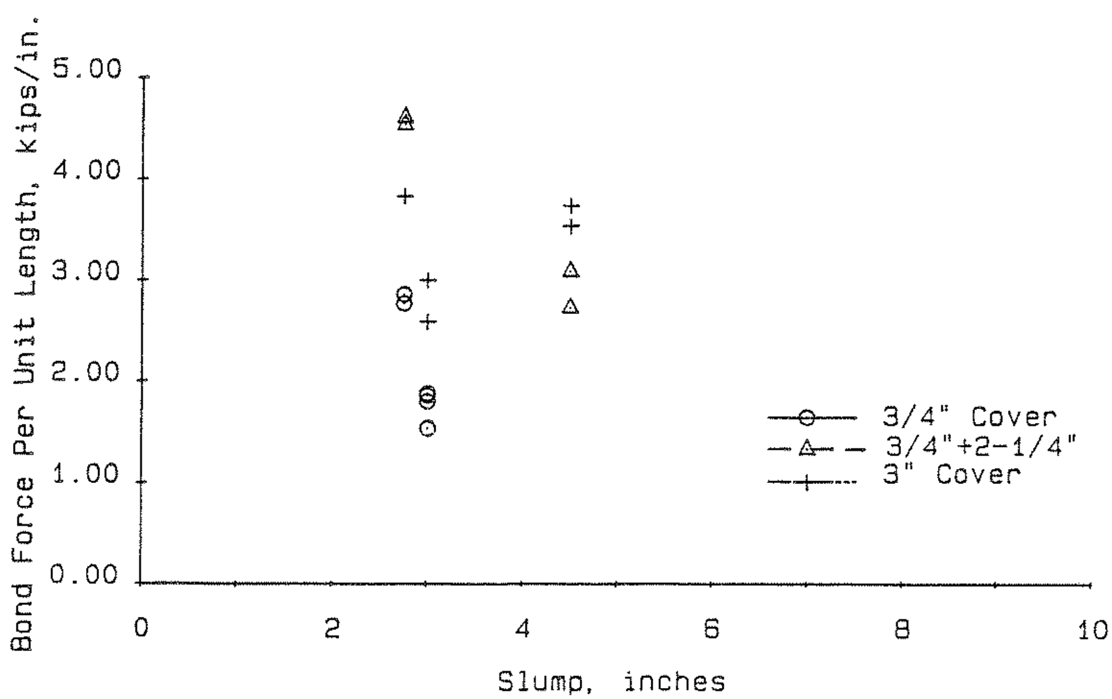

Fig. 3.11 Bond Forces Per Unit Length at Ultimate Load for #5 Bars Versus Slump (High Density Vibration Slabs from Groups 4, 5, and 6).

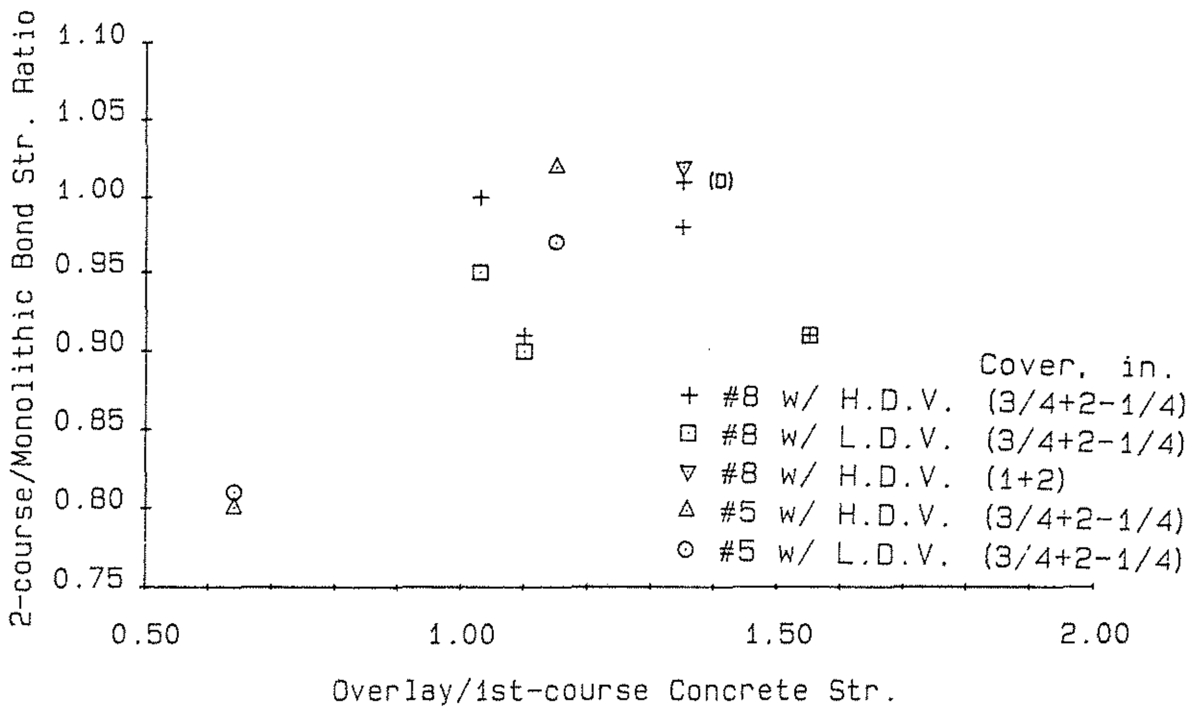

Fig. 3.12 Ratio of Two-Course to Monolithic Bond Strength Versus Ratio of Overlay to First Course Concrete Strength.

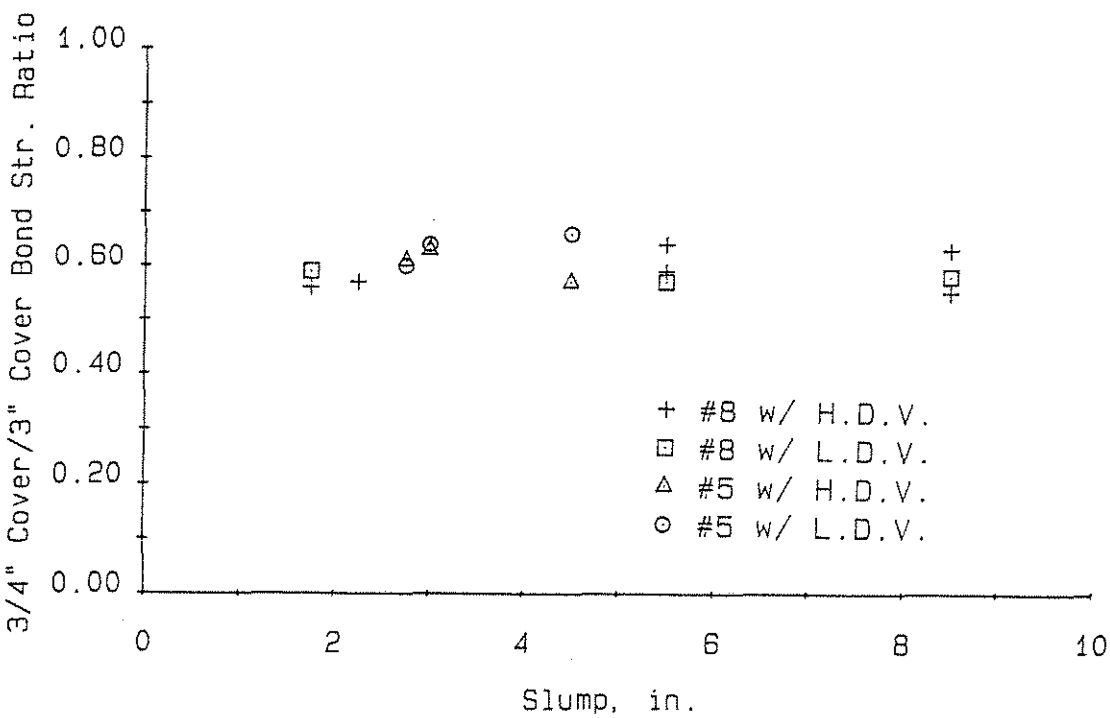

Fig. 3.13 Ratio of Bond Strength for 3/4 Inch Cover to 3 Inch Cover Versus Slump.

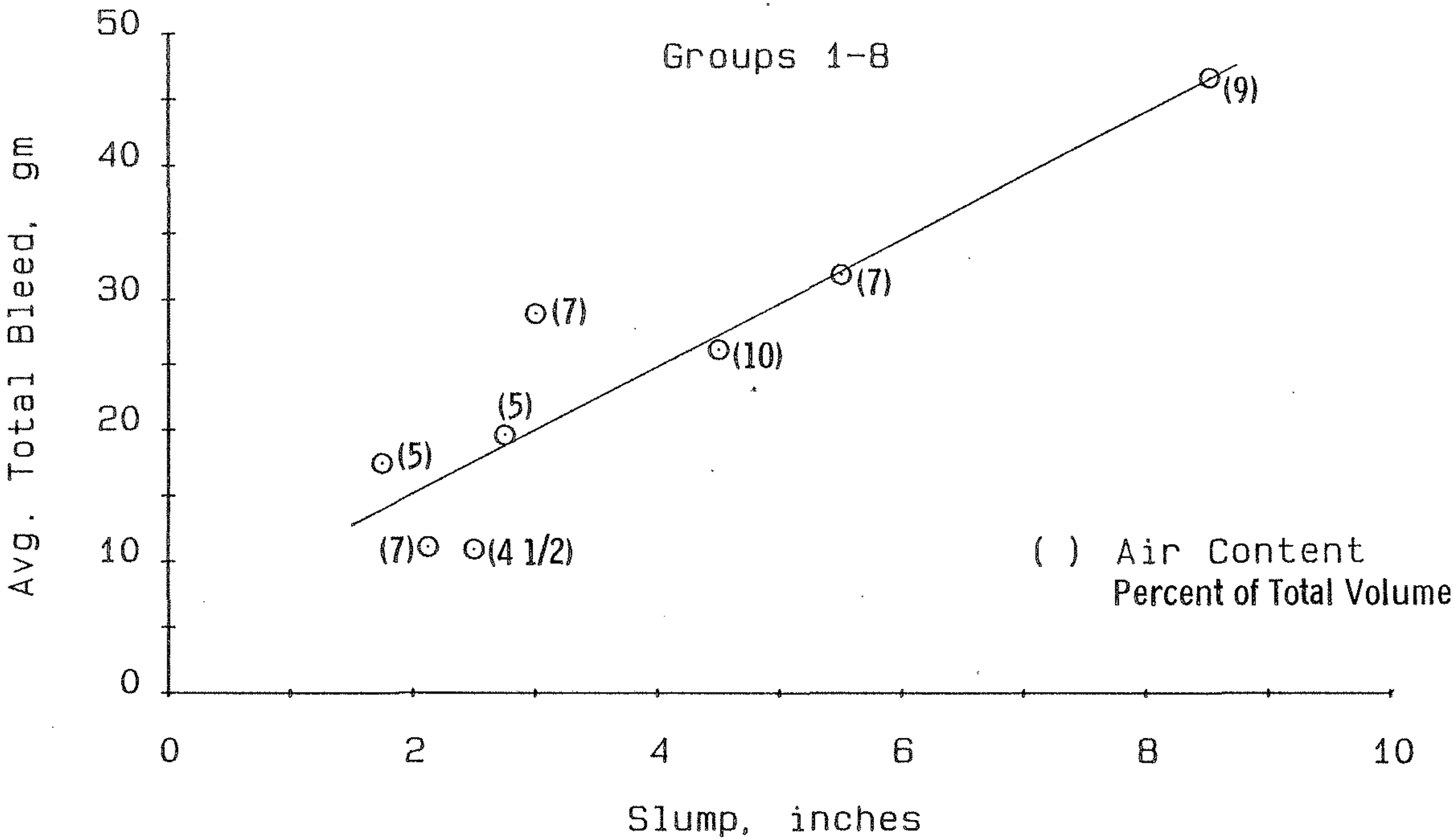

Fig. 3.14 Average Total Bleed at Two Hours for All Slab Groups Versus Concrete Slump.

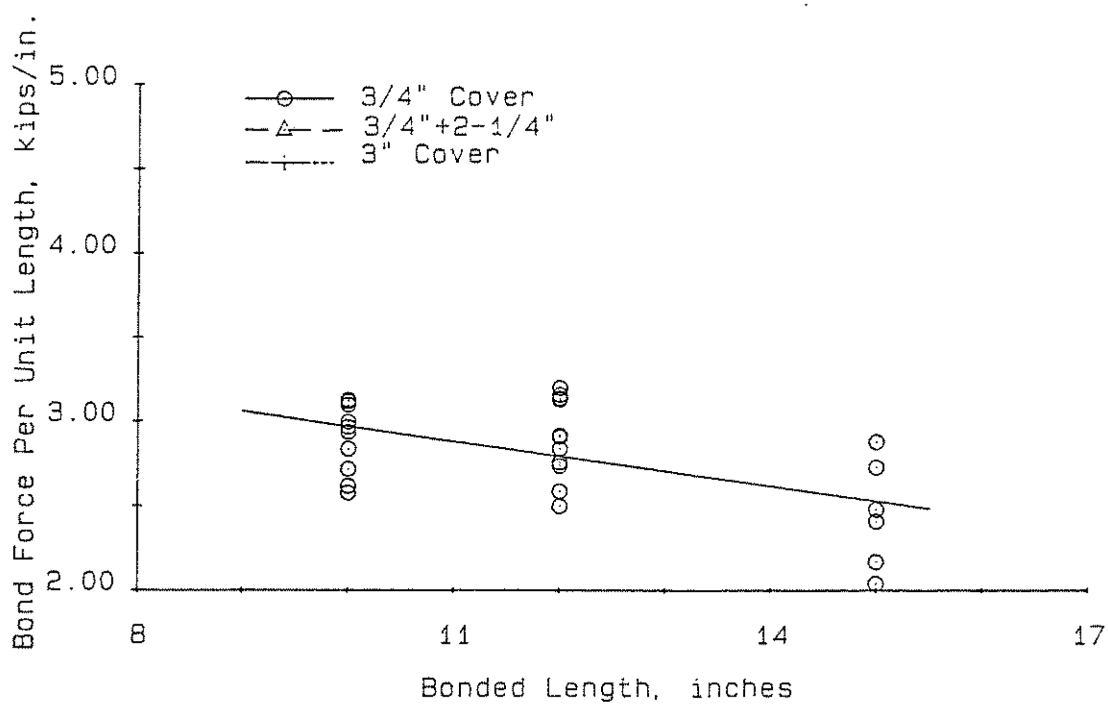

Fig. 3.15 Bond Forces Per Unit Length at Ultimate Load for #8 Bars Versus Bonded Length.

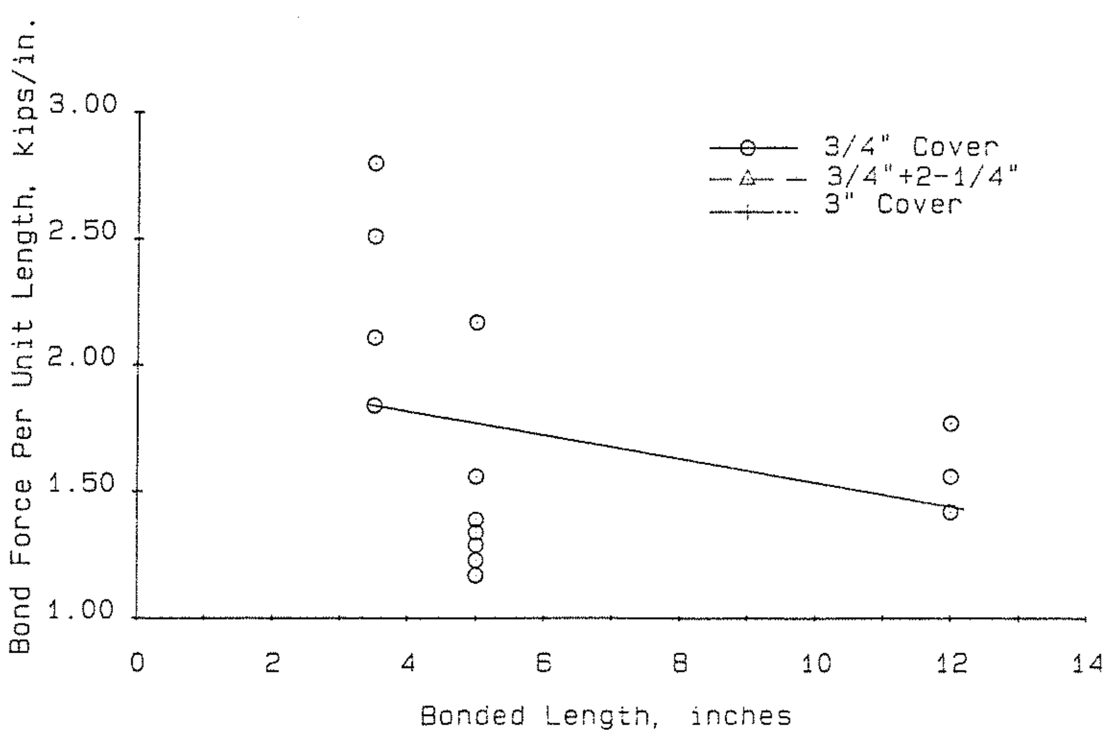

Fig. 3.16 Bond Forces Per Unit Length at 0.010 Inch End Slip for #5 Bars Versus Bonded Length.

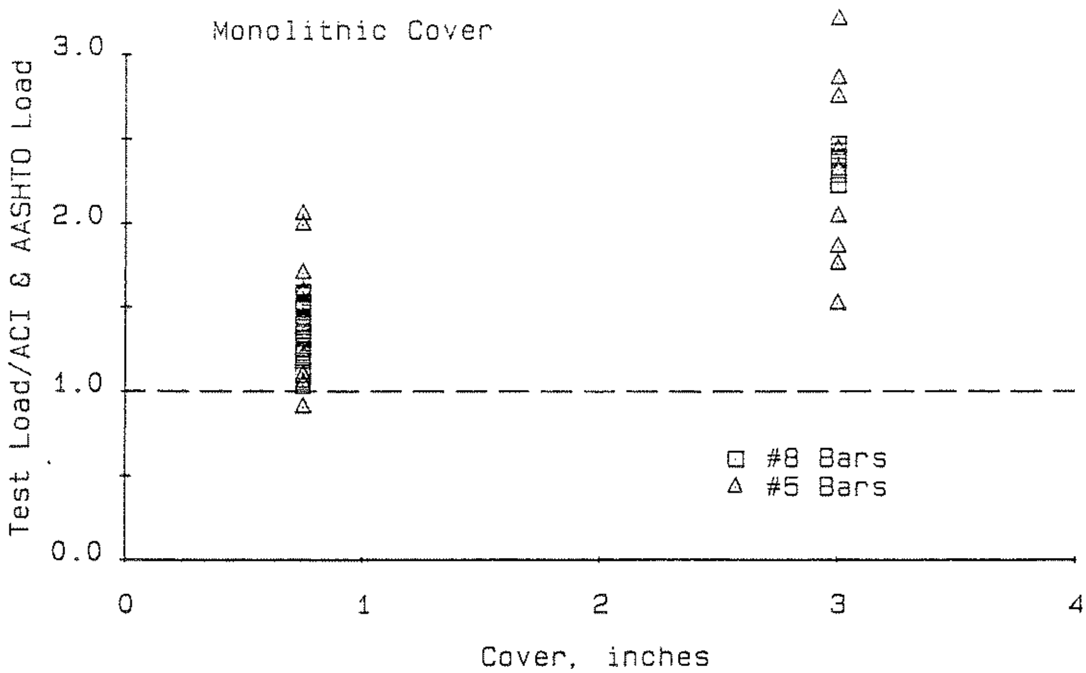

Fig. 3.17 Comparison of Ultimate Test Loads for Bars with 3/4 Inch Monolithic Cover with ACI (4) and AASHTO (1) Loads.

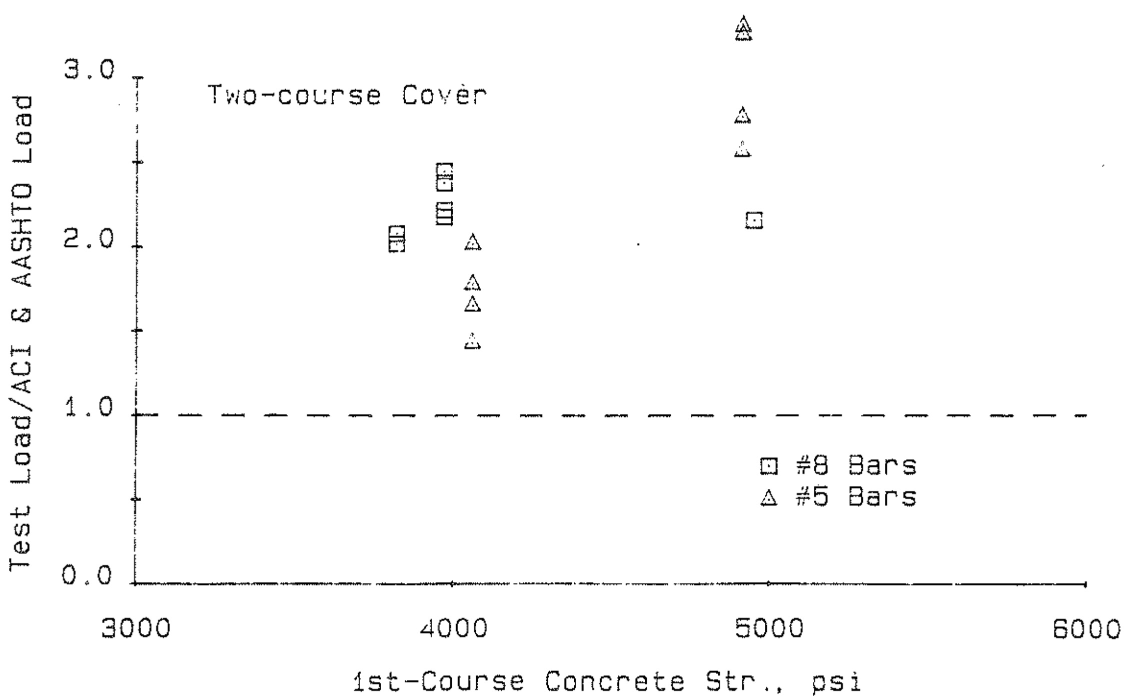

Fig. 3.18 Comparison of Ultimate Test Loads for Bars with Two-Course Cover with ACI (4) and AASHTO (1) Loads.

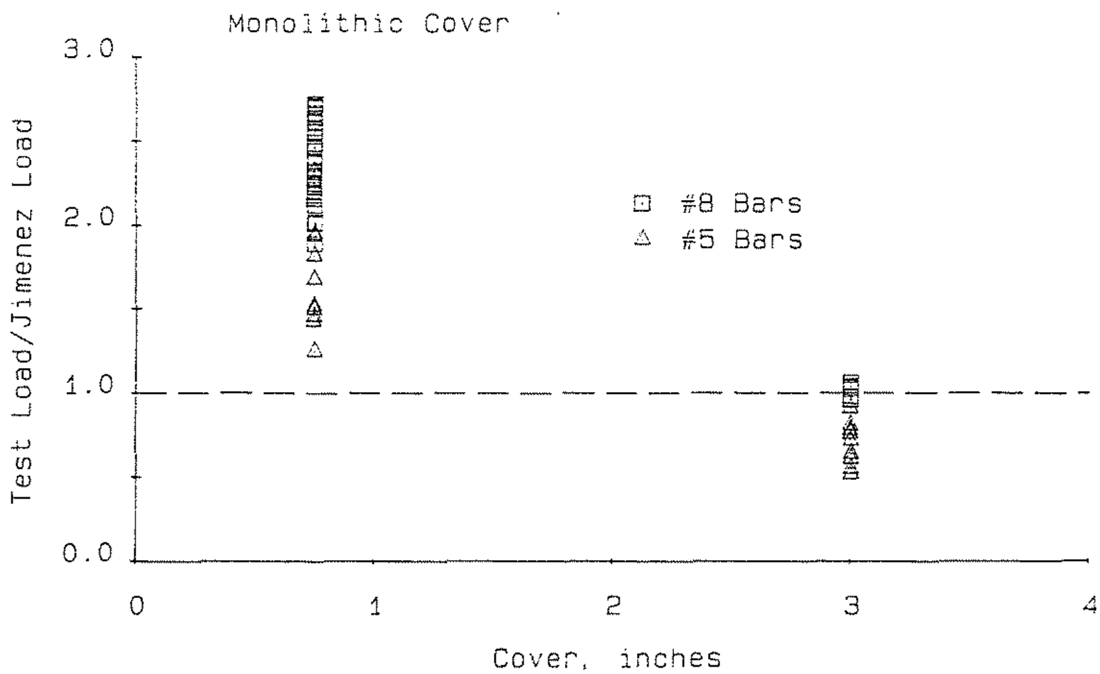

Fig. 3.19 Comparison of Ultimate Test Loads with Loads Predicted by the Jimenez Bond Relationship (22).

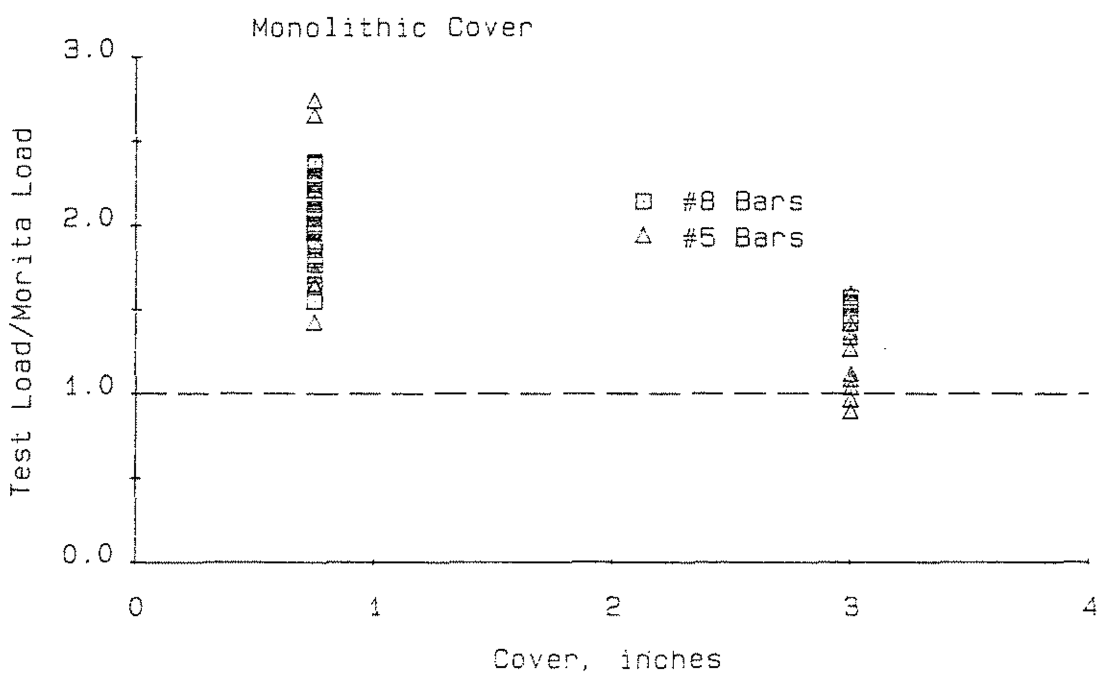

Fig. 3.20 Comparison of Ultimate Test Loads with Loads Predicted by the Morita and Fujii Relationship (29).

Appendix A

Notation

c	minimum cover (inches)
d	bar diameter (inches)
f'_c	concrete compressive strength (pounds per square inch)
L	embedment length (inches)
T	total ultimate bond force based on ultimate average bond stress (pounds)
T_a	total ultimate bond force based on 1977 ACI (4) and 1977 AASHTO (1) bond requirements for #11 bars and smaller (pounds)
T_j	total ultimate bond force derived by Jimenez et al. (22) (kips)
T_m	total ultimate bond force derived by Morita and Fujii (29) (kips)
U	ultimate average bond force per unit length (pounds per inch)